

**PARAMETRIC STUDY ON SEISMIC VULNERABILITY  
OF SYMMETRIC AND ASYMMETRIC BUILDINGS BY  
PUSHOVER ANALYSIS**

THESIS SUBMITTED FOR PARTIAL FULFILMENT OF THE REQUIREMENT FOR

THE DEGREE OF

**MASTER OF CONSTRUCTION ENGINEERING**

WITH SPECIALIZATION IN

**STRUCTURAL REPAIR AND RETROFIT ENGINEERING**

By

**ACHIRA ADHYA**

**Examination Roll no. – M6CNE1604**

**Registration no. – 73899 of 1999 – 2000**

Under the esteemed Guidance of

**PROF. DR. DEBASISH BANDYOPADHYAY**

**DEPARTMENT OF CONSTRUCTION ENGINEERING**

**FACULTY OF ENGINEERING AND TECHNOLOGY**

**JADAVPUR UNIVERSITY**

**KOLKATA – 700098**

**May – 2016**

**FACULTY OF ENGINEERING & TECHNOLOGY**  
**DEPARTMENT OF CONSTRUCTION ENGINEERING**  
**JADAVPUR UNIVERSITY**  
**KOLKATA, INDIA**

**CERTIFICATE OF RECOMMENDATIONS**

**TO WHOM IT MAY CONCERN**

This is to certify that the thesis entitled “**Parametric study on seismic vulnerability of symmetric and asymmetric buildings by pushover analysis**” submitted by **Achira Adhya** is absolutely based upon her own work under our supervision and neither her thesis nor any part of the thesis has been submitted for any degree/diploma or any other academic award anywhere before.

**Prof. (Dr.) Debasish Bandyopadhyay**  
Thesis Supervisor,  
Department of Construction Engineering,  
Jadavpur University, Kolkata, India

Countersigned by,

---

**Prof. (Dr.) Kaushik Bandyopadhyay**  
Head,  
Department of Construction Engineering,  
Jadavpur University, Kolkata, India

---

**Dean,**  
Faculty of Engineering and Technology  
Jadavpur University, Kolkata, India

**FACULTY OF ENGINEERING & TECHNOLOGY  
DEPARTMENT OF CONSTRUCTION ENGINEERING  
JADAVPUR UNIVERSITY  
KOLKATA, INDIA**

**CERTIFICATE OF APPROVAL**

This foregoing thesis is hereby approved as a credible study of an engineering subject carried out and presented in a manner satisfactory to warrant its acceptance as a prerequisite to the degree for which it has been submitted. It is understood that by this approval the undersigned do not endorse or approve any statement made, opinion expressed or conclusion drawn therein but approve the thesis only for the purpose for which it has been submitted.

**Board of Examiners**

\_\_\_\_\_  
**(Signature of Examiner)**

\_\_\_\_\_  
**(Signature of Examiner)**

**\* Only in case of thesis is approved.**

# **FACULTY OF ENGINEERING & TECHNOLOGY**

## **DEPARTMENT OF CONSTRUCTION ENGINEERING**

### **JADAVPUR UNIVERSITY**

**Kolkata, India**

#### **DECLARATION OF ORIGINALITY AND COMPLIANCE OF ACADEMIC ETHICS**

It is hereby declared that the thesis entitled “**Parametric study on seismic vulnerability of symmetric and asymmetric buildings by pushover analysis**” contains literature survey and original research work done by the undersigned candidate, and have been submitted for the partial fulfilment of the continuous assessment of the course of **Master of Construction Engineering with** specialization in “**Structural Repair and Retrofit Engineering**” of Jadavpur University.

All information in this document have been obtained and presented in accordance with academic rules and ethical conduct.

It is also declared that, as required by these rules and conduct, all materials and results that are not original to this work have been fully cited and referenced.

**Name** : **ACHIRA ADHYA**

**Examination Roll No** : **M6CNE1604**

**Registration No** : **73899 of 1999 – 2000**

**Thesis Title** : **Parametric study on seismic vulnerability of symmetric and asymmetric buildings by pushover analysis**

**Signature** :

**Date** : **.5.2016**

**Place** : **Kolkata**

## **ACKNOWLEDGEMENT**

I would like to express my deep sense of gratitude to **Prof. (Dr.) Debasish Bandyopadhyay** for his valuable guidance and supervision.

It is my pleasure to take this opportunity to extend my sincere thanks to Head, Department of Construction Engineering, Jadavpur University for his co-operation and advice.

I would like to thank Mr. **Jafar Sadak Ali**, Assistant Professor, Department of Civil Engineering, Aliah University and visiting Lecturer, Department of Construction Engineering, Jadavpur University, Kolkata for providing necessary academic helps whenever required.

I would also like to express my gratitude to other respected teachers of the department for the continuous encouragement, support and valuable advices they provided throughout my work.

I would like to thank all the librarians, assistant librarians and library staffs of the Central Library and the Departmental Library of Jadavpur University for their kind cooperation during preparation of this report by providing me the books and documents as and when necessary.

Everything in this nature is time bound, so thanks to ‘Almighty’ for successful completion of the work in time.

Finally, it is difficult to express my heartfelt respect in words for my parents, whose blessing has made me to reach my destination.

**(Achira Adhya)**

**Examination Roll no. – M6CNE1604**

**Registration no. – 73899 of 1999 – 2000**

## **TABLE OF CONTENTS**

---

<b>CONTENTS</b>	<b>PAGE No</b>
<b>Certificate of Recommendation</b>	<b>ii</b>
<b>Certificate of Approval</b>	<b>iii</b>
<b>Declaration of Originality and Compliance of Academic Ethics</b>	<b>iv</b>
<b>Acknowledgement</b>	<b>v</b>
<b>Table of contents</b>	<b>vi-ix</b>
<b>List of Tables</b>	<b>x-xi</b>
<b>List of Figures</b>	<b>xii- xvii</b>
<b>Abbreviations or symbols</b>	<b>xviii</b>
<b>Abstract</b>	<b>xix</b>
<b>Chapter 1: Introduction</b>	
1.1 General	
1.1.1 Analytical procedures	
1.2 Objective of work	
1.3 Scope of work	
<b>Chapter 2: Literature Review</b>	
2.0 General	
2.1 Pushover Analysis of Structure	
2.2 Critical view on literatures	
<b>Chapter 3: NSP based Evaluation</b>	
3.1 General	
3.2 Pushover Analysis	
3.2.1 Evaluation result	
3.3 Pushover Analysis using FEMA 356 CM	

- 3.3.1 Basis of the procedure
- 3.3.2 Modeling and Analysis Considerations
  - 3.3.2.1 Control Node Displacement
  - 3.3.2.2 Lateral Load Distribution
  - 3.3.2.3 Idealized Force-Displacement Curve
  - 3.3.2.4 Period Determination
- 3.3.3 Determination of Forces and Deformations
  - 3.3.3.1 Target Displacement
- 3.3.4 Acceptance Criteria
- 3.4 Pushover Analysis using ATC 40 CSM
  - 3.4.1 Capacity Spectrum method
    - 3.4.1.1 Basis of the procedure
    - 3.4.1.2 Modeling and Analysis Considerations
      - 3.4.1.2.1 Capacity
      - 3.4.1.2.2 Demand
      - 3.4.1.2.3 Conversion of the Capacity Curve to the capacity Spectrum
      - 3.4.1.2.4 Conversion of the Demand Curve to the Response Spectrum in ADRS format
      - 3.4.1.2.5 Reduced Response Spectrum
      - 3.4.1.2.6 Performance
      - 3.4.1.2.7 Intersection of Capacity Spectrum and Demand Spectrum
  - 3.4.2 Capacity Spectrum method
    - 3.4.2.1 Calculating Demand Displacement using the Displacement Coefficient Method
    - 3.4.2.2 Effective fundamental period & Target displacement
    - 3.4.2.3 Checking Performance at the Expected Maximum Displacement
- 3.5 Comparative chart for capacity spectrum, Displacement Coefficient Methods

- 3.6 Performance level of structure and element
- 3.7 Types of non-linearity
  - 3.7.1 Geometric non-linearity
  - 3.7.2 Material non-linearity
- 3.8 Pushover Analysis Solution Control
- 3.9 Vulnerability Index
- 3.10 Limitation of Conventional Pushover Analysis

#### **Chapter 4: Pushover analysis by SAP 2000**

- 4.0 General
- 4.1 Begin a New Model
- 4.2 Define Material
- 4.3 Define Frame Section
- 4.4 Add Frame Objects
- 4.5 Define Load Patterns
- 4.6 Assign Gravity Loads
- 4.7 Define Response Spectrum Function
- 4.8 Define Response Spectrum Load Case
- 4.9 Define Mass Sources
- 4.10 Define Load Combinations
- 4.11 Concrete Frame Design
- 4.12 Linear Analysis & Unlock the Model
- 4.13 New Load Case of Gravity Loads
- 4.14 Assignment of Hinges to Frame Elements
- 4.15 Define Pushover Load Case
- 4.16 Graphically review the Results

#### **Chapter 5: Numerical study**

- 5.1 General
- 5.2 Case Study
  - 5.2.1 Load Calculations



- 5.3 Four storied O.M.R.F building
- 5.4 Models symmetric about both X & Y axes
  - 5.4.1 Rectangular model
  - 5.4.2 Model H
  - 5.4.3 Model I
  - 5.4.4 Model O
  - 5.4.5 Result discussion of symmetric models
- 5.5 Models asymmetric about one or both of the axes
  - 5.5.1 Model C
  - 5.5.2 Model L
  - 5.5.3 Model Br L
  - 5.5.4 Model T
  - 5.5.5 Model U
  - 5.5.6 Result discussion of asymmetric models
- 5.6 Result discussion of all models

## **Chapter 6: Conclusion**

- 6.1 General
- 6.2 Observation and conclusion
- 6.3 Future scope of work

## **References**

**Appendix** – Load calculations and response spectrum text file

## LIST OF TABLES

---

<b>Table No</b>	<b>Description of Tables</b>
Table 1-1	List of earthquakes in India after year 2000
Table 3-1	Values for Modification Factor $C_0$
Table 3-2	Values for Modification Factor $C_2$
Table 3-3	Performance level and inter storey drift limit
Table 3-4	Performance range and weight age factor
Table 5-1	Slab loading intensity
Table 5-2	Comparison of various seismic resisting features of symmetric models along X direction
Table 5-3	Comparison of various seismic resisting features of symmetric models along Y direction
Table 5-4	$VI_{\text{bldg}}$ in both direction for Symmetric models
Table 5-5	$VI_{\text{storey}}$ in both direction for Symmetric models at all levels
Table 5-6	Comparison of various seismic resisting features of asymmetric models along X direction
Table 5-7	Comparison of various seismic resisting features of asymmetric models along Y direction
Table 5-8	$VI_{\text{bldg}}$ in both direction for Asymmetric models
Table 5-9	$VI_{\text{storey}}$ in both direction for Asymmetric models at all levels
Table 5-10	Comparison of various seismic resisting features of all models along X direction
Table 5-11	Comparison of various seismic resisting features of all models along Y direction
Table 5-12	Global Ductility & Global Stiffness in X direction of all models

Table 5-13	Global Ductility & Global Stiffness in Y direction of all models
Table 5-14	$VI_{\text{bldg}}$ & $VI_{\text{storey}}$ of all models in details in both X and Y direction
Table 5-15	$VI_{\text{storey}}$ in both directions for all models in all levels
Table A-1	Trapezoidal/Triangular load ordinate (max) calculations

## LIST OF FIGURES

---

FIGURE	CONTENTS
Fig. 1.1	Ratio of Types of Structure to Total Surveyed Buildings
Fig. 1.2	Severely damaged and collapsed buildings in Nepal earthquake
Fig. 3.1.1	Building model and Pushover curve
Fig. 3.1.2	Demand and capacity spectra
Fig. 3.2	Idealized Force-Displacement Curves
Fig. 3.3	Capacity Curve
Fig. 3.4	Multiple Capacity Curves Required To Global strength Degradation Modeled
Fig. 3.5	Capacity curve with Model strength Degradation
Fig. 3.6	Demand Spectrum
Fig. 3.7	Equal Displacement Approximation
Fig. 3.8	Capacity curve and capacity spectrum
Fig. 3.9.1	Response spectra in traditional and ADRS format
Fig. 3.9.2	Spectral acceleration and spectral displacement
Fig. 3.10	Capacity spectrum superimposed over Response spectra in Traditional and ADRS Formats
Fig. 3.11	Intersection point of Demand and capacity spectrums within acceptable tolerance
Fig. 3.12	Intersection point of Reduced Demand and capacity spectrums to meet acceptance criteria
Fig. 3.13	Bilinear representation of Capacity Curve for Displacement coefficient Method
Fig. 3.14	Pushover curve and performance levels
Fig. 4.1	New model initialization
Fig. 4.2	Quick grid lines and grid system data forms
Fig. 4.3	Materials data form
Fig. 4.4	Material property data forms for concrete and rebar

- Fig. 4.5 Concrete section property and rectangular section property data forms
- Fig. 4.6 Reinforcement data forms for beam and column
- Fig. 4.7 Properties of object data form
- Fig. 4.8 Joint restraints data form
- Fig. 4.9 Load patterns data form
- Fig. 4.10 Frame distributed loads data form
- Fig. 4.11 Response Spectrum function definition form and display graph
- Fig. 4.12 Response Spectrum load case data form
- Fig. 4.13 Mass source data form
- Fig. 4.14 Load combination data form
- Fig. 4.15 Concrete frame design data form
- Fig. 4.16 Window for unlocking the model after linear analysis and design
- Fig. 4.17 Gravity load case data form
- Fig. 4.18 Window for assignment of frame hinges
- Fig. 4.19 Hinge assignment data form for concrete beams
- Fig. 4.20 Frame hinge assignment data form
- Fig. 4.21 Hinge assignment data form for concrete columns
- Fig. 4.22 Pushover load case data form
- Fig. 4.23 Load application control data form
- Fig. 4.24 Minimum and maximum number of saved states form
- Fig. 4.25 Solution control form for nonlinear parameters
- Fig. 4.26 Display window for Static pushover curve
- Fig. 4.27 Deformed shape data form
- Fig. 5.1 Typical gridline plan of models
- Fig. 5.2 Typical Y face elevation of models
- Fig. 5.3 Plan of rectangular model
- Fig. 5.4 Isometric view of rectangular model with slab diaphragm
- Fig. 5.5 Slab loading pattern of rectangular model
- Fig. 5.6 Isometric view of rectangular model with wall diaphragm
- Fig. 5.7 Wall loading pattern of rectangular model

- Fig. 5.8 Rectangular model ATC 40 (X)
- Fig. 5.9 Rectangular model ATC 40 (Y)
- Fig. 5.10 Plan of model H
- Fig. 5.11 Isometric view of model H with slab diaphragm
- Fig. 5.12 Slab loading pattern of model H
- Fig. 5.13 Isometric view of model H with wall diaphragm
- Fig. 5.14 Wall loading pattern of model H
- Fig. 5.15 Model H ATC 40 (X)
- Fig. 5.16 Plan of model I
- Fig. 5.17 Isometric view of model I with slab diaphragm
- Fig. 5.18 Slab loading pattern of model I
- Fig. 5.19 Isometric view of model I with wall diaphragm
- Fig. 5.20 Wall loading pattern of model I
- Fig. 5.21 Model I ATC 40 (X)
- Fig. 5.22 Model I ATC 40 (Y)
- Fig. 5.23 Plan of model O
- Fig. 5.24 Isometric view of model O with slab diaphragm
- Fig. 5.25 Slab loading pattern of model O
- Fig. 5.26 Isometric view of model O with wall diaphragm
- Fig. 5.27 Wall loading pattern of model O
- Fig. 5.28 Model O ATC 40 (X)
- Fig. 5.29 Model O ATC 40 (Y)
- Fig. 5.30 Base shear ( $V$ ) of symmetric models in X & Y Direction
- Fig. 5.31 Roof displacement ( $D_{rf}$ ) of symmetric models in X & Y Direction
- Fig. 5.32 Spectral Acceleration of symmetric models ( $S_a$ ) in X & Y Direction
- Fig. 5.33 Spectral Displacement ( $S_d$ ) of symmetric models in X & Y Direction
- Fig. 5.34 Global Stiffness of symmetric models in X & Y Direction
- Fig. 5.35 Building Vulnerability ( $VI_{\text{bdg}}$ ) of symmetric models in X & Y Direction
- Fig. 5.36 Storey Vulnerability ( $VI_{\text{storey}}$ ) of symmetric models at 1.8 m level in X & Y Direction

- Fig. 5.37 Plan of model C
- Fig. 5.38 Isometric view of model C with slab diaphragm
- Fig. 5.39 Slab loading pattern of model C
- Fig. 5.40 Isometric view of model C with wall diaphragm
- Fig. 5.41 Wall loading pattern of model C
- Fig. 5.42 Model C ATC 40 (X)
- Fig. 5.43 Model C ATC 40 (Y)
- Fig. 5.44 Plan of model L
- Fig. 5.45 Isometric view of model L with slab diaphragm
- Fig. 5.46 Slab loading pattern of model L
- Fig. 5.47 Isometric view of model L with wall diaphragm
- Fig. 5.48 Wall loading pattern of model L
- Fig. 5.49 Model L ATC 40 (X)
- Fig. 5.50 Plan of model Broader L
- Fig. 5.51 Isometric view of model Broader L with slab diaphragm
- Fig. 5.52 Slab loading pattern of model Broader L
- Fig. 5.53 Isometric view of model Broader L with wall diaphragm
- Fig. 5.54 Wall loading pattern of model Broader L
- Fig. 5.55 Model Broader L ATC 40 (X)
- Fig. 5.56 Model Broader L ATC 40 (Y)
- Fig. 5.57 Plan of model T
- Fig. 5.58 Isometric view of model T with slab diaphragm
- Fig. 5.59 Slab loading pattern of model T
- Fig. 5.60 Isometric view of model T with wall diaphragm
- Fig. 5.61 Wall loading pattern of model T
- Fig. 5.62 Model T ATC 40 (X)
- Fig. 5.63 Model T ATC 40 (Y)
- Fig. 5.64 Plan of model U
- Fig. 5.65 Isometric view of model U with slab diaphragm
- Fig. 5.66 Slab loading pattern of model U
- Fig. 5.67 Isometric view of model U with wall diaphragm

- Fig. 5.68 Wall loading pattern of model U
- Fig. 5.69 Model U ATC 40 (X)
- Fig. 5.70 Model U ATC 40 (Y)
- Fig. 5.71 Base shear (V) of asymmetric models in X & Y Direction
- Fig. 5.72 Roof displacement (Drf) of asymmetric models in X & Y Direction
- Fig. 5.73 Spectral Acceleration of asymmetric models (Sa) in X & Y Direction
- Fig. 5.74 Spectral Displacement (Sd) of asymmetric models in X & Y Direction
- Fig. 5.75 Global Stiffness of asymmetric models in X & Y Direction
- Fig.5.76 Building Vulnerability ( $VI_{\text{bldg}}$ ) of asymmetric models in X & Y Direction
- Fig. 5.77 Storey Vulnerability ( $VI_{\text{storey}}$ ) of asymmetric models at 1.8 m level in X & Y Direction
- Fig. 5.78 Base shear (V) in X & Y Direction for all models
- Fig. 5.79 Roof displacement (Drf) in X & Y Direction for all models
- Fig. 5.80 Global Ductility in X & Y Direction for all models
- Fig. 5.81 Global Stiffness in X & Y Direction for all models
- Fig.5.82 Building Vulnerability ( $VI_{\text{bldg}}$ ) in X & Y Direction for all models
- Fig. 5.83 Storey Vulnerability ( $VI_{\text{storey}}$ ) at 0 m level in X & Y Direction for all models
- Fig. 5.84 Storey Vulnerability ( $VI_{\text{storey}}$ ) at 1.8 m level in X & Y Direction for all models
- Fig. 5.85 Storey Vulnerability ( $VI_{\text{storey}}$ ) at 11.4 m level in X & Y Direction for all models
- Fig. A.1 Trapezoidal loading with shorter span length of slab 3 m
- Fig. A.2 Triangular loading with shorter span length of slab 3 m
- Fig. A.3 Trapezoidal loading with shorter span length of slab 4 m



Fig. A.4 Triangular loading with shorter span length of slab 4 m

Fig. B.1 Response Spectrum text file

## ABBREVIATION

---

ADRS	Acceleration Displacement Response Spectrum
B	Basic Safety
C	Collapse
COLA	City of Los Angeles
CP	Collapse Prevention
CSM	Capacity Spectrum Method
DBE	Design Basis Earthquake
PGA	Peak Ground Acceleration
IO	Immediate Occupancy
LDP	Linear Dynamic Procedure
LS	Life Safety
MCE	Maximum Credible Earthquake
MDOF	Multiple Degree of Freedom
IS	Indian Standards
NSP	Non linear Static Procedure
OMRF	Ordinary Moment Resisting Frame
RC	Reinforced Concrete
SAP	System, Applications and Products in date Processing
SDOF	Single Degree of Freedom
SMRF	Special Moment Resisting Frame
VI	Vulnerability Index

## ABSTRACT

Many urban multi storey frame buildings in India today have asymmetric plan configurations to give a different aesthetics which is highly demanding and appreciated by the clients. Although these asymmetric buildings performances are poor against seismic forces. Many of these buildings may have adequate strength to cater the gravity load. However, the overall safety of these structures essentially require satisfactory performance against seismic demand. This paper involves seismic resistance evaluation of such kind of frame buildings and a comparative study among symmetric and asymmetric building plan configurations from the seismic resistance point of view as in past few years both the occurrence and intensity of major earthquakes has been increased significantly. The structural engineering profession has been using the nonlinear static procedure (NSP) or pushover analysis as modelling for such structures requires the determination of the nonlinear properties of each component in the structure, quantified by strength and deformation capacities, which depend on the modelling assumptions.. This paper aims to carry out pushover analysis of the building based on the FEMA-356 and ATC-40 guidelines. The pushover analysis shows the pushover curves, capacity spectrum, plastic hinges and performance level of the building. This non-linear static analysis gives better understanding and more accurate seismic performance of buildings of the damage or failure element.

**Keywords:** Pushover Analysis, Vulnerability Index

## 1.1 General

**Earthquake** is a very relevant issue in recent days specially for structural engineers as it is a low probability but high consequence event causing structural damage which in turn results in loss of lives and loss of economy. Structures designed according to the existing seismic codes provide minimum safety to preserve life and in a major earthquake, they assure at least gravity-load-bearing elements of non essential facilities will still function and provide some margin of safety. However, compliance with the standard does not guarantee such performance. They typically do not address performance of non-structural components neither provide differences in performance between different structural systems. This is because it cannot accurately estimate the inelastic strength and deformation of each member due to linear elastic analysis.

The non-engineered structure, which does not follow the seismic resistance stipulations have suffered severe damages in past earthquake. However, it is unfortunate to have huge numbers of such non-engineered structured in the countries prove to high seismic risk. The typical percentages of non-engineered buildings in countries having severe seismic zones have shown in figure 1.1.

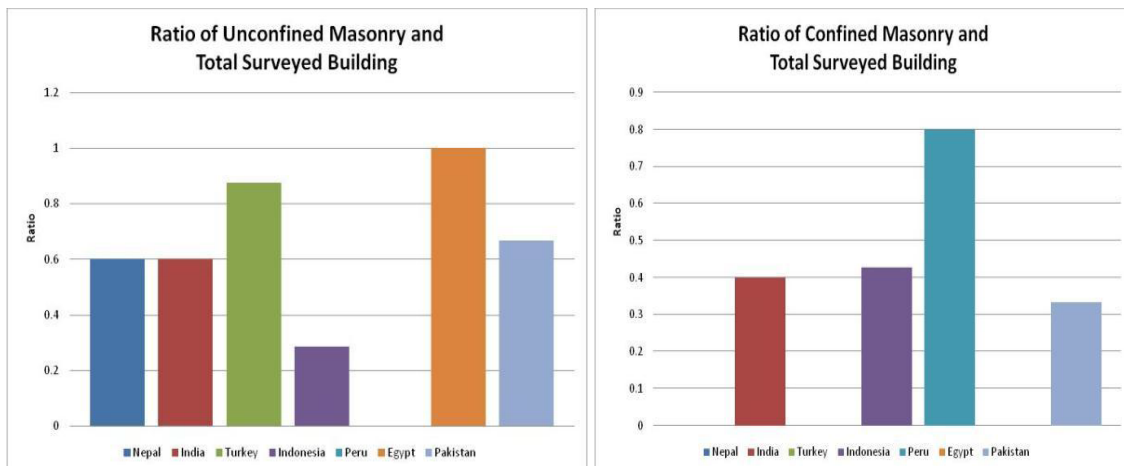


**Figure 1.1:** Ratio of Types of Structure to Total Surveyed Buildings

**Table 1-1: List of earthquakes in India after year 2000**

The Indian subcontinent has a history of earthquakes. The reason for the intensity and high frequency of earthquakes is the Indian plate driving into Asia at a rate of approximately 49 mm/year. The following is a list of **major earthquakes which have occurred in India**.

Date	Time	Location	Lat	Long	Deaths	Comments	M
January 3, 2016	23:05:16 UTC	North East India	24.8°N	93.6°E	11 dead, 200 injured in Manipur & Assam	Regional event that affected India, Myanmar, and Bangladesh.	6.7
October 26, 2015	09:09 UTC	Northern India, Pakistan, Afghanistan	36°14'45"N	71°50'38"E	280 in Pakistan, 115 in Afghanistan and 4 in India		7.7
June 28, 2015	06:35 IST	Dibrugarh, Assam	26.5°N	90.1°E	0	3 injured in Assam earthquake, tremors felt in West Bengal, Meghalaya and Bhutan	5.6
May 12, 2015	12:35 IST	Northern India, North East India	27.794°N	85.974°E	218	Epicentre 17 km S of Kodari, Nepal; Felt in Delhi, West Bengal, Bihar, U.P.; 44 killed in India	7.3

<b>Date</b>	<b>Time</b>	<b>Location</b>	<b>Lat</b>	<b>Long</b>	<b>Deaths</b>	<b>Comments</b>	<b>M</b>
April 26, 2015	12:39 IST	Northern India, North East India	27.794°N	85.974°E	Aftershock	Aftershock (Epicentre 17 km S of Kodari, Nepal)	6.7
April 25, 2015	12:19 IST	Northern India	28.193°N	84.865°E	Aftershock	Aftershock (Epicentre 49 km east of Lamjung, Nepal)	6.6
April 25, 2015	11:41 IST	Northern India, North East India	28.147°N	84.708°E	8,900+	Epicentre 34 km ESE of Lamjung, Nepal. Felt in eastern, northern, north eastern India and parts of Gujarat	7.8
March 21, 2014	18:41 IST	Andaman and Nicobar Islands	7.6°N	94.4°E	0	Moderate earthquake in Andaman Islands	6.7
April 25, 2012	08:45 IST	Andaman and Nicobar Islands	9.9°N	94.0°E	0	Big earthquake in Andaman and Nicobar Islands	6.2
March 5, 2012	13:10 IST	New Delhi	28.6°N	77.4°E	1	Moderate earthquake in national capital, CBSE Physics board exam disrupted in Delhi	5.2
September 18, 2011	18:10 IST	Gangtok, Sikkim	27.723°N	88.064°E	118	Strong earthquake in NE India, tremors felt in Delhi, Kolkata, Lucknow and Jaipur	6.9
August 10, 2009	01:21 IST	Andaman Islands	14.1°N	92.8°E	26	Tsunami Warning issued	7.7
October 8, 2005	08:50 IST	Kashmir	34.493°N	73.629°E	130,000	95 km (59 mi) NE of Islamabad, Pakistan, 125 km (78 mi) WNW of Srinagar, Kangra, Jammu and Kashmir, India (pop 894,000)	7.6

Date	Time	Location	Lat	Long	Deaths	Comments	M
December 26, 2004	09:28 IST	off west coast northern Sumatra India Sri-Lanka, Maldives	3.30°N	95.87°E	283,106	Third deadliest earthquake in the history of the world, the tsunami generated killed 15,000 people in India	9.1
January 26, 2001	08:50 IST	Gujarat	23.6°N	69.8°E	20,000	Indian Republic Day Gujarat earthquake, thousands killed	7.6/ 7.7

In April, 2015 **Nepal earthquake** (also known as the Gorkha earthquake) more than 8,000 people were dead and injured more than 19,000. It occurred at 11:56 NST on 25 April, with a magnitude of 7.8Mw or 8.1Ms and a maximum Mercalli Intensity of VIII (Severe). Its epicentre was the village of Barpak, Gorkha district, and its hypocenter was at a depth of approximately 15 km (9.3 mi). It was the worst natural disaster to strike Nepal since the 1934 Nepal-Bihar earthquake. The earthquake triggered in avalanche on Mount Everest, killing at least 19, making it the deadliest day on the mountain in history. It triggered another huge avalanche in the Langtang valley, where 250 were reported missing. Continued aftershocks occurred throughout Nepal within 15-20 minute intervals, with one shock reaching a magnitude of 6.7 on 26 April at 12:54:08 NST. The country also had a continued risk of landslides. A second major earthquake occurred on 12 May 2015 at 12:35 NST with a moment magnitude (Mw) of 7.3 Mw. The epicenter was near the Chinese border between the capital of Kathmandu and Mt. Everest. More than 125 people were killed and more than 2,500 were injured by this aftershock. Many buildings, most of them belongs to non-engineered category have suffered severe damage and even collapsed are shown in figure 1.2.



**Figure 1.2:** Severely damaged and collapsed buildings in Nepal earthquake

Repair Restoration and strengthening are very common words now-a-days. However, they have different meaning with respect to their functional objective. The purpose of repairs is to rectify the observed defects and bring the building to reasonable architectural shape so that all services start functioning. This enables the use of building for its intended purpose. Repairs do not improve structural strength or stability. In fact a repaired building may be deceptive. It may hide the structural defects. Outwardly it may appear good. It may suffer from structural weakness. Such weakness may cause collapse during future earthquakes. However, the main purpose of restoration is to structurally treat the building with an aim to restore its original strength. This intervention is undertaken for a damaged building if one is sure that the original strength provides an adequate level of safety for future earthquake disasters. Strengthening of building against earthquake loads are also quite significantly important in seismic disaster mitigation. Seismic forces are the most serious dynamic forces.

Earthquake being uncertain in terms of amplitude, duration and frequency content, proper seismic analysis and design is a major challenge for structural engineers. Moreover,



seismic loading is dynamic in nature, lateral (multi component), cyclic and induce reversal of stresses. Various analysis methods, both elastic (linear) and inelastic (nonlinear), are available for the seismic analysis of existing structures. Elastic analysis methods available include code static lateral force procedures, code dynamic lateral force procedures and elastic procedures using demand capacity ratios. The most basic inelastic analysis method is the complete nonlinear time history analysis, which at this time is considered overly complex and impractical for general use. Available simplified nonlinear analysis methods, referred to as nonlinear static analysis procedures, include the capacity spectrum method (CSM) that uses the intersection of the capacity (pushover) curve and a reduced response spectrum to estimate maximum displacement; the displacement coefficient method (e.g., FEMA-356 (ATC 1996a)) that uses pushover analysis and a modified version of the equal displacement approximation to estimate maximum displacement; and the secant method (e.g., City of Los Angeles, Division 95 (COLA 1995)) that uses a substitute structure and secant stiffnesses. Different analytical procedures for seismic analysis of structures are given below:

### **1.1.1 Analytical procedures:**

- **Elastic:** 1. Codal procedures  
2. Demand capacity ratios
- **Static non linear:** Pushover analysis, Secant method, Time history analysis

- **Dynamic non linear**

**Elastic method:** This method is a force based procedure with an assumption that every structure respond elastically to earthquakes. The demand forces on each member of the structure are obtained and compared with calculated capacities by performing an elastic analysis. Elastic analysis methods include IS code static lateral force procedure, dynamic procedure and elastic procedure using Demand capacity ratio(DCR).In IS code static lateral force procedure, a static analysis is performed by subjecting the structure to lateral forces. In IS code dynamic procedure, force demands on various structural members are determined by an elastic dynamic analysis. Dynamic analysis may be either a response spectrum

analysis or an elastic Time history analysis. Sufficient number of modes is considered to have a mass participation of at least 90% for response spectrum analysis. Any effects of higher modes is automatically included in Time history analysis. Although force based procedures are well known and easy to apply, they have certain drawbacks. Post-elastic behavior of structures could not be identified by an elastic analysis. However, post- elastic behavior should be considered as almost all structures are expected to deform in inelastic range during a strong earthquake.

**Inelastic method:** Displacement based procedures are mainly based on inelastic deformations rather than elastic forces and use non linear analysis procedures considering seismic demands and available capacities explicitly. By inelastic Analytical procedures we can understand the actual behavior of structures by identifying failure modes. Among the inelastic static analysis methods **Pushover analysis** is a simplified non linear analysis and is very popular due to its simplicity. Other non linear methods are complex and time consuming. **Pushover analysis** could be done by Capacity Spectrum method or displacement Coefficient method.

### **1.2 Objective of present work:**

To study the seismic resistance features including the seismic vulnerability based on non linear pushover analysis of different regular and irregular building configurations.

**1.3 Scope of work:** The present scope of work includes the following

- Evaluation of base shear resisting capacity, roof displacement, Spectral acceleration, Spectral displacement, Global Stiffness, Global ductility, Vulnerability index, Storey vulnerability of different buildings with symmetric plan configurations by Pushover analysis.
- Evaluation of base shear resisting capacity, roof displacement, Spectral acceleration, Spectral displacement, Global Stiffness, Global ductility, Vulnerability index, Storey vulnerability of different buildings with asymmetric plan configurations by Pushover analysis.
- Comparative study of above mentioned seismic resistant features for symmetric and asymmetric building configurations.

## LITERATURE REVIEW

---

**2.0 General** :It is important to review the research literatures on this particular field to get acquainted with the state of art prior to involve in actual research. The summary of the literature review are as follows :

**2.1 Pushover Analysis of Structure:** Non linear static analysis is used to quantify the resistance of the structure to lateral deformation and to read the mode of deformation and intensity of local demands. Various techniques have been recommended, developed, described in many literatures including the use of constant lateral force profiles and the use of adaptive pushover and multimode pushover approaches. Pushover technique provide useful information on the overall characteristics of the structural system and can be used to identify some (but not necessarily all) of the likely mechanism. Because the prescribed loading used in pushover analysis can't represent the potential range of loading experienced in dynamic response, the results obtained by pushover analysis at best represent and approximation of the non linear behaviour expected to develop in the response to earthquake ground motions. The applicability of pushover analysis is less clear for systems having discontinuities in strength and stiffness. The development of pushover analysis and various techniques have been studied in various literatures are described below briefly:

**Vojko Kilar and Peter Fajfar (September ,1996):** Discussed a simple method for the nonlinear static analysis of complex building structures subjected to monotonically increasing horizontal loading (push-over analysis) is presented. The

method is designed to be a part of new methodologies for the seismic design and evaluation of structures. It is based on the extension of a pseudo three-dimensional mathematical model of a building structure into the nonlinear range. The structure consists of planar macro elements. For each planar macro element, a simple bilinear or multilinear base shear - top displacement relationship is assumed. By a step-by-step analysis an approximate relationship between the global base shear and top displacement is computed. During the analysis the development of plastic hinges throughout the building can be monitored. The method has been implemented into a prototype computer program. In the paper the mathematical model, the base shear – top displacement relationships for different types of macro elements, and the step-by-step computational procedure are described. The method has been applied for the analysis of a symmetric and an asymmetric variant of a seven-story reinforced concrete frame-wall building, as well as for the analysis of a complex asymmetric 21-story reinforced concrete wall building. The influence of torsion on structural behaviour is discussed.

**Joseph M. Bracci et al. (January ,1997):**In this paper a procedure for evaluating the seismic performance and retrofit of existing low-to-midrise reinforced concrete (RC) buildings is proposed. The procedure is derived from the well-known capacity spectrum method and is intended to provide practicing engineers with a methodology for estimating the margin of safety against structural failure. A series of seismic story demand curves is established from modal superposition analyses wherein changes in the dynamic characteristics of the structure at various response phases ranging from elastic to full failure mechanism are considered. These demands are compared to the lateral story capacities as determined from an independent inelastic pushover analysis. The distribution of lateral forces used in the progressive pushover analysis is based on stiffness dependent incremental story shear demands and forms a critical aspect of the methodology. The proposed technique is applied to a one-third scale model, three-story reinforced concrete frame building that was subjected to repeated shaking table excitations, and that was later retrofitted and tested again at the same intensities. This study indicates

that the procedure can provide reliable estimates of story demands versus capacities for use in seismic performance and retrofit evaluation of structures.

**Eduardo Miranda(1999, April):** Studied Both structural and non structural damage sustained during earthquake ground motions produced primarily by lateral displacements. Thus, adequate damage control can be achieved if lateral deformations are controlled by providing enough lateral stiffness, lateral strength, and energy dissipation capacity to a structure. However, current building codes are based on lateral forces and give a secondary importance to lateral displacements. Furthermore, maximum lateral displacements are typically checked near the end of the design process for serviceability limits, by comparing the computed displacements to an allowable upper limit on the maximum inter story drift. Lateral displacements are typically computed as the displacements computed with a linear elastic analysis of the structure when subjected to code-specified (reduced) lateral forces multiplied by a displacement amplification factor that is intended to account for the inelastic deformation expected in the structure during severe earthquake ground motions. This approach has been criticized for being inconsistent, for underestimating displacement demands, and for often relying on startlingly different relationships between elastic and inelastic displacements. The objectives of this paper are (1) to present an approximate method to estimate lateral displacements and maximum inter story drifts in multi story buildings subjected to earthquake ground motions; and (2) to compare the results of the proposed method with those computed with detailed step-by-step time history analyses. The approximate method is intended to be used during the preliminary design of new buildings and for a rapid evaluation of existing buildings and is not intended to be a substitute of more detailed analyses, which are appropriate during the final evaluation of the proposed design of a new building or during the detailed evaluation of existing buildings.

**A. S. Elnashai AND A. M. Mwafy( 2002):**This paper addresses the issue of horizontal over strength in modern code-designed reinforced-concrete (RC) buildings. The relationship between the lateral capacity, the design force reduction factor, the ductility level and the over strength factor are investigated. The lateral capacity and the over strength factor are estimated by means of inelastic static pushover as well as time-history collapse analysis for 12 buildings of various characteristics representing a wide range of contemporary RC buildings. The importance of employing the elongated periods of structures to obtain the design forces is emphasized. Predicting this period from free vibration analysis by employing 'effective' flexural stiffnesses is investigated. A direct relationship between the force reduction factor used in design and the lateral capacity of structures is confirmed in this study. Moreover, conservative over strength of medium and low period RC buildings designed according to Euro code 8 is proposed. Finally, the implication of the force reduction factor on the commonly utilized over strength definition is highlighted. Advantages of using an additional measure of response alongside the over strength factor are emphasized. This is the ratio between the over strength factor and the force reduction factor and is termed the inherent over strength ( $\_i$ ). The suggested measure provides more meaningful results of reserve strength and structural response than over strength and force reduction factors.

**Rahul Rana et al. (August ,2004):** In this study pushover analysis was performed on a nineteen story, slender concrete tower building located in San Francisco with a gross area of 430,000 square feet. Lateral system of the building consists of concrete shear walls. The building is newly designed conforming to 1997 Uniform Building Code, and pushover analysis was performed to verify code's underlying intent of Life Safety performance under design earthquake. Procedure followed for carrying out the analysis and results are presented in this paper.

**X.-K. Zou, C.-M. Chan(May ,2005):** Studied on Performance-based design using nonlinear pushover analysis, which generally involves tedious and intensive computational effort and is a highly iterative process needed to meet designer-specified and code requirements. This paper presents an effective computer-based technique that incorporates pushover analysis together with numerical optimization procedures to automate the pushover drift performance design of reinforced concrete (RC) buildings. Steel reinforcement, as compared with concrete materials, appears to be the more cost-effective material, that can be effectively used to control drift beyond the occurrence of first yielding and to provide the required ductility of RC building frameworks. In this study, steel reinforcement ratios are taken as design variables during the design optimization process. Using the principle of virtual work, the nonlinear inelastic seismic drift responses generated by the pushover analysis can be explicitly expressed in terms of element design variables. An optimality criteria technique is presented in this paper for solving the explicit performance-based seismic design optimization problem for RC buildings. Two building frame examples are presented to illustrate the effectiveness and practicality of the proposed optimal design method.

**Mehmet Inel (March,2006):** Ascertained due to its simplicity, the structural engineering profession has been using the nonlinear static procedure (NSP) or pushover analysis. Modelling for such analysis requires the determination of the nonlinear properties of each component in the structure, quantified by strength and deformation capacities, which depend on the modelling assumptions. Pushover analysis is carried out for either user-defined nonlinear hinge properties or default-hinge properties, available in some programs based on the FEMA-356 and ATC-40 guidelines. While such documents provide the hinge properties for several ranges of detailing, programs may implement averaged values. The user needs to be careful; the misuse of default-hinge properties may lead to unreasonable displacement capacities for existing structures. This paper studies the possible differences in the results of pushover analysis due to default and user-defined nonlinear component properties. Four- and seven-story buildings are considered to



represent low- and medium- rise buildings for this study. Plastic hinge length and transverse reinforcement spacing are assumed to be effective parameters in the user-defined hinge properties. Observations show that plastic hinge length and transverse reinforcement spacing have no influence on the base shear capacity, while these parameters have considerable effects on the displacement capacity of the frames. Comparisons point out that an increase in the amount of transverse reinforcement improves the displacement capacity. Although the capacity curve for the default-hinge model is reasonable for modern code compliant buildings, it may not be suitable for others. Considering that most existing buildings in Turkey and in some other countries do not conform to requirements of modern code detailing, the use of default hinges needs special care. The observations clearly show that the user-defined hinge model is better than the default-hinge model in reflecting nonlinear behaviour compatible with the element properties.

**Curt B. Haselton (December ,2006):** This study finds that that aspects of the structural design (height, framing layout, etc.) have less impact on the final performance prediction than the aspects of the collapse assessment methodology (structural modelling uncertainties, and spectral shape). This emphasizes the importance of developing a systematic codified assessment method that can be used to demonstrate the performance of a structural system. Without a codified assessment method, a collapse performance prediction will depend almost entirely on how the analyst carried out the performance assessment.

**Carlos Augusto Fernandes Bhatt (2007):** Seen Catastrophes occurring due to strong earthquakes, throughout the several regions of the planet revealed the deficiencies of many constructions concerning its seismic resistance. In this study, design/building problems were addressed, pointing out the best solutions to reduce the buildings seismic vulnerability. Nowadays, seismic design of buildings in design offices is performed in the majority of the cases using linear dynamic analysis affecting the results obtained by a behaviour coefficient. In spite of the celerity of this process meet the extremely rigid project time demands which must

be accomplished in this area of business, it is important to develop and improve methods that can better describe, for the particular situations, the real seismic behaviour of the structures. When the structure is submitted to a seismic action with enough intensity to cause significant damage, it stops working in a linear regime, being therefore essential the proper description of the nonlinear behaviour. In this work, besides the linear dynamic analysis, the nonlinear dynamic analysis and nonlinear static Pushover analysis were presented and applied to two reinforced concrete buildings. These later analyses allowed assessing and describing, in a more rigorous way than the linear analysis, the structures nonlinear behaviour when submitted to a seismic action.

**A. Kadid and A. Boumrkik (2008):** Discussed about the Boumerdes 2003 earthquake which has devastated a large part of the north of Algeria has raised questions about the adequacy of framed structures to resist strong motions, since many buildings suffered great damage or collapsed. To evaluate the performance of framed buildings under future expected earthquakes, a non linear static pushover analysis has been conducted. To achieve this objective, three framed buildings with 5, 8 and 12 stories respectively were analyzed. The results obtained from this study show that properly designed frames will perform well under seismic loads.

**Mehmed Causevic ,Sasa Mitrovic (July ,2010):** According to their study several procedures for non-linear static and dynamic analysis of structures have been developed in recent years. This paper discusses those procedures that have been implemented into the latest European and US seismic provisions: non-linear dynamic time-history analysis; N2 non-linear static method (Euro code 8); non-linear static procedure NSP (FEMA 356) and improved capacity spectrum method CSM (FEMA 440). The presented methods differ in respect to accuracy, simplicity, transparency and clarity of theoretical background. Non-linear static procedures were developed with the aim of overcoming the insufficiency and limitations of linear methods, whilst at the same time maintaining a relatively

simple application. All procedures incorporate performance-based concepts paying more attention to damage control. Application of the presented procedures is illustrated by means of an example of an eight-storey reinforced concrete frame building. The results obtained by non-linear dynamic time-history analysis and non-linear static procedures are compared. It is concluded that these non-linear static procedures are sustainable for application. Additionally, this paper discusses a recommendation in the Euro code 8/1 that the capacity curve should be determined by pushover analysis for values of the control displacement ranging between zero and 150% of the target displacement. Maximum top displacement of the analyzed structure obtained by using dynamic method with real time-history records corresponds to 145% of the target displacement obtained using the non-linear static N2 procedure.

**M. K. Rahman et al. (2012):** According to their version the Western region of Saudi Arabia lies in a moderate seismic zone and seismic events of magnitude 5.7 were recorded in 2009 in areas near the holy city of Madinah. A historical event involving ground cracking and fissuring with volcanic activity took place in the year 1256. The recent seismic events have led to concerns on safety and vulnerability of RC buildings, which were designed only for gravity loads in the past devoid of any ductile detailing of joints. This paper presents a 3D nonlinear static analysis for seismic performance evaluation of an existing eight-story reinforced concrete frame-shear wall building in Madinah. The building has a dome, reinforced concrete frame, elevator shafts and ribbed and flat slab systems at different floor levels. The seismic displacement response of the RC frame-shear wall building is obtained using the 3D pushover analysis. The 3D static pushover analysis was carried out using SAP2000 incorporating inelastic material behavior for concrete and steel. Moment curvature and P-M interactions of frame members were obtained by cross sectional fiber analysis using XTRACT. The shear wall was modeled using mid-pier approach. The damage modes includes a sequence of yielding and failure of members and structural levels were obtained for the target

displacement expected under design earthquake and retrofitting strategies to strengthen the building were evaluated.

**Aswin Prabhu T (2013):** A 50-year old four story (8-bay and 3-frame) reinforced concrete structure has been considered in this study, which lies in Zone II, according to IS 1893:2000 classification of seismic zones in India. Masonry in fills have been considered as non-structural members during this entire study. The structure has been evaluated using Pushover Analysis, a non-linear static procedure, which may be considered as a series of static analysis carried out to develop a pushover curve for the building. The structure is simulated in SeismoStruct Version 5.2.2 after being designed in STAAD.Pro v8i by considering M15 concrete and Fe250 steel reinforcement. The pushover curve is generated by pushing the top node of structure to the limiting displacement and setting appropriate performance criteria. The target displacement for the structure is derived by bi linearization of the obtained pushover curve and subsequent use of Displacement Coefficient Method according to ASCE 41-06.

**A. E. Hassaballaet al. (2014):** In this paper a four-story residential existing reinforced concrete building in the city of Khartoum-Sudan, subjected to seismic hazard ,was analyzed. Plastic hinge is used to represent the failure mode in the beams and columns when the member yields. The pushover analysis was performed on the building using SAP2000 software (Ver.14) and equivalent static method according to UBC 97. The principles of Performance Based Seismic Engineering are used to govern the analysis, where inelastic structural analysis is combined with the seismic hazard to calculate expected seismic performance of a structure. Base shear versus tip displacement curve of the structure, called pushover curve, is an essential outcomes of pushover analysis. The pushover analysis is carried out in both positive and negative x and y directions. Default hinge properties, available in some programs based on the FEMA -356 and Applied Technology Council (ATC-40) guidelines are used for each member. One

case study has been chosen for this purpose. The evaluation has proved that the four-story residential building is not seismically safe.

**Akshay V. Raut, Prof. RVRK Prasad (July ,2014):** According to them many urban multi storey buildings in India today have open first storey as an unavoidable feature. This is primarily being adopted to accommodate parking or reception lobbies in the first storey. This paper highlights the importance of explicitly recognizing the presence of the open first storey in the analysis of the building and also for immediate measures to prevent the indiscriminate use of soft first storeys in buildings. Alternate measures, involving stiffness balance of the open first storey and the storey above, are proposed to reduce the irregularity introduced by the open first storey. The structural engineering profession has been using the nonlinear static procedure (NSP) or pushover analysis. Modeling for such analysis requires the determination of the nonlinear properties of each component in the structure, quantified by strength and deformation capacities, which depend on the modeling assumptions. Pushover analysis is carried out for either user-defined nonlinear hinge properties or default-hinge properties, available in some programs based on the FEMA-356 and ATC-40 guidelines. This paper aims to evaluate the zone –II selected reinforced concrete building to conduct the non-linear static analysis (Pushover Analysis). The pushover analysis shows the pushover curves, capacity spectrum, plastic hinges and performance level of the building. This non-linear static analysis gives better understanding and more accurate seismic performance of buildings of the damage or failure element.

## 2.1 Critical view on literatures:

- The seven-story building, have clearly demonstrated the unfavourable influence of torsion in asymmetric structures. The results indicate that, in general, larger displacements and larger ductilities are required in an asymmetric structure in order to develop the same strength as in the symmetric structure, especially at the flexible and/or weak side of the building. If a torsional plastic mechanism is formed the available strength of some macro elements can not be fully exploited. Torsional rotations and the formation of a torsional mechanism strongly depend on the structural elements which resist loads in the direction perpendicular to the direction of the applied loading.
- From the standpoint of evaluating the adequacy of the retrofit behavior, it can be observed that the story demands intersect the capacity envelopes with sufficient strength and displacement reserves. Although inelastic response is evident during these base motions, collapse of the retrofitted structure is not imminent for these levels of ground motion excitation.
- The effect of the number of stories, of the lateral loading pattern, and of the ratio of overall flexural and shear deformations on the ratio of spectral displacement and maximum roof displacement was studied. It was concluded that the difference between the spectral displacement and the maximum roof displacement increases with the number of stories. Furthermore, for a given number of stories, the difference between spectral displacement and maximum roof displacement increases as overall flexural deformations increase with respect to shear deformations. The lateral loading pattern has a very small effect on the ratio of spectral displacement to the maximum roof displacement. For buildings where overall shear deformations dominate over flexural deformations, the ratio of the maximum IDR to the roof drift ratio is significantly larger than for buildings where overall shear deformations are

negligible with respect to overall flexural deformations, which means that MRF buildings are likely to have larger concentrations of inter story drifts than flexible-type buildings (shear wall buildings). The effect of the lateral loading pattern on the concentration of inter story drifts is more pronounced for shear-type buildings than for flexural-type buildings.

- Over strength during earthquakes should be higher than the values obtained from inelastic static analyses using the code lateral load distribution. The triangular load is conservative in predicting the ultimate capacity. Also, contributions of nonstructural elements should produce higher capacity and hence higher over strength. If over strength is not accurately evaluated by means of inelastic analysis, a lower bound may be utilized. A conservative over strength factor of 2.0 is suggested for medium period RC buildings designed and detailed to EC8 (in principle, this applies to other modern codes). This limit can be applied to low-rise buildings since they usually possess higher over strength than do medium-rise buildings.
- Rigid end offsets significantly influence model behavior and force distribution between elements. In shear wall buildings where pushover model uses frame elements to model shear walls, the clear span of spandrels and any slender columns formed due to wall openings is usually much smaller than the center to-center span. These elements should be modeled with rigid end offsets and nonlinear hinges should be assigned outside of the offset.
- Steel reinforcement plays a significant role in controlling the lateral drift beyond first yielding and in providing ductility to an RC building framework. Using the principle of virtual work and the Taylor series approximation, the inelastic performance based seismic design problem has been explicitly expressed in terms of the steel reinforcement design variables. Axial moment

hinges and moment hinges should be considered in the nonlinear pushover analysis of a frame structure so that the behavior of columns and beams can be effectively modeled. It is important that uplifting tension induced by seismic loading should be prevented in an RC building as the net tension in columns tends to weaken the lateral resistance of such a structure and to result in a less economical design.

- The base shear capacity of models with the default hinges and with the user-defined hinges for different plastic hinge length and transverse reinforcement spacing are similar; the variation in the base shear capacity is less than 5%. Thus, the base shear capacity does not depend on whether the default or user-defined hinge properties are used. Plastic hinge length ( $L_p$ ) has considerable effects on the displacement capacity of the frames. Comparisons show that there is a variation of about 30% in displacement capacities due to  $L_p$ . Displacement capacity depends on the amount of transverse reinforcement at the potential hinge regions. Comparisons clearly point out that an increase in the amount of transverse reinforcement improves the displacement capacity. The improvement is more effective for smaller spacing. For example, reducing the spacing from 200 mm to 100 mm provides an increase of up to 40% in the displacement capacity, while reducing the spacing from 200 mm to 150 mm provides an increase of only 12% for the 4-story frame.
- The modeling uncertainty work in Chapter 5 was based on analyses of a single four-story RC SMF building. While we used this estimate of uncertainty for all buildings assessed in this study, further work could be done to generalize the uncertainty calculations. We found that structural modeling uncertainties have significant impacts on predicted collapse risk. Therefore, significant future research is warranted to more fully understand the impacts that these uncertainties have in collapse assessment. This study only addressed uncertainties in structural design and modeling. We did not fully consider



many other important uncertainties, such as construction uncertainty, human error, etc. Future research is warranted to better understand the impact of not accounting for such uncertainties in the collapse assessment process.

- The inter storey drifts decreased in height for all the analyses and for the two directions. This is a characteristic of framed structures; The inter storey drifts were higher in the X direction than in the Y direction, because the structure, as previously mentioned, is more stiff according to Y; Along the X direction, the inter storey drift value between the floor 0 and floor 1 was higher for the pushover analysis than for the nonlinear dynamic analysis. In the later case the value obtained with the artificial accelerograms was closer to the pushover analysis result than the one obtained with the semi-artificial accelerograms. For the remaining inter storey drifts in this direction, between the floor 1 and floor 2 and between the floor 2 and floor 3, the values obtained were higher for the nonlinear dynamic analysis than for the Pushover analysis and, within the nonlinear dynamic analysis, higher to the ones corresponding to semi-artificial accelerograms; According to Y, the inter storey drifts values are higher to the nonlinear dynamic analysis with semi artificial accelerograms, followed by the Pushover analysis and finally by the nonlinear dynamic analysis with artificial accelerograms.
- The causes of failure of reinforced concrete during the Boumerdes earthquake may be attributed to the quality of the materials of the used and also to the fact that most of buildings constructed in Algeria are of strong beam and weak column type and not to the intrinsic behaviour of framed structures. The results obtained in terms of demand, capacity and plastic hinges gave an insight into the real behaviour of structures.

**3.1 General:** Present study tries to explore the applicability of non linear static procedure (NSP) developed for assessment of existing building structures. The entire study is hinged on static pushover analysis.

### **3.2 Pushover analysis:**

**Pushover analysis**, a widely used method for **seismic performance evaluation** of a structure, is a **static nonlinear procedure** in which the magnitude of the lateral loading is **incrementally increased** in accordance with a certain predefined pattern along the height of the building. With an increase in magnitude of loads weak links and failure modes of the building can be observed. Pushover analysis can determine the behaviour of the building including the ultimate load and maximum inelastic deformation. The structure is pushed until a collapse mechanism develops. Local non linear effects are modelled in the pushover analysis. The roof displacement against increased base shear may be plotted to generate the pushover curve gives an idea about the maximum base shear the structure is capable of resisting. The NSP is generally a more reliable approach to characterizing the performance of a structure than are linear procedures. However, it is not exact, and cannot accurately account for changes in dynamic response as the structure degrades in stiffness or account for higher mode effects. When the NSP is utilized on a structure that has significant higher mode response, the LDP is also employed to verify the adequacy of the design. When this approach is taken, less restrictive criteria are permitted for the LDP, recognizing the significantly improved knowledge that is obtained by performing both analysis procedures. Although an elastic analysis gives a good indication of the elastic capacity of structures and indicates where first yielding will occur, it cannot predict failure mechanisms and account for redistribution of forces

during progressive yielding. Inelastic analysis procedures help demonstrate how buildings really work by identifying modes of failure and the potential for progressive collapse. The use of inelastic procedures for design and evaluation is an attempt to help engineers better understand how structures will behave when subjected to major earthquakes, where it is assumed that the elastic capacity of the structure will be exceeded. This resolves some of the uncertainties associated with code and elastic procedures. Thus the **static pushover analysis** is becoming a popular tool for seismic performance evaluation of existing and new structures. The expectation is that the pushover analysis will provide adequate information on seismic demands imposed by the design ground motion on which the structural system and its component. The aim of basic safety objective is to have a low risk of life threatening injury during a moderate earthquake (DBE) and to check the collapse of vertical load resisting system during severe earthquake(MCE).As per IS-1893(2002),the DBE is assumed to be fifty percent that of MCE but not rationally defined based on probabilistic approach. The collapse prevention level under MCE can be selected which is only one performance level and though this does not meet the damage control requirement for frequent earthquake, by pushover analysis the consequences under MCE can be predicted. The reserve strength of building, non linear behaviour and the amount it can be pushed until collapse are under the focus of this study.

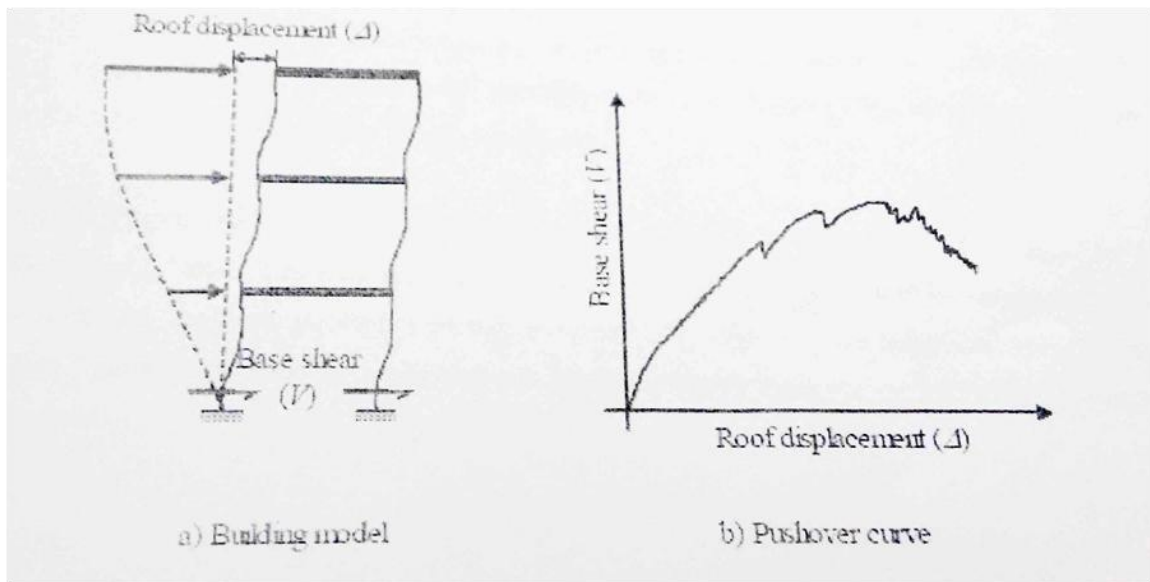


Fig 3.1.1 : Building model and Pushover curve

### 3.2.1 Evaluation result:

Pushover analysis may provide

- a) Pushover curve
  - b) Demand and capacity spectrum and their tabulated values
- 
- a) **Pushover curve:** It will provide base shear capacity and inelastic roof displacement. Global ductility of the structure can be calculated as the ratio of roof displacement at ultimate base shear to roof displacement at the onset of yielding.
  - b) **Capacity spectrum:** If the base acceleration is plotted with respect to the roof displacement, it is termed as capacity spectrum. The spectral acceleration and the spectral displacement, as calculated from linear elastic response spectrum for a certain damping value is plotted as acceleration- displacement-response spectrum. With the increase of nonlinear deformation of the components, the equivalent damping and the time period increases. The spectral acceleration and displacement values can be modified by multiplying factor as per IS-1893(2002).
  - c) **Demand spectrum:** The instantaneous spectral acceleration and displacement point, which is called demand point, shifts to a different response spectrum for higher damping. The locus of the demand point in the ADRS plot is referred to as demand spectrum which corresponds to the inelastic deformation of the building.
  - d) **Performance point:** It is a point where the capacity curve crosses the demand curve. If the performance point exists and the damage state at this point is acceptable, the structure is assumed to satisfy the target performance level. If the capacity spectrum is always less than demand spectrum performance point could not be reached, the structure fails to achieve target performance level (CP

performance level). Again if the performance level is achieved at a substantially greater roof drift than the typical specified value of the selected performance level then the performance of the structure seems to be unsatisfactory.

Pushover analysis will also provide the deflected shape, formation of hinges with increasing load and the performance levels of the hinges at the performance point. The deflected shape and the concentration of hinges in a storey can reveal soft storey mechanism. The inelastic drift profile can be plotted from the displacement values of the centre of mass of the storey, which can also reveal soft storey mechanism. The no of hinges formed in the beams and the columns at the performance point or at the point of termination of performance point of pushover analysis can be used to study the vulnerability of the structure. The Pushover analysis is approximate in nature and based on statically applied load. It estimates an envelope curve of the behavior under dynamic loading and must be interpreted with caution to understand the actual behavior under seismic loading.

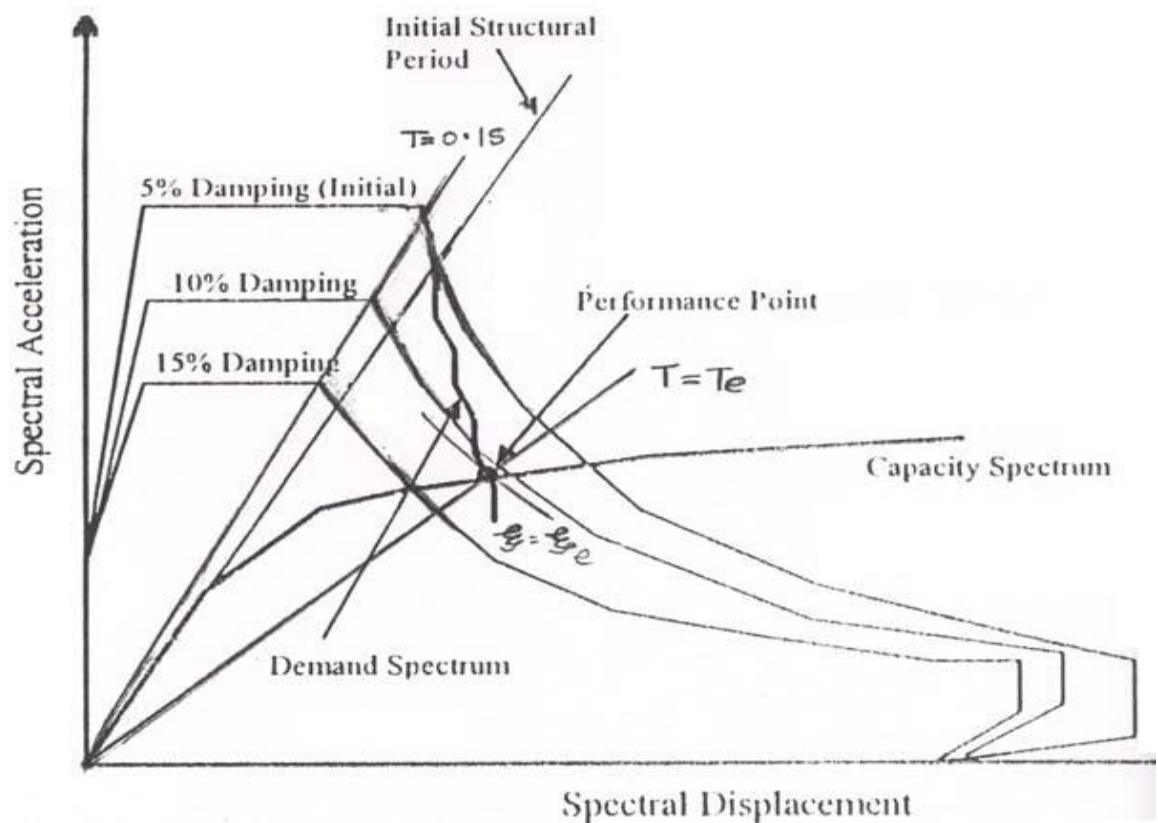


Fig 3.1.2 : Demand and capacity spectra

### **3.3 Pushover Analysis using FEMA 356 CM:**

#### **3.3.1 Basis of the procedure:**

For seismic analysis of the building by Nonlinear Static Procedure (NSP), a mathematical model directly incorporating the nonlinear load-deformation characteristics of individual components and elements of the building shall be subjected to monotonically increasing lateral loads representing inertia forces in an earthquake until a target displacement is exceeded.

#### **3.3.2 Modelling and Analysis Considerations:**

The selection of a control node, the selection of lateral load patterns, the determination of the fundamental period, and analysis procedures shall comply with the requirements of this section. The relation between base shear force and lateral displacement of the control node shall be established for control node displacements ranging between zero and 150% of the target displacement,  $\delta_t$ .

The component gravity loads shall be included in the mathematical model for combination with lateral loads as specified in this document. The lateral loads shall be applied in both the positive and negative directions, and the maximum seismic effects shall be used for design. The analysis model shall be discretized to represent the load-deformation response of each component along its length to identify locations of inelastic action. All primary and secondary lateral-force-resisting elements shall be included in the model. The force-displacement behaviour of all components shall be explicitly included in the model using full backbone curves that include strength degradation and residual strength, if any.

Alternatively, the use of a simplified NSP analysis shall be permitted. In a simplified NSP analysis only primary lateral force resisting elements are modelled, the force displacement characteristics of such elements are bilinear, and the degrading portion of the backbone curve is not explicitly modelled. The simplified NSP analysis shall only be used in conjunction with the acceptance criteria described in this

document. Elements not meeting the acceptance criteria for primary components shall be designated as secondary, and removed from the mathematical model.

### 3.3.2.1 Control Node Displacement:

The control node shall be located at the centre of mass at the roof of a building. For buildings with a penthouse, the floor of the penthouse shall be regarded as the level of the control node. The displacement of the control node in the mathematical model shall be calculated for the specified lateral loads.

### 3.3.2.2 Lateral Load Distribution:

Lateral loads shall be applied to the mathematical model in proportion to the distribution of inertia forces in the plane of each floor diaphragm. For all analyses, at least two vertical distributions of lateral load shall be applied. One pattern shall be selected from each of the following two groups:

1. A modal pattern selected from one of the following:

- A vertical distribution proportional to the values of  $C_{vx}$  given in Equation below. Use of this distribution shall be permitted only when more than 75% of the total mass participates in the fundamental mode in the direction under consideration, and the uniform distribution is also used.

$$F_x = C_{vx} \cdot V$$
$$C_{vx} = \frac{W_x h_x^k}{\sum_1^n w_i h_i^k}$$

Where:  $C_{vx}$  = Vertical distribution factor

$$k = 2.0 \text{ for } T \geq 2.5 \text{ seconds}$$
$$= 1.0 \text{ for } T \leq 0.5 \text{ seconds}$$

$$V = \text{Pseudo lateral load} = C_1 C_2 C_3 C_m S_a W$$

$C_1$  = Modification factor to relate expected maximum inelastic displacements to displacements calculated for linear elastic response.

$C_2$  = Modification factor to represent the effects of pinched hysteresis shape, stiffness,

degradation, and strength deterioration on maximum displacement response. For linear procedures *C2* shall be taken as 1.0.

$C_3$  = Modification factor to represent increased displacements due to dynamic P- $\Delta$  effects.

$C_m$  = Effective mass factor to account for higher mode mass participation effects.

$S_a$  = Response spectrum acceleration

$W$  = Effective seismic weight of the building

$w_i$  = Portion of the total building weight  $W$  located on or assigned to floor level  $i$

$w_x$  = Portion of the total building weight  $W$  located on or assigned to floor level  $x$

$h_i$  = Height (in ft) from the base to floor level  $i$

$h_x$  = Height (in ft) from the base to floor level  $x$

- A vertical distribution proportional to the shape of the fundamental mode in the direction under consideration. Use of this distribution shall be permitted only when more than 75% of the total mass participates in this mode.
- A vertical distribution proportional to the story shear distribution calculated by combining modal responses from a response spectrum analysis of the building, including sufficient modes to capture at least 90% of the total building mass, and using the appropriate ground motion spectrum. This distribution shall be used when the period of the fundamental mode exceeds 1.0 second.

2. A second pattern selected from one of the following:

- A uniform distribution consisting of lateral forces at each level proportional to the total mass at each level.



- An adaptive load distribution that changes as the structure is displaced. The adaptive load distribution shall be modified from the original load distribution using a procedure that considers the properties of the yielded.

### 3.3.2.3 Idealized Force-Displacement Curve:

The nonlinear force-displacement relationship between base shear and displacement of the control node shall be replaced with an idealized relationship to calculate the effective lateral stiffness,  $K_e$ , and effective yield strength,  $V_y$ , of the building as shown in Figure 3-1. This relationship shall be bilinear, with initial slope  $K_e$  and post-yield slope  $\alpha$ . Line segments on the idealized force-displacement curve shall be located using an iterative graphical procedure that approximately balances the area above and below the curve. The effective lateral stiffness, shall be taken as the secant stiffness calculated at a base shear force equal to 60% of the effective yield strength of the structure. The post-yield slope,  $\alpha$ , shall be determined by a line segment that passes through the actual curve at the calculated target displacement. The effective yield strength shall not be taken as greater than the maximum base shear force at any point along the actual curve.

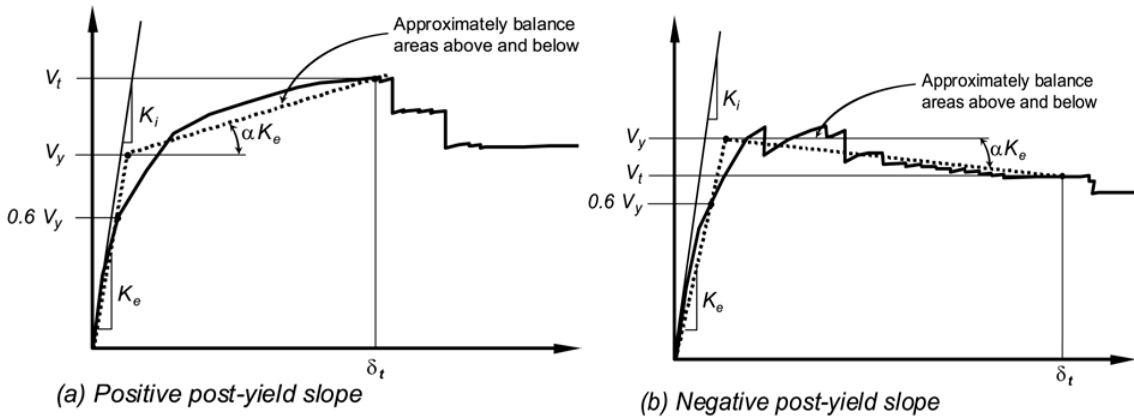


**Fig 3.2: Idealized Force-Displacement Curves**

### 3.3.2.4 Period Determination

The effective fundamental period in the direction under consideration shall be based on the idealized force displacement curve. The effective fundamental period, shall be calculated by the following equation:

$$T_e = T_i \sqrt{\frac{K_i}{K_e}}$$

Where,

$T_i$  = Elastic fundamental period (in seconds) in the direction under consideration calculated by elastic dynamic analysis

$K_i$  = Elastic lateral stiffness of the building in the direction under consideration

$K_e$  = Effective lateral stiffness of the building in the direction under consideration

### 3.3.3 Determination of Forces and Deformations:

For buildings with rigid diaphragms at each floor level, the target displacement,  $\delta_t$ , shall be calculated in accordance with Equation for target displacement given below or by an approved procedure that accounts for the nonlinear response of the building.

### 3.3.3.1 Target Displacement

The target displacement,  $\delta_t$ , at each floor level shall be calculated from the Equation below:

$$\delta_t = C_0 C_1 C_2 C_3 S_a \frac{T_e^2}{4\pi^2} g$$

Where,

$C_0$  = Modification factor to relate spectral displacement of an equivalent SDOF system to the roof displacement of the building MDOF system calculated using one of the following procedures:

$C_1$  = Modification factor to relate expected maximum inelastic displacements to displacements calculated for linear elastic response:

$$=1.0 \quad \text{for } T_e \geq T_s$$

$$=[1.0+(R-1)T_s/T_e]/R \quad \text{for } T_e < T_s$$

$T_e$  = Effective fundamental period of the building in the direction under consideration, sec.

$T_s$  = Characteristic period of the response spectrum, defined as the period associated with the transition from the constant acceleration segment of the spectrum to the constant velocity segment of the spectrum

$R$  = Ratio of elastic strength demand to calculated yield strength coefficient calculated by,

$$R = \frac{S_a}{V_y/W} \times C_m$$

$S_a$  = Response spectrum acceleration, at the effective fundamental period and damping ratio of the building in the direction under consideration

$V_y$  = Yield strength calculated using results of the NSP for the idealized nonlinear force displacement curve developed for the building

$W$  = Effective seismic weight of the structure

$C_m$  = Effective mass factor from Table 3-1. Alternatively,  $C_m$  taken as the effective model mass calculated for the fundamental mode using an Eigen value analysis.

$C_2$  = Modification factor to represent the effect of pinched hysteretic shape, stiffness degradation and strength deterioration on maximum displacement response. Values of for different framing systems and Structural Performance Levels shall be obtained from Table 3-3. Alternatively, use of  $C_2 = 1.0$  shall be permitted for nonlinear procedures.

$C_3$  = Modification factor to represent increased displacements due to dynamic P- $\Delta$  effects. For buildings with positive post-yield stiffness, shall be set equal to 1.0. For buildings with negative post-yield stiffness, values of shall be calculated using Equation (3-17) but not to exceed the values set forth in

$$C_3 = 1.0 + \frac{\alpha (R - 1)^{1.5}}{T_e}$$

$\alpha$  = Ratio of post-yield stiffness to effective elastic stiffness, where the nonlinear force displacement relation shall be characterized by a bilinear relation shown in fig 3-1

$g$  = acceleration of gravity

	Shear Buildings <sup>2</sup>		Other Buildings
Number of Stories	Triangular Load Pattern (1.1, 1.2, 1.3)	Uniform Load Pattern (2.1)	Any Load Pattern
1	1.0	1.0	1.0
2	1.2	1.15	1.2
3	1.2	1.2	1.3
5	1.3	1.2	1.4
10 <sup>+</sup>	1.3	1.2	1.5

1. Linear interpolation shall be used to calculate intermediate values.

2. Buildings in which, for all stories, inter story drift decreases with increasing height.

Structural Performance Level	$T \leq 0.1$ second <sup>3</sup>		$T \geq Ts$ seconds	
	Framing Type 1 <sup>1</sup>	Framing Type 2 <sup>2</sup>	Framing Type 1 <sup>1</sup>	Framing Type 2 <sup>2</sup>
Immediate Occupancy	1.0	1.0	1.0	1.0
Life Safety	1.3	1.0	1.1	1.0
Collapse Prevention	1.5	1.0	1.2	1.0

1. Structures in which more than 30% of the story shear at any level is resisted by any combination of the following components, elements, or frames:  
Ordinary moment-resisting frames, concentrically-braced frames, frames with partially-restrained connections, tension-only braces, unreinforced masonry walls, shear-critical, piers, and spandrels of reinforced concrete or masonry.

2. All frames not assigned to Framing Type 1.

3. Linear interpolation shall be used for intermediate values of  $T$ .

### **3.3.4 Acceptance Criteria:**

Components and elements analyzed using the nonlinear procedures shall satisfy the following requirements. Prior to selecting component acceptance criteria, components shall be classified as primary or secondary, and actions shall be classified as deformation-controlled or force-controlled.

#### **Deformation-Controlled Actions for the Simplified Nonlinear Static Analysis**

Primary and secondary components modelled using the alternative simplified NSP analysis shall meet the requirements of this section. Expected deformation capacities shall not be less than maximum deformation demands calculated at the target displacement. Primary component demands shall be within the acceptance criteria for primary components at the selected Structural Performance Level. Demands on other components shall be within the acceptance criteria for secondary components at the selected Structural Performance Level.

#### **Force-Controlled Actions**

Primary and secondary components shall have lower bound strengths not less than the maximum design forces. Lower-bound strengths shall be determined considering all coexisting forces and deformations.

### **3.4 Pushover Analysis using ATC 40 CSM:**

#### **3.4.1 Capacity Spectrum method:**

**3.4.1.1 Basis of the procedure:** The capacity spectrum method, a nonlinear static procedure that provides a graphical representation of the global force-displacement capacity curve of the structure (i.e., pushover) and compares it to the response spectra representations of the earthquake demands, is a very useful tool in the evaluation and retrofit design of existing concrete buildings. The graphical representation provides a clear picture of how a building responds to earthquake ground motion, and it provides an immediate and clear picture of how various

retrofit strategies, such as adding stiffness or strength, will impact the building's response to earthquake demands.

**3.4.1.2 Modelling and Analysis Considerations:** Two key elements of a performance-based design procedure are demand and capacity. Demand is a representation of the earthquake ground motion. Capacity is a representation of the structure's ability to resist the seismic demand. The performance is dependent on the manner that the capacity is able to handle the demand. In other words, the structure must have the capacity to resist the demands of the earthquake such that the performance of the structure is compatible with the objectives of the design.

**3.4.1.2.1 Capacity:** The overall capacity of a structure depends on the strength and deformation capacities of the individual components of the structure. In order to determine capacities beyond the elastic limits, some form of nonlinear analysis, such as the pushover procedure, is required. This procedure uses a series of sequential elastic analyses, superimposed to approximate a force-displacement capacity diagram of the overall structure. The mathematical model of the structure is modified to account for reduced resistance of yielding components. A lateral force distribution is again applied until additional components yield. This process is continued until the structure becomes unstable or until a predetermined limit is reached. For two dimensional models, computer programs are available that directly model nonlinear behaviour and can create a pushover curve directly. The pushover capacity curve approximates how structures behave after exceeding their elastic limit. This represents the lateral displacement as a function of the force applied to the structure. The capacity curve is generally constructed to represent the first mode response of the structure based on the assumption that the fundamental mode of vibration is the predominant response of the structure. This is generally valid for buildings with fundamental periods of vibration up to about one second. For more flexible buildings with a fundamental period greater than

one second, the analyst should consider addressing higher mode effects in the analysis.

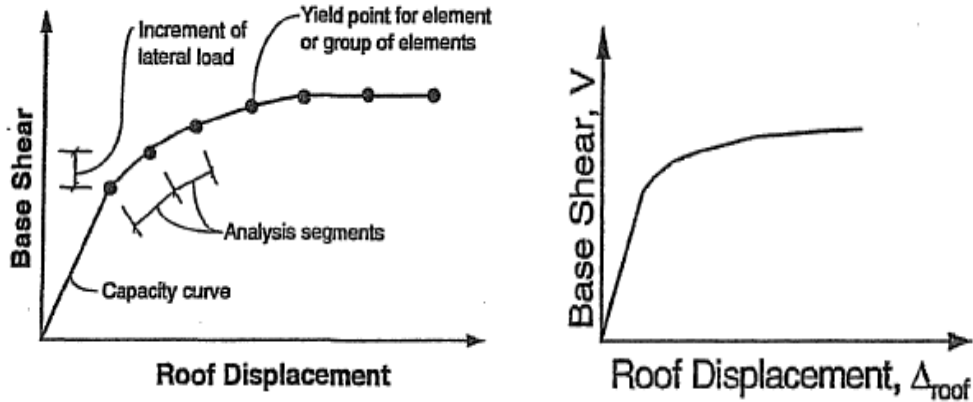


Fig3.3: Capacity Curve

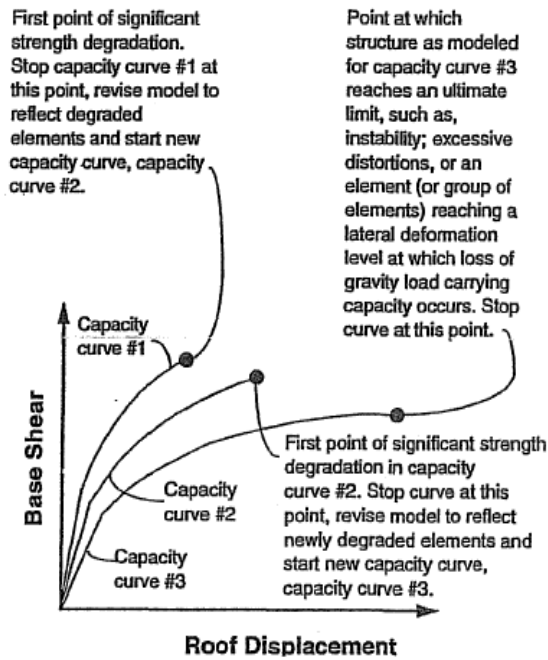


Fig 3.4: Multiple Capacity Curves Required to strength Degradation Modelled

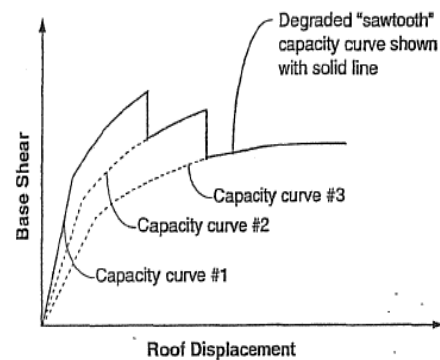
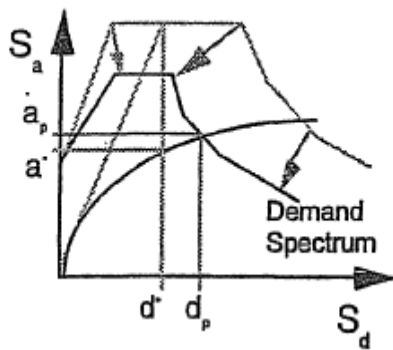


Fig 3.5: Capacity curve With Global Model strength Degradation



**3.4.1.2.2 Demand (displacement):** Ground motions during an earthquake produce complex horizontal displacement patterns in structures that may vary with time. Tracking this motion at every time-step to determine structural design requirements is -judged impractical. Traditional linear analysis methods use lateral forces to represent a design condition. For nonlinear methods it is easier and more direct to use a set of lateral displacements as a design condition. For a given structure and ground motion, the displacement demand is an estimate of the maximum expected response of the building during the ground motion.



**Fig 3.6: Demand Spectrum**

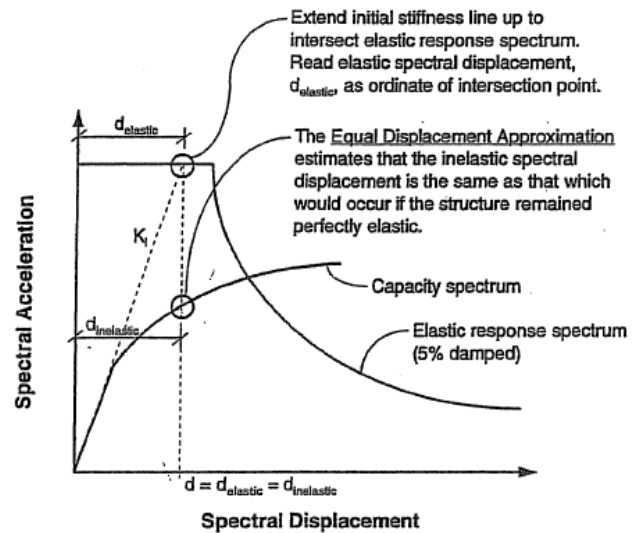


**Fig 3.7: Equal Displacement Approximation**

**3.4.1.2.3 Conversion of the Capacity Curve to the Capacity Spectrum:** To use the capacity spectrum method it is necessary to convert the capacity curve, which is in terms of base shear and roof displacement to what is called a capacity spectrum, which is a representation of the capacity curve in Acceleration-Displacement Response Spectra (ADRS) format (i.e.,  $S_a$  versus  $S_d$ ).

The required equations to make the transformation are:

$$PF_1 = \frac{\left[ \sum_{i=1}^N (w_i \phi_{i1}) / g \right]}{\left[ \sum_{i=1}^N (w_i \phi_{i1}^2) / g \right]} \quad (8-1)$$

$$\alpha_1 = \frac{\left[ \sum_{i=1}^N (w_i \phi_{i1}) / g \right]^2}{\left[ \sum_{i=1}^N w_i / g \right] \left[ \sum_{i=1}^N (w_i \phi_{i1}^2) / g \right]} \quad (8-2)$$

$$S_a = \frac{V / W}{\alpha_1} \quad (8-3)$$

$$S_d = \frac{\Delta_{roof}}{PF_1 \phi_{roof,1}} \quad (8-4)$$

where:

- PF<sub>1</sub> = modal participation factor for the first natural mode.
- α<sub>1</sub> = modal mass coefficient for the first natural mode.
- w<sub>i</sub> / g = mass assigned to level i.
- φ<sub>i1</sub> = amplitude of mode 1 at level i.
- N = level N, the level which is the uppermost in the main portion of the structure.
- V = base shear.
- W = building dead weight plus likely live loads, see Section 9.2.
- Δ<sub>roof</sub> = roof displacement (V and the associated Δ<sub>roof</sub> make up points on the capacity curve).
- S<sub>a</sub> = spectral acceleration.
- S<sub>d</sub> = spectral displacement (S<sub>a</sub> and the associated S<sub>d</sub> make up points on the capacity spectrum).

Any point  $V_i, \Delta_{roof}$  on the capacity curve is converted to the corresponding point  $S_{ai}, S_{di}$  on the capacity spectrum using the above equations.

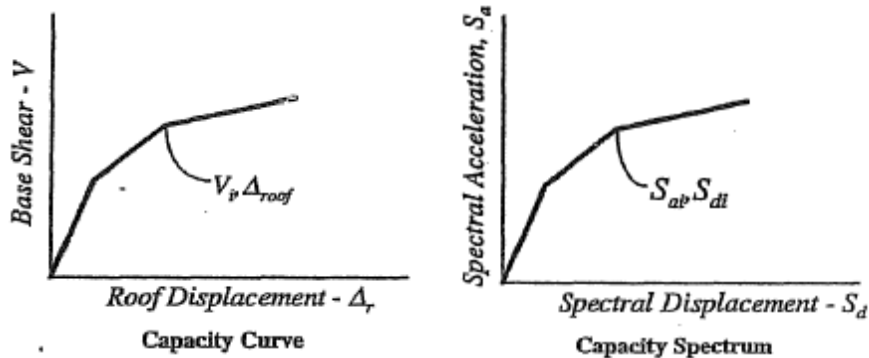


Fig 3.8: Capacity curve and capacity spectrum

#### 3.4.1.2.4 Conversion of the Demand Curve to the Response Spectrum in ADRS format:

Every point on a response spectrum curve has associated with it a unique spectral acceleration,  $S_a$ , spectral velocity,  $S_v$ , spectral displacement,  $S_d$  and period,  $T$ . To convert a spectrum from the standard  $S_a$  vs.  $T$  format found in the building code to

ADRS format, it is necessary to determine the value of  $S_{di}$  for each point on the curve,  $S_{ai}$ ,  $T_i$ . This can be done with the equation:

$$S_{di} = \frac{T_i^2}{4\pi^2} S_{ai} g \quad T = 2\pi \sqrt{\frac{S_d}{S_a}}$$

Standard demand response spectra contain a range of constant spectral acceleration and a second range of constant spectral velocity. Spectral acceleration and displacement at period  $T$ , are given by:

$$S_{ai} g = \frac{2\pi}{T_i} S_v \quad S_{di} = \frac{T_i}{2\pi} S_v$$

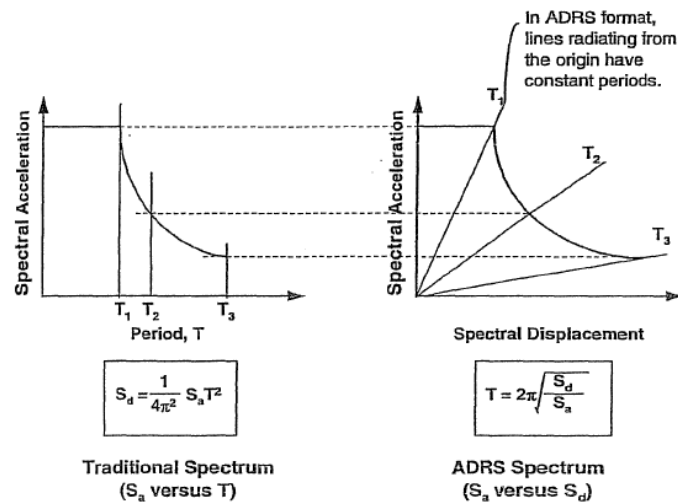


**Fig 3.9.1: Response Spectra in Traditional and ADRS format**

**3.4.1.2.5 Reduced Response Spectrum:** The equivalent viscous damping values can be used to estimate spectral reduction factors ( $SR=1/B$ ,  $B$ =Damping Coefficient) using relationships developed by Newmark and Hall. As shown in Figure 8-14, spectral reduction factors are used to decrease the elastic (5% damped) response spectrum to a reduced response spectrum with damping greater than 5% of critical damping. For damping values less than about 25 percent, spectral reduction factors calculated using the  $\beta_{eq}$  from equation below:

1.  $C_A$  &  $C_V$  are seismic coefficients depending on Site geology & soil characteristics, Site seismicity characteristics & Site response Spectra.
2.  $SR_A$  is Spectral reduction value in constant acceleration range of spectrum.
3.  $SR_V$  is spectral reduction value in constant velocity range of spectrum.

Where,

$$SR_A = \frac{1}{B_s} \approx \frac{3.21 - 0.68 \ln(\beta_{eff})}{2.12}$$

$$SR_V = \frac{1}{B_L} \approx \frac{2.31 - 0.41 \ln(\beta_{eff})}{1.65}$$

$$\beta_{eff} = \kappa \beta_0 + 5$$

$\beta_0$  = hysteretic damping represented as equivalent viscous damping

$\kappa$  = damping modification factor,

The term  $\beta_0$  can be calculated as

$$\beta_0 = \frac{1}{4\pi} \frac{E_D}{E_{S_0}}$$

where,

$E_D$  = energy dissipated by damping

$E_{S_0}$  = maximum strain energy

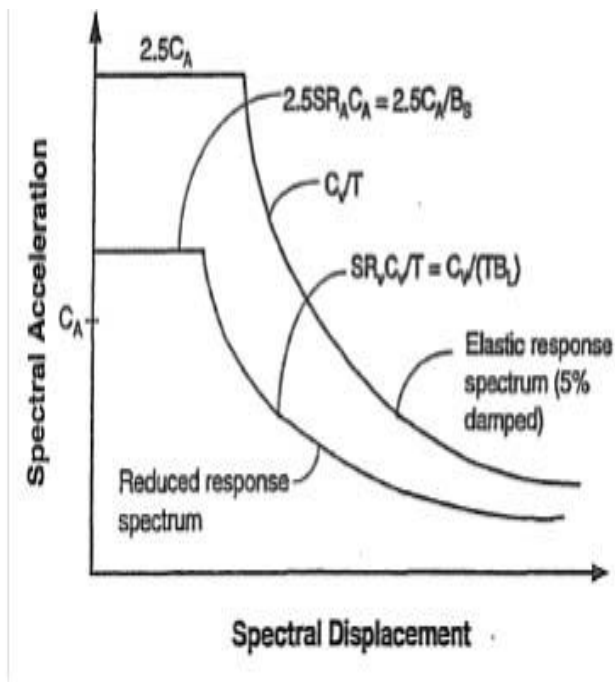


**Fig 3.9.2: Spectral acceleration and spectral displacement**

**3.4.1.2.6 Performance:** Once a capacity curve and demand displacement is defined, a performance check can be done. A performance check verifies that structural and non structural components are not damaged beyond the acceptable limits of the performance objective for the forces and displacements implied by the displacement demand.

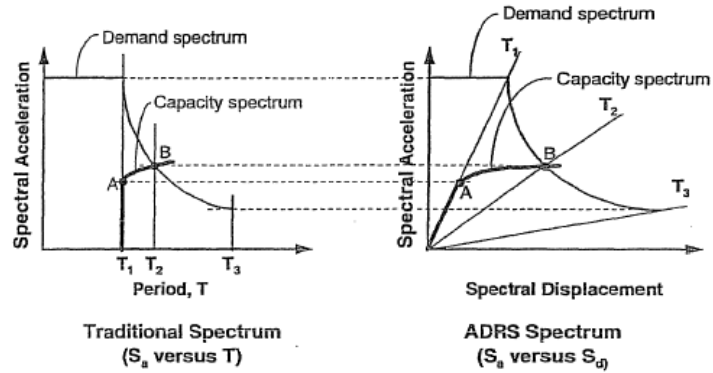


**Fig3.10: Capacity spectrum superimposed over Response spectra in Traditional and ADRS Formats**

**3.4.1.2.7 Intersection of Capacity Spectrum and Demand Spectrum:** When the displacement at the intersection of the demand spectrum and the capacity spectrum,  $d_i$ , is within 5 percent- ( $0.95d_{pi} \leq d_i \leq 1.05 d_{pi}$ ) of the displacement of the trial performance point,  $a_{pi}$ ,  $d_{pi}$ ,  $d_{pi}$  becomes the performance point. If the intersection of the demand spectrum and the capacity spectrum is not within the acceptable tolerance, then a new  $a_{pi}$ ,  $d_{pi}$  point is selected and the process is repeated. Figure 8-22 illustrates the concept. The performance point represents the maximum structural displacement expected for the demand earthquake ground motion.

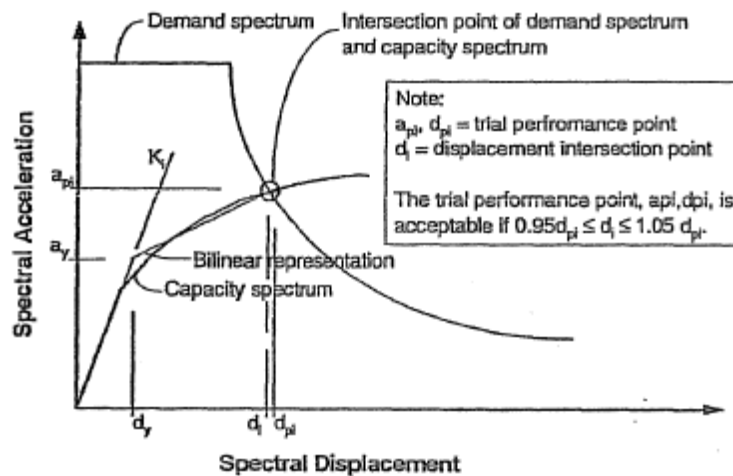


**Figure3.11: Intersection point of Demand and capacity spectrums within Acceptable Tolerance**

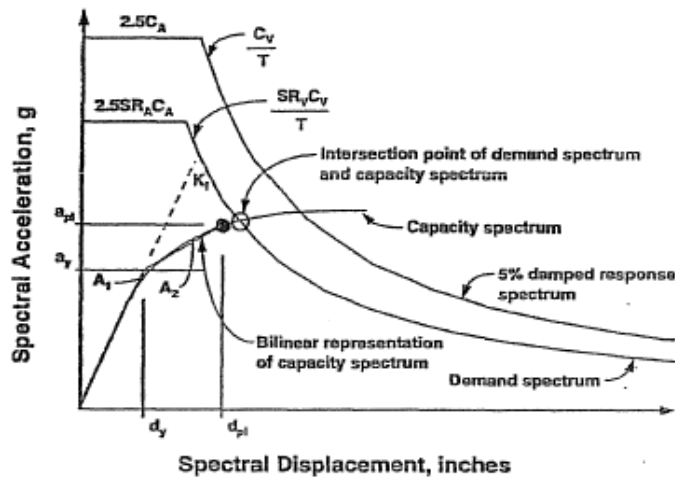


Figure 3.12: Intersection point of Reduced Demand and capacity spectrums to meet acceptance criteria

### 3.4.2 Displacement Coefficient Method:

#### 3.4.2.1 Calculating Demand Displacement using the Displacement Coefficient Method:

The displacement coefficient method provides a direct numerical process for calculating the displacement demand. It does not require converting the capacity curve to spectral coordinates. Construction of a bilinear representation of the capacity curve has been done in this method. The post-elastic stiffness,  $K_s$ , by judgment is drawn to represent an average stiffness in the range in which the structure strength has levelled off. The effective elastic stiffness,  $K_e$ , is drawn by constructing a secant line passing through the point on the capacity curve corresponding to a base shear of  $0.6V_y$ , where  $V_y$  is defined by the intersection of the  $K_e$  and  $K_s$  lines. The above process requires some trial and error effort because the value for  $V_y$  is not known until after the  $K_e$  line is drawn.

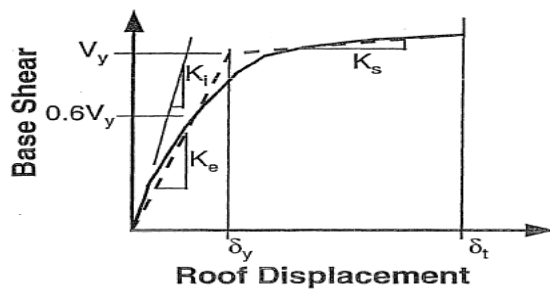


Fig 3.13: Bilinear representation of Capacity Curve for Displacement coefficient Method

The bilinear curve constructed for the displacement coefficient method will generally be different from one constructed for the capacity spectrum method.

**3.4.2.2 Effective fundamental period ( $T_e$ ) & Target displacement ( $\delta_t$ ):** Same as calculated by using FEMA 356 except in change of few notations though the basis and concept are same.

**3.4.2.3 Checking Performance at the Expected Maximum Displacement:** The following steps should be followed in the performance check:

1. For global building response verify the following:
  - The lateral force resistance has not degraded by more than 20 percent of the peak resistance
  - The lateral drifts satisfy the limits given in Table below-

**Table: 3-3 : Performance level and inter storey drift limit**

Inter storey drift limit	Performance Level			
	Immediate Occupancy	Damage control	Life safety	Structural stability
Maximum total drift	0.01	0.01-0.02	0.02	$0.33 \frac{V_t}{P_t}$
Maximum inelastic drift	0.005	0.005-0.015	No limit	No limit

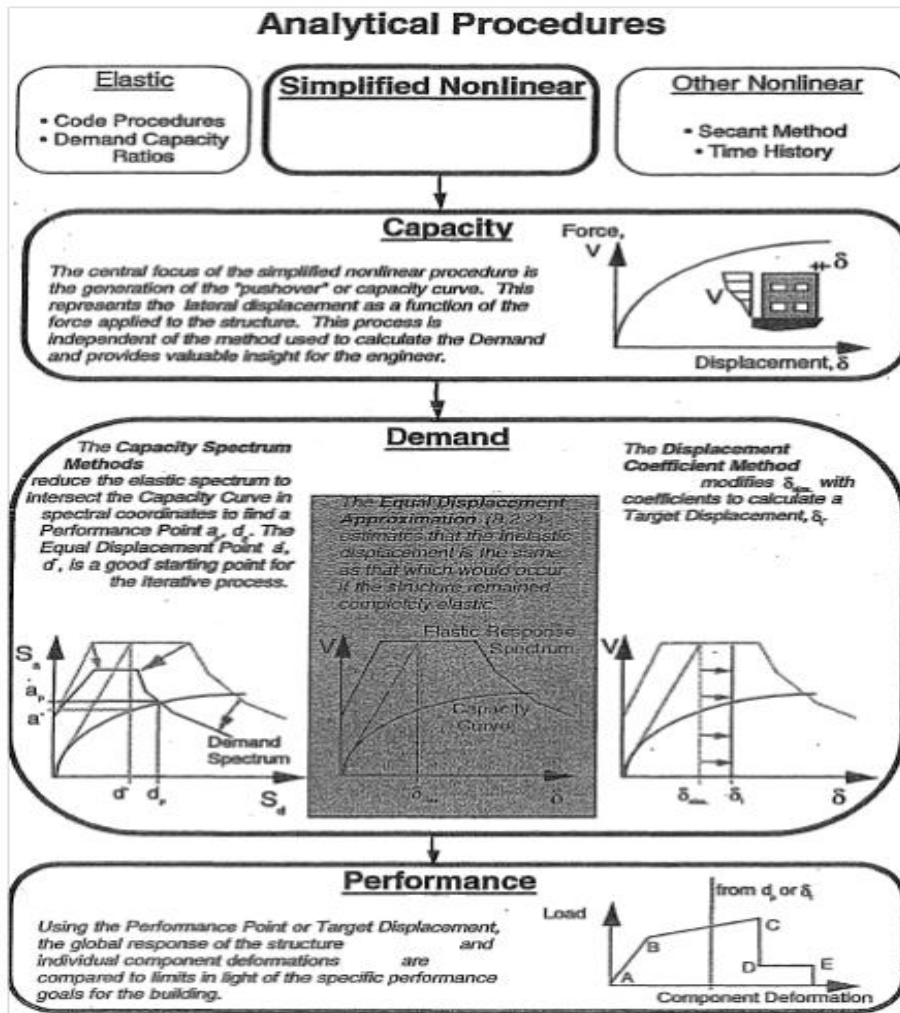
2. Identify and classify the different elements in the building. Any of the following element types may be present: beam-column frames, slab-column frames, solid walls, coupled walls, perforated walls, punched walls, floor diaphragms and foundations.

3. Identify all primary and secondary components. This classification is needed for the deformation check in step 5.

4. For each element, identify the critical components and actions to be checked.

5. The strength and deformation demands at the structure's performance point shall be equal to or less than their respective capacities considering all co-existing forces acting with the demand spectrum.
6. The performance of structural elements not carrying vertical load shall be reviewed for acceptability for the specified performance level.
7. Non structural elements shall be checked for acceptability for the specified performance level.

### 3.5 Comparative chart for capacity spectrum & Displacement Coefficient Methods:





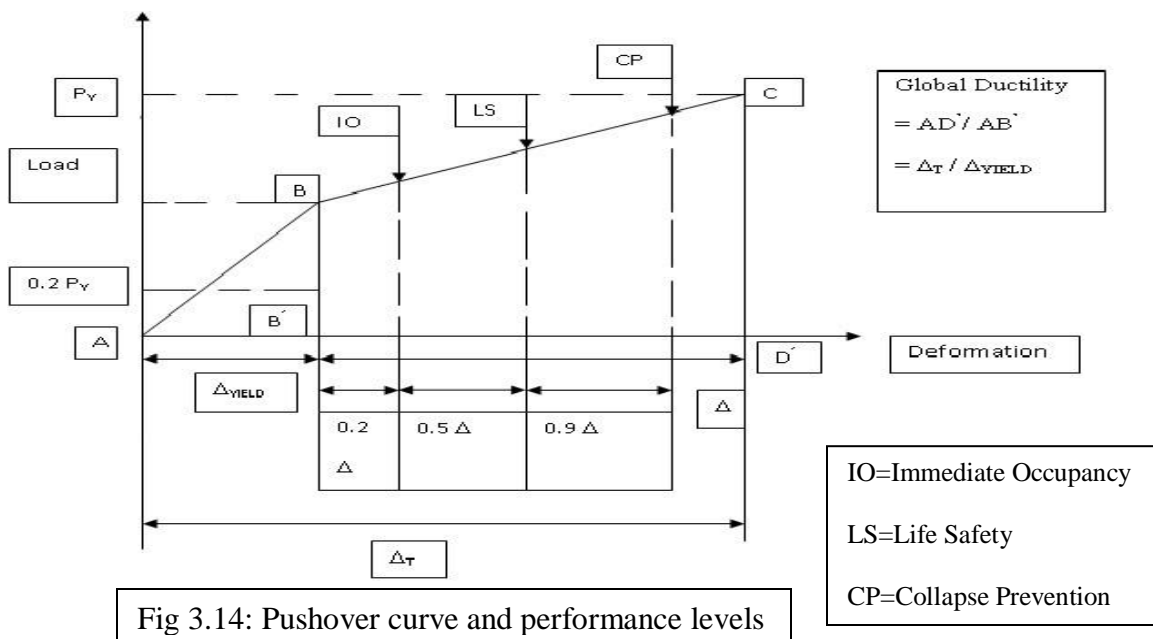
### 3.6 Performance level of structure and element:

The performance levels are discrete damaged states identified from a continuous spectrum of possible damage states. The structural performance levels are

- i) Immediate Occupancy
- ii) Life Safety
- iii) Collapse Prevention

These three levels are arranged according to decreasing performance of lateral load & vertical load resisting system. A target performance is defined by a typical value of roof drift, as well as limiting value of deformation of the structural element. To determine whether a building meets a specified performance objective response quantities from the pushover analysis should be compared with limits for each of the performance levels. According to FEMA 356, typical values of the roof drift are as follows:

- a) For immediate occupancy, transient drift is about 1% with negligible permanent drift.
- b) For life safety, transient drift is 2% with 1% permanent drift.
- c) Total 4% inelastic drift, whether transient or permanent.



Performance levels of a structural element are specified in the load-deformation curve as shown above. The actual value of these levels can be obtained from test results. However in absence of test data, the following may be adopted as per ATC 40.

- i) Immediate Occupancy =20% of  $\Delta$  from point B, where  $\Delta$  is the length of the plastic plateau.
- ii) Life safety =50% of  $\Delta$  from point B
- iii) Collapse Prevention =90% of  $\Delta$  from point B

### **3.7 Types of non-linearity:**

Both geometric and material non-linearities are considered in this static nonlinear pushover analysis.

#### **3.7.1 Geometric non-linearity:**

This is a type of non-linearity where the structure is still elastic, but the effects of large deflections cause the geometry of the structure to change, so that linear elastic theory breaks down. Typical problems that lie in this category are the elastic instability of structures, such as in the Euler buckling of struts and the large deflection analysis of a beam-column member. In general, it can be said that for geometrical non-linearity, an axially applied compressive force in a member decreases its bending stiffness, but an axially applied tensile force increases its bending stiffness. In addition, P-Delta effect is also included in this concept.

#### **3.7.2 Material non-linearity:**

In this type of non-linearity, material undergoes plastic deformation. Material non-linearity can be modelled as discrete hinges at a number of locations along the length of a frame (beam or column) element and a discrete hinge for a brace element as discrete material fibres distributed over the cross-section of the element, or as a series of material points throughout the element.

### **3.8 Pushover Analysis Solution Control :**

Pushover analysis will continue until any of the following three conditions is satisfied:

- a) Cumulative base shear is less than or equal to the base shear defined by the user :

-

User needs to define base shear until which pushover analysis will be performed since design base shear (specific to particular seismic code) excludes non-linear effect. When the structure is subjected to strong earthquake the actual base shear may be very high compared to the design base shear. Under this condition there is no guarantee that the structure will maintain desired performance level. This option is chosen when the magnitude of base shear is known and the structure will be able to support that load.

- b) Displacement at the control joint in the specified direction exceeds specified displacement : -

This option is chosen when the amount of displacement is known i.e. how far the structure will move but the amount of base shear that the structure will be subjected to is not known. While defining this option please make sure that the displacement component chosen at the control joint increases monotonically during loading. The control node shall be located at the centre of mass at the roof of the building.

- c) The structure becomes unstable : -

This happens whenever hinge formation is such that it renders the structure on the verge of collapse. If neither base shear nor displacement at control joint is known, define a higher value for both these options. During analysis instability will arise due to collapse of different members and make the structure unstable.

### 3.9 Vulnerability Index:

Vulnerability function may be defined as test of repair / damage against seismic excitation. In case of pushover analysis the function of plastic hinges are considered to be a measure of damage and non linear push are considered to be equivalent seismic excitation.

The vulnerability index is a measure of the damage in a building obtained from the pushover analysis. It is defined as a scaled linear combination (weighted average) of performance measures of the hinges in the components, and is calculated from performance levels of the components at the performance point or at the point of termination of the pushover analysis. It has been mentioned earlier that the load deformation curve for a particular hinge is assumed to be piece wise linear. The plastic plateau (B-C) in the load deformation curve is subdivided into the performance ranges, namely, B-IO, IO-LS, LS-CP, CP-C, D-E, AND >E.

After the pushover analysis, performance ranges of the hinges formed in the component can be noted from the deformed shape output. The number of hinges formed in the beams and columns for each performance range are available the output. A “weight age factor” ( $X_i$ ) is assigned to each performance range. The proposed values of  $X_i$  are given in table. As columns are more important than beam in global safety of building, an importance factor of 1.5 is additionally assigned for columns. The building vulnerability index “ $VI_{\text{bldg}}$ ” is accordingly given by the following weighted average.

$$VI_{\text{bldg}} = \frac{1.5 \sum N_i^C X_i + \sum N_i^h X_i}{\sum N_i^C + \sum N_i^h}$$

Here  $N_i^C$  and  $N_i^h$  are the numbers of hinges in columns and beams, respectively, for the  $i^{\text{th}}$  performance range. The summation sign intended to over the performance range,  $i=1, 2, \dots$ .  $VI_{\text{bldg}}$  is measure of overall vulnerability of building. A high value of  $VI_{\text{bldg}}$  reflects poor performance of the building components (i.e. high risk) as obtained from the

pushover analysis. However, this index may not reflect a soft storey mechanism, in which a performance point may not be achieved. A storey vulnerability index  $VI_{storey}$  can be defined to quality the possibility of a soft/weak storey with the formation of flexural hinges. For each storey  $VI_{storey}$  is defined as

$$VI_{storey} = \frac{\sum X_i N_i^C}{\sum N_i^C}$$

Where N is the number of column hinges in the storey under investigation for a particular performance range. In a given building, the presence of soft / weak storey is reflected by a relatively high value of  $VI_{storey}$  for that storey, in relation to the other storey. If the analysis is terminated due to the formation of shear hinges, then the above definition is not applicable.

**Table 3-4: Performance range and weight age factor**

PERFORMANCE RANGE (i)	WEIGHTAGE FACTOR (X <sub>i</sub> )
<B	0.000
B- I.O.	0.125
I.O.-L.S.	0.375
L.S.-C.P.	0.625
C.P.-C	0.875
C-D,D-E AND >E	1.000

### 3.10 Limitation of Conventional Pushover Analysis:

Although pushover analysis has advantages over elastic analysis procedures, underlying assumptions, the accuracy of pushover predictions and limitations of current pushover procedures must be identified. The estimate of target displacement, selection of lateral load patterns and identification of failure mechanisms due to higher modes of vibration are important issues that affect the accuracy of pushover results. Target displacement is the global displacement expected in a design earthquake. Most of the time, roof displacement at mass centre of the structure is used as target displacement. The

accurate estimation of target displacement associated with specific performance objective affect the accuracy of seismic demand predictions of pushover analysis. In pushover analysis, the target displacement for a multi degree of freedom (MDOF) system is usually estimated as the displacement demand for the corresponding equivalent single degree of freedom (SDOF) system.

Lateral loads represent, the possible distribution of inertia forces imposed on structure during an earthquake. The distribution of inertia forces vary with the severity of earthquake and with the duration of earthquake.

$$F_{ij} = \frac{W_i}{g} \ddot{u}_j$$

Where,

$F_{ij}$  = Inertia force at  $i$ th storey at time  $j$        $\ddot{u}_j$  = Instantaneous storey acceleration

$W_i$  = Weight of  $i$ th storey

However, in pushover analysis, generally an invariant lateral load pattern is used that the distribution of inertia forces is assumed to be constant during earthquake and the deformed configuration of structure under the action of invariant lateral load pattern is expected to be similar to that experienced in design earthquake. As the response of structure, thus the capacity curve is very sensitive to the choice of lateral load distribution, selection of lateral load pattern is more critical than the accurate estimation of target displacement. Whether lateral loading is invariant or adaptive, it is applied to the structure statically that a static loading cannot represent inelastic dynamic response with a large degree of accuracy. From the above discussion on target displacement and lateral load pattern it can be concluded that in pushover analysis assumes that response of structure can be related to that of an equivalent SDOF system. Actually the response is controlled by fundamental mode which remains constant throughout the response history without considering progressive yielding.

## 4.0 General :

Sap is an integrated software for structural analysis and design in which the Push-over analysis features is included. The stepwise description of Push-over analysis procedure is given below.

### 4.1 Step 1 Begin a New Model

- File menu > New Model

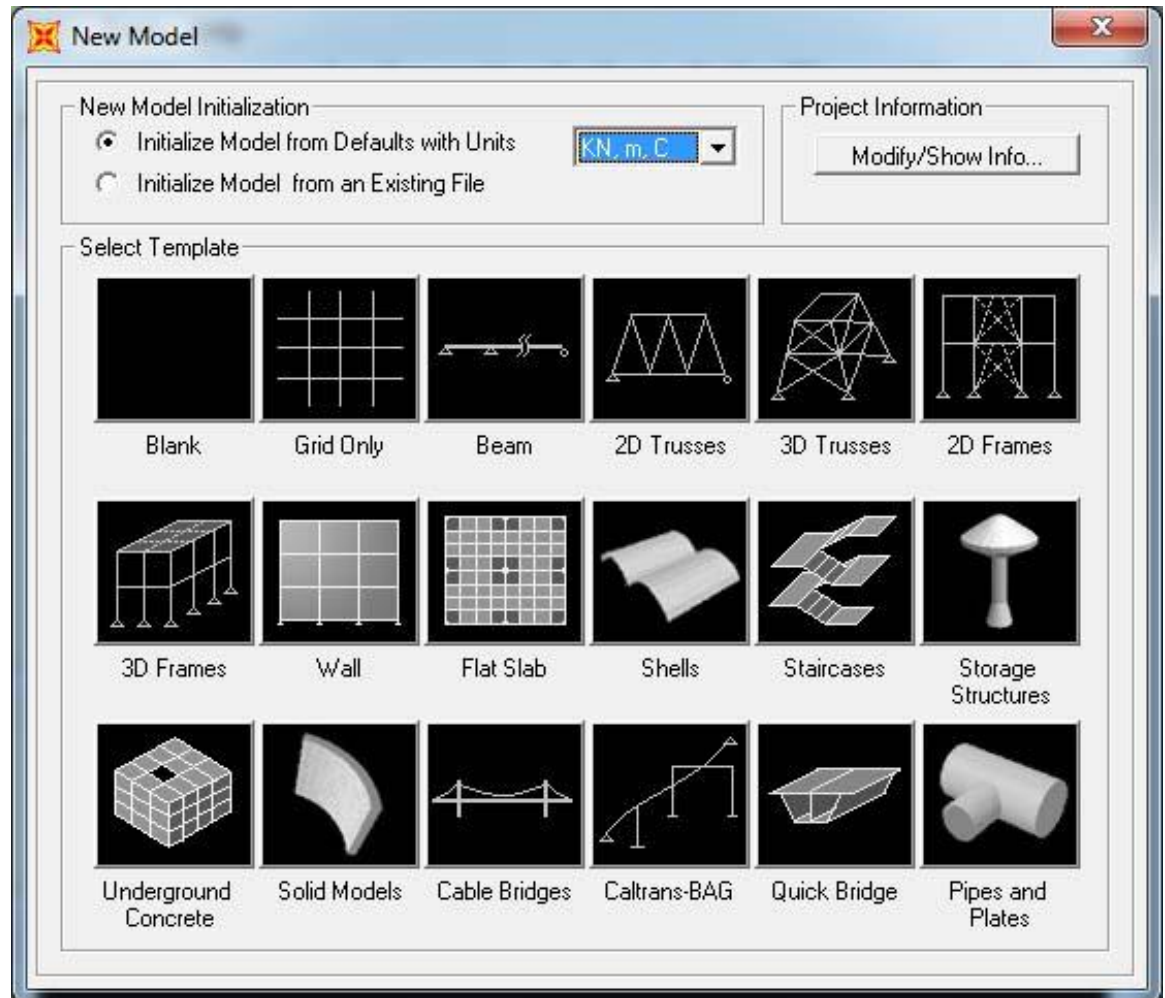
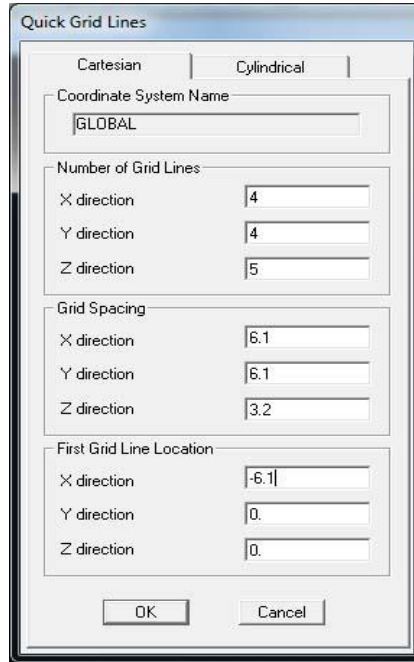


Fig 4.1: New model initialization

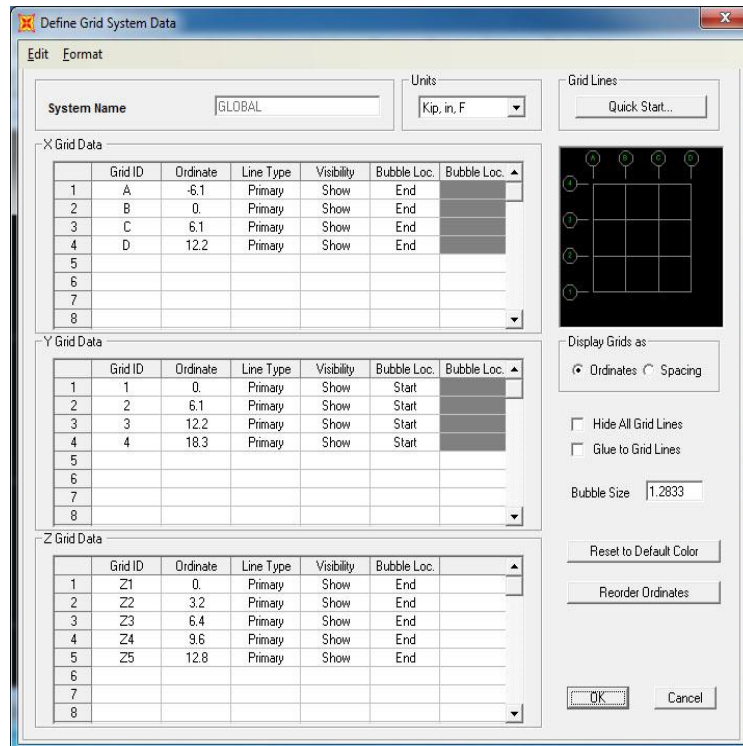
- Define Menu > Coordinate Systems / Grids
  - ❖ Quick Grid Lines Form
  - ❖ Define Grid Data Form



The 'Quick Grid Lines' dialog box is shown with the 'Cartesian' tab selected. It contains the following fields:

- Coordinate System Name: GLOBAL
- Number of Grid Lines:
  - X direction: 4
  - Y direction: 4
  - Z direction: 5
- Grid Spacing:
  - X direction: 6.1
  - Y direction: 6.1
  - Z direction: 3.2
- First Grid Line Location:
  - X direction: -6.1
  - Y direction: 0.
  - Z direction: 0.

Buttons for 'OK' and 'Cancel' are at the bottom.



The 'Define Grid System Data' dialog box is shown with the 'GLOBAL' system name and 'Kip, in, F' units. It displays three data tables for X, Y, and Z grid lines, along with a grid visualization and display options.

**-X Grid Data**

	Grid ID	Ordinate	Line Type	Visibility	Bubble Loc.	Bubble Loc.
1	A	-6.1	Primary	Show	End	
2	B	0.	Primary	Show	End	
3	C	6.1	Primary	Show	End	
4	D	12.2	Primary	Show	End	
5						
6						
7						
8						

**-Y Grid Data**

	Grid ID	Ordinate	Line Type	Visibility	Bubble Loc.	Bubble Loc.
1	1	0.	Primary	Show	Start	
2	2	6.1	Primary	Show	Start	
3	3	12.2	Primary	Show	Start	
4	4	18.3	Primary	Show	Start	
5						
6						
7						
8						

**-Z Grid Data**

	Grid ID	Ordinate	Line Type	Visibility	Bubble Loc.
1	Z1	0.	Primary	Show	End
2	Z2	3.2	Primary	Show	End
3	Z3	6.4	Primary	Show	End
4	Z4	9.6	Primary	Show	End
5	Z5	12.8	Primary	Show	End
6					
7					
8					

**Grid Lines** section includes a 'Quick Start...' button and a grid visualization with numbered points 1-4.

**Display Grids as:**  Ordinates  Spacing

Hide All Grid Lines  
 Glue to Grid Lines

Bubble Size: 1.2833

Buttons: 'Reset to Default Color', 'Reorder Ordinates', 'OK', 'Cancel'.

Fig 4.2: Quick grid lines and grid system data forms



## 4.2 Step 2 Define Material

- Define menu > Materials

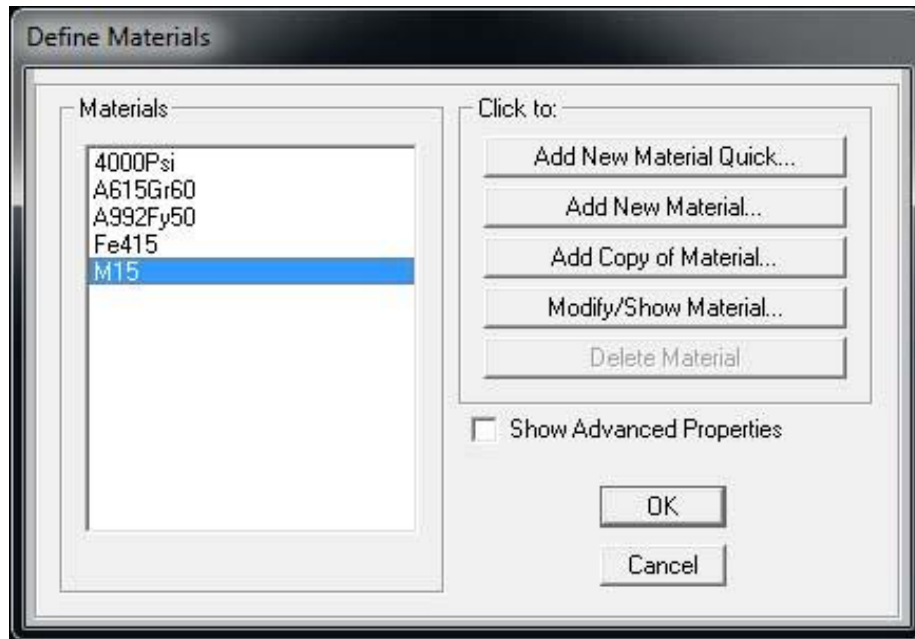


Fig 4.3: Materials data form

- ❖ Material Property Data Form – Concrete
- ❖ Material Property Data Form – Rebar

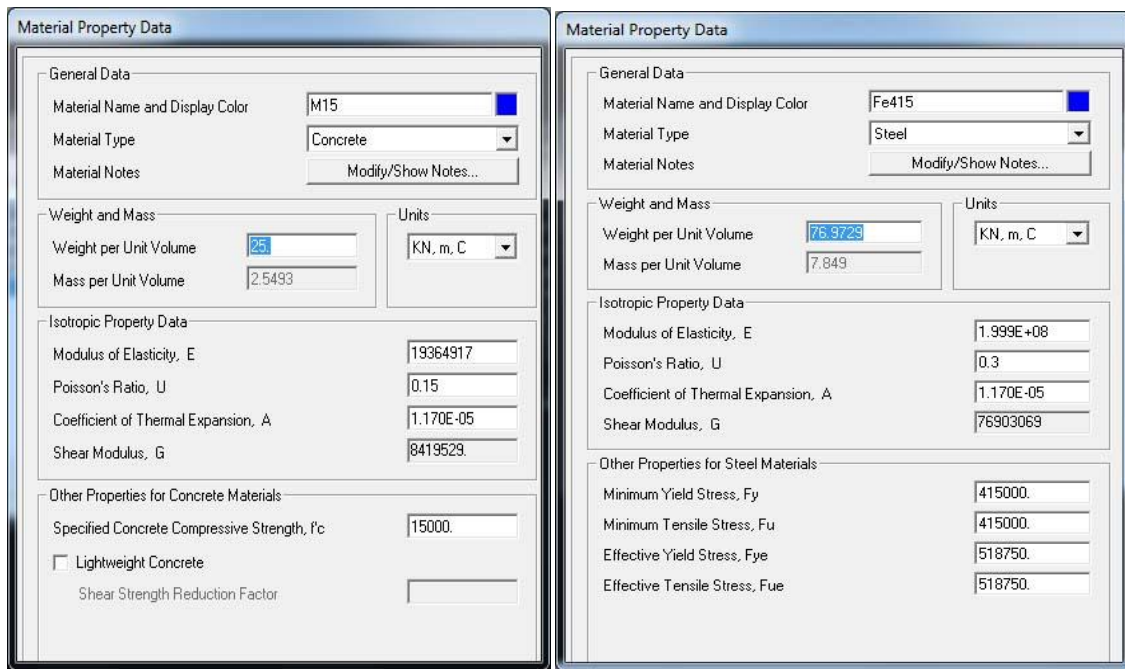


Fig 4.4: Material property data forms for concrete and rebar

### 4.3 Step 3 Define Frame Section

- Define menu > Section Properties > Frame Sections
- ❖ Add Frame Section Property Form
- ❖ Rectangular Section Form
- ❖ Reinforcement Data Form for Column
- ❖ Reinforcement Data Form for Beam

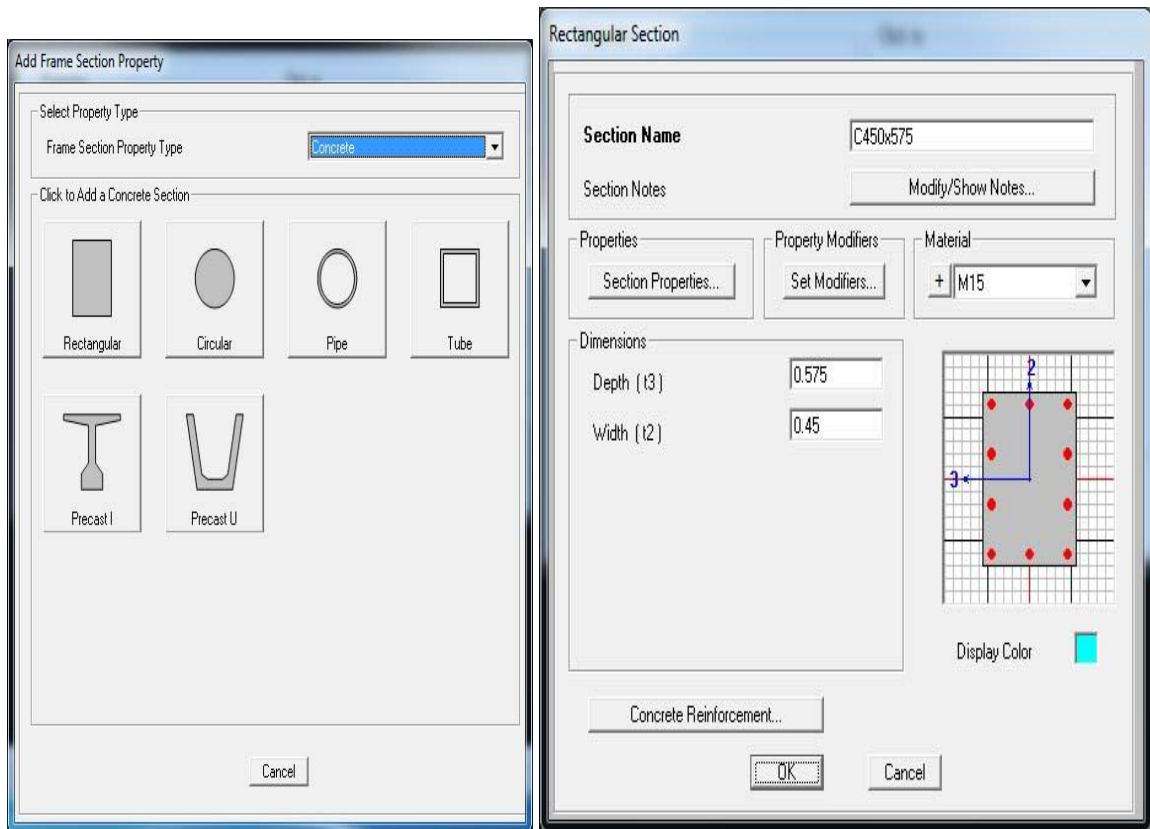


Fig 4.5: Concrete section property and rectangular section property data forms

The image shows two side-by-side dialog boxes titled "Reinforcement Data".

**Left Dialog (Beam):**

- Rebar Material:** Longitudinal Bars: A615Gr60; Confinement Bars (Ties): A615Gr60.
- Design Type:**  Beam (M3 Design Only);  Column (P-M2-M3 Design).
- Concrete Cover to Longitudinal Rebar Center:** Top: 0.04; Bottom: 0.04.
- Reinforcement Overrides for Ductile Beams:**

	Left	Right
Top	0.	0.
Bottom	0.	0.

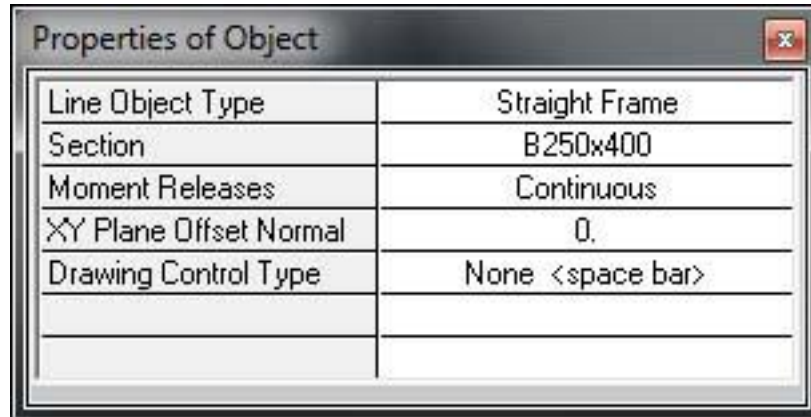
**Right Dialog (Column):**

- Rebar Material:** Longitudinal Bars: A615Gr60; Confinement Bars (Ties): A615Gr60.
- Design Type:**  Column (P-M2-M3 Design);  Beam (M3 Design Only).
- Reinforcement Configuration:**  Rectangular;  Circular.
- Confinement Bars:**  Ties;  Spiral.
- Longitudinal Bars - Rectangular Configuration:**
  - Clear Cover for Confinement Bars: 0.04
  - Number of Longit Bars Along 3-dir Face: 3
  - Number of Longit Bars Along 2-dir Face: 4
  - Longitudinal Bar Size: + 28d
- Confinement Bars:**
  - Confinement Bar Size: + #8
  - Longitudinal Spacing of Confinement Bars: 0.3
  - Number of Confinement Bars in 3-dir: 4
  - Number of Confinement Bars in 2-dir: 4
- Check/Design:**  Reinforcement to be Checked;  Reinforcement to be Designed.

Fig 4.6: Reinforcement data forms for beam and column

#### 4.4 Step 4 Add Frame Objects

- Draw Menu > Snap to > Points and Grid
- View Menu > Set 2D View



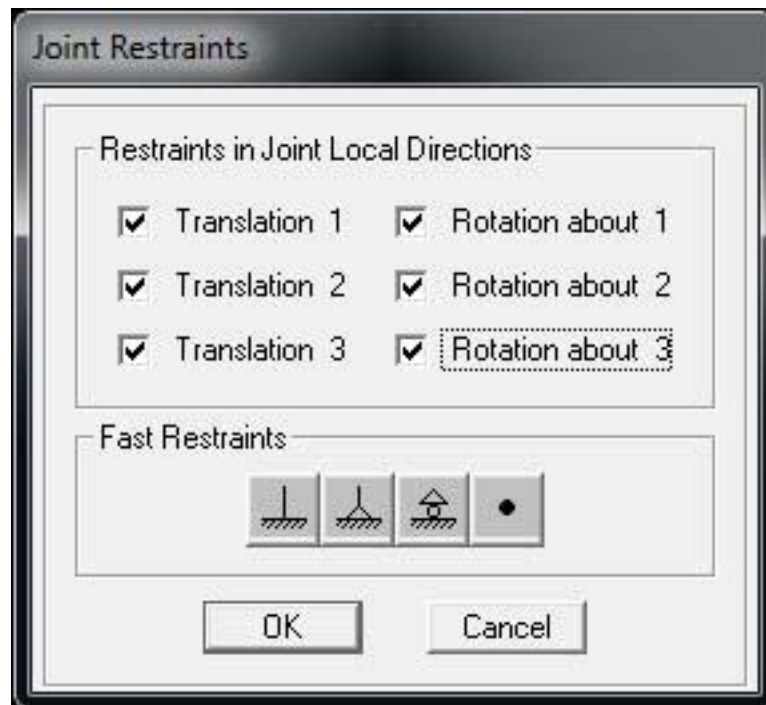
The 'Properties of Object' dialog box displays the following data:

Line Object Type	Straight Frame
Section	B250x400
Moment Releases	Continuous
XY Plane Offset Normal	0.
Drawing Control Type	None <space bar>

Fig 4.7: Properties of object data form

#### Add Restraints

- Assign Menu > Joint > Restraints



The 'Joint Restraints' dialog box shows the following configuration:

Restraints in Joint Local Directions

<input checked="" type="checkbox"/> Translation 1	<input checked="" type="checkbox"/> Rotation about 1
<input checked="" type="checkbox"/> Translation 2	<input checked="" type="checkbox"/> Rotation about 2
<input checked="" type="checkbox"/> Translation 3	<input checked="" type="checkbox"/> Rotation about 3

Fast Restraints

Four icons are shown: a pin, a roller, a support, and a dot. The dot icon is selected.

Buttons: OK, Cancel

Fig 4.8: Joint restraints data form

## 4.5 Step 5 Define Load Patterns

- Define Menu > Load Patterns

Load Pattern Name	Type	Self Weight Multiplier	Auto Lateral Load Pattern
DEAD	DEAD	1	
DEAD	DEAD	1	
dead wall	SUPER DEAD	0	
dead stair	SUPER DEAD	0	
dead point	SUPER DEAD	0	
dead slab	SUPER DEAD	0	
live stair	LIVE	0	
live slab	LIVE	0	
live roof slab	ROOF LIVE	0	

Fig 4.9: Load patterns data form

## 4.6 Step 6 Assign Gravity Loads

- Assign Menu > Frame Loads > Distributed

Load Pattern Name: + DEAD Units: KN, m, C

Load Type and Direction:  Forces  Moments  
Coord Sys: GLOBAL Direction: Gravity

Options:  Add to Existing Loads  Replace Existing Loads  Delete Existing Loads

Trapezoidal Loads:

	1.	2.	3.	4.
Distance	0.	0.25	0.75	1.
Load	0.	0.	0.	0.

Relative Distance from End-I  Absolute Distance from End-I

Uniform Load: Load: 6.5

Fig 4.10: Frame distributed loads data form

## 4.7 Step 7 Define Response Spectrum Function

- Define Menu > Functions > Response Spectrum Functions
  - ❖ Response Spectrum Function Definition Form

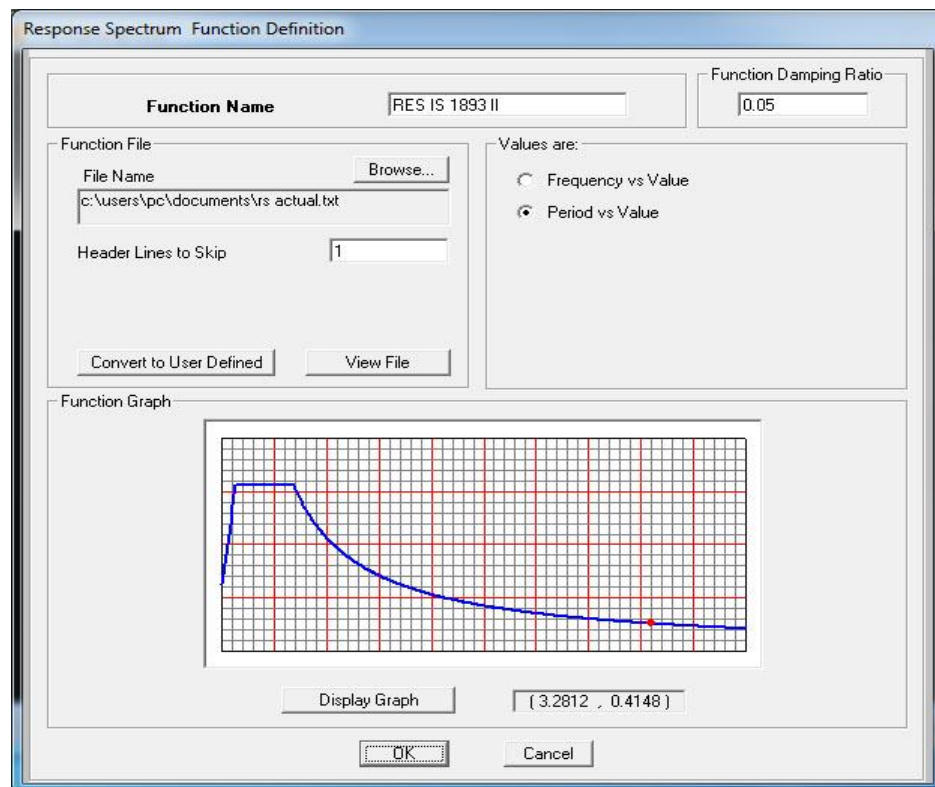
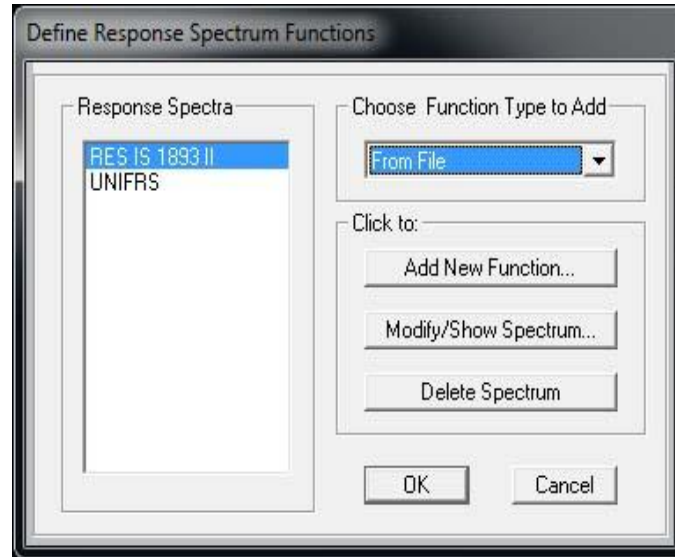


Fig 4.11: Response Spectrum function definition form and display graph

## 4.8 Step 8 Define Response Spectrum Load Case

- Define Menu > Load Cases

Load Type	Load Name	Function	Scale Factor
Accel	U1	RES IS 1893 I	0.479
Accel	U1	RES IS 1893 II	0.479

Fig 4.12: Response Spectrum load case data form

## 4.9 Step 9 Define Mass Sources

- Define Menu > Mass Source

Load	Multiplier
DEAD	1.
DEAD	1.
dead wall	1.
dead stair	1.
dead point	1.
dead slab	1.
live stair	0.25
live slab	0.25

Fig 4.13: Mass source data form

## 4.10 Step 10 Define Load Combinations

- Define Menu > Combinations

**Load Combination Data**

Load Combination Name (User-Generated): 1.5(DL+LL)

Notes: Modify/Show Notes...

Load Combination Type: Linear Add

Options: Convert to User Load Combo, Create Nonlinear Load Case from Load Combo

Define Combination of Load Case Results

Load Case Name	Load Case Type	Scale Factor
DEAD	Linear Static	1.5
DEAD	Linear Static	1.5
dead point	Linear Static	1.5
dead slab	Linear Static	1.5
dead stair	Linear Static	1.5
dead wall	Linear Static	1.5
live roof slab	Linear Static	1.5
live slab	Linear Static	1.5
live stair	Linear Static	1.5

Buttons: Add, Modify, Delete, OK, Cancel

Fig 4.14: Load combination data form

## 4.11 Step 11 Concrete Frame Design

- Define Menu > Concrete Frame Design > View/Review Preferences
  - ❖ Design Menu > Concrete Frame Design > Start De-sign / Check of Structure

**Concrete Frame Design Preferences for Indian IS 456-2000**

Item	Value
1 Design Code	Indian IS 456-2000
2 Multi-Response Case Design	Envelopes
3 Number of Interaction Curves	24
4 Number of Interaction Points	11
5 Consider Minimum Eccentricity	Yes
6 Gamma (Steel)	1.15
7 Gamma (Concrete)	1.5
8 Pattern Live Load Factor	0.75
9 Utilization Factor Limit	0.95

Item Description: Explanation of Color Coding for Values  
**Blue:** Default Value  
**Black:** Not a Default Value  
**Red:** Value that has changed during the current session

Buttons: Set To Default Value (All Items, Selected Items), Reset To Previous Values (All Items, Selected Items), OK, Cancel

Fig 4.15: Concrete frame design data form



## 4.12 Step 12 Linear Analysis & Unlock the Model

- After completing the design of the building **Unlock** the Model.

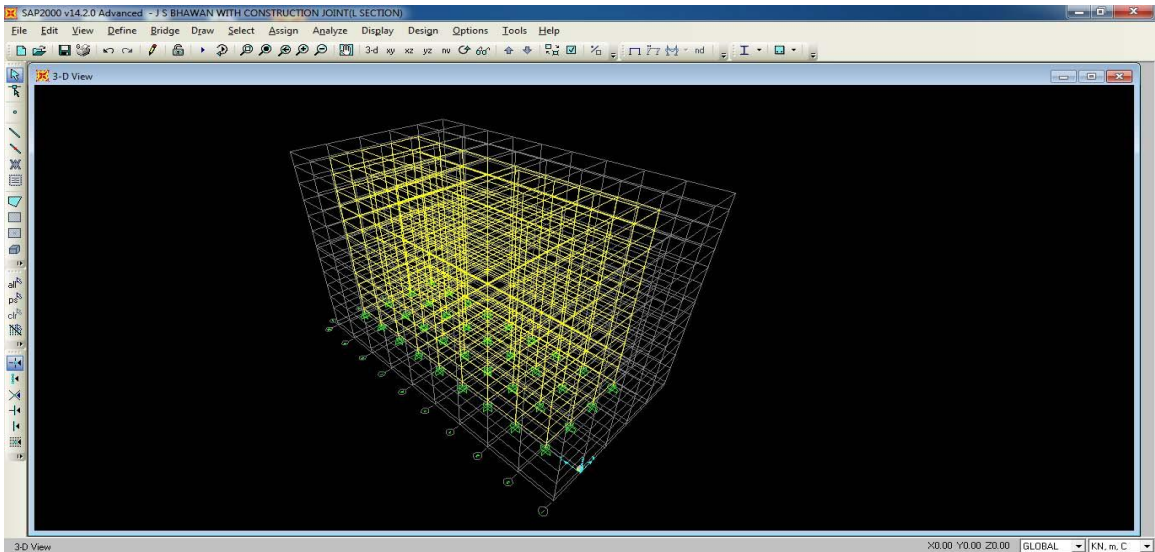


Fig 4.16: Window for unlocking the model after linear analysis and design

## 4.13 Step 13 New Load Case of Gravity Loads

- **Define > Load Case > Add New Load Case** consisting of Gravity loads (i.e. dead load and % of live load). This load case consists of force controlled loads since load application type is full load.

Load Type	Load Name	Scale Factor
Load Pattern	DEAD	1.
Load Pattern	dead point	1.
Load Pattern	dead slab	1.
Load Pattern	dead stair	1.
Load Pattern	dead wall	1.
Load Pattern	live slab	0.25
Load Pattern	live stair	0.25

Fig 4.17: Gravity load case data form

#### 4.14 Step 14 Assignment of Hinges to Frame Elements

- Assign > Frame > Hinges

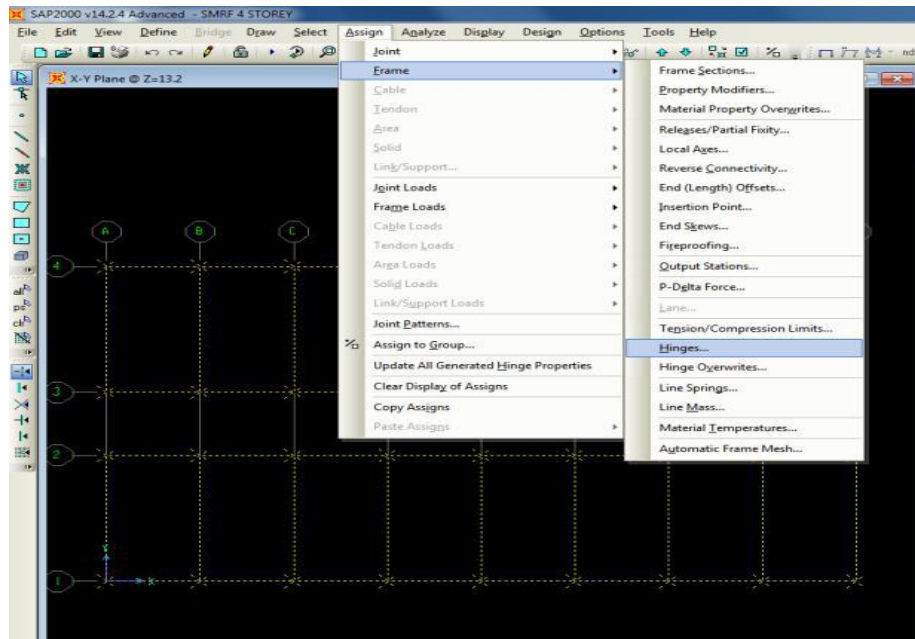
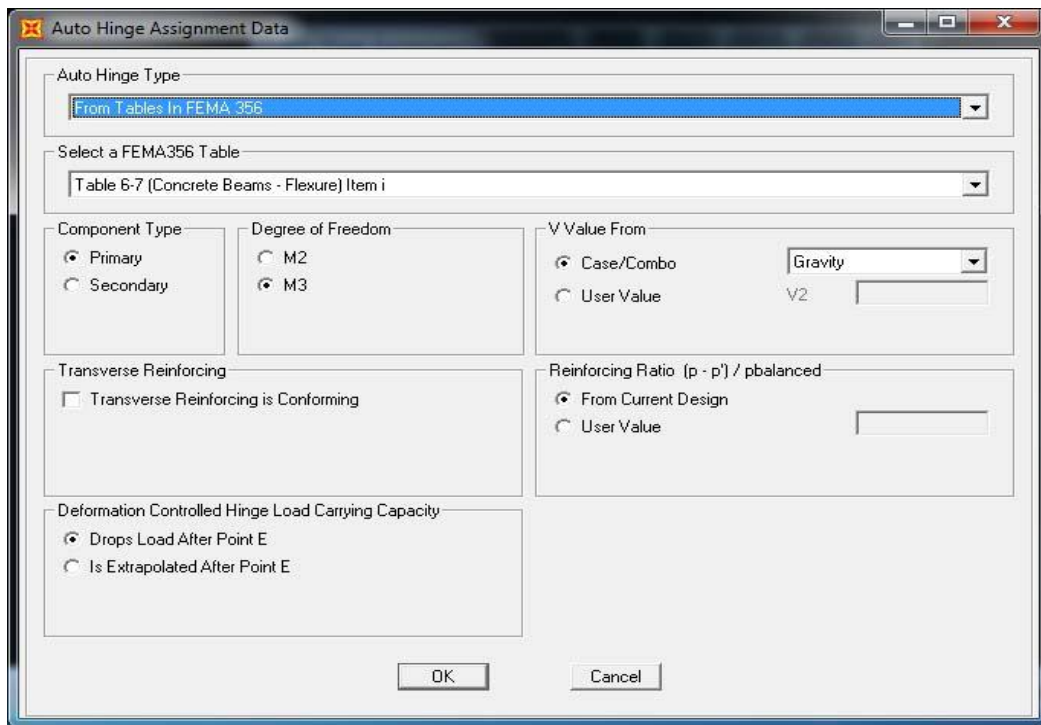


Fig 4.18: Window for assignment of frame hinges

- Add Hinges to the selected beams the hinge type form will appear



Auto Hinge Assignment Data

Auto Hinge Type  
From Tables In FEMA 356

Select a FEMA356 Table  
Table 6-7 (Concrete Beams - Flexure) Item i

Component Type  
 Primary  
 Secondary

Degree of Freedom  
 M2  
 M3

V Value From  
 Case/Combo Gravity  
 User Value V2

Transverse Reinforcing  
 Transverse Reinforcing is Conforming

Reinforcing Ratio  $(p - p') / p_{balanced}$   
 From Current Design  
 User Value

Deformation Controlled Hinge Load Carrying Capacity  
 Drops Load After Point E  
 Is Extrapolated After Point E

OK Cancel

Fig 4.19: Hinge assignment data form for concrete beams

- The hinges should be assigned at both the ends which means at the relative distance of 0.05 and 0.95 and form will appear.

Hinge Property	Relative Distance
Auto	0.
Auto M3	0.
Auto M3	1.

Auto Hinge Assignment Data  
 Type: From Tables In FEMA 356  
 Table: Table 6-7 (Concrete Beams - Flexure) Item i  
 DOF: M3

Fig 4.20 Frame hinge assignment data form

- In similar manner assign hinges to all columns by repeating steps as previously carried out for beams the only difference is that column should be assigned P-M2-M3 hinges instead of M3 hinges.

Auto Hinge Type: From Tables In FEMA 356

Select a FEMA356 Table: Table 6-8 (Concrete Columns - Flexure) Item i

Component Type:  Primary  Secondary

Degree of Freedom:  M2  M3  M2-M3  P-M2  P-M3  P-M2-M3

P and V Values From:  Case/Combo  User Value  
 Gravity

Transverse Reinforcing:  Transverse Reinforcing is Conforming

Deformation Controlled Hinge Load Carrying Capacity:  Drops Load After Point E  Is Extrapolated After Point E

Fig 4.21: Hinge assignment data form for concrete columns

#### 4.15 Step 15 Define Pushover Load Case

- **Define > Load Case > Add New Load Case > Push** consisting of load in proportion to the fundamental mode. This load case is deformation controlled load case.

Load Case Data - Nonlinear Static

Load Case Name: PUSH [Set Def Name] [Modify/Show...]

Notes: [Modify/Show...]

Load Case Type: Static [Design...]

Initial Conditions:  
 Zero Initial Conditions - Start from Unstressed State  
 Continue from State at End of Nonlinear Case [Gravity]

Important Note: Loads from this previous case are included in the current case

Modal Load Case:  
All Modal Loads Applied Use Modes from Case: MODAL

Loads Applied

Load Type	Load Name	Scale Factor
Mode	1	1.0
Mode	1	1.0

[Add] [Modify] [Delete]

Other Parameters:  
Load Application: [Displ Control] [Modify/Show...]  
Results Saved: [Multiple States] [Modify/Show...]  
Nonlinear Parameters: [Default] [Modify/Show...]

[OK] [Cancel]

Fig 4.22: Pushover load case data form

- **Load Case Type > Static, Analysis Type > Nonlinear and Geometric Nonlinearity Parameters as P-Delta.**

Load Application Control for Nonlinear Static Analysis

Load Application Control:  
 Full Load  
 Displacement Control

Control Displacement:  
 Use Conjugate Displacement  
 Use Monitored Displacement

Load to a Monitored Displacement Magnitude of: 0.789

Monitored Displacement:  
 DOF [U1] at Joint [451]  
 Generalized Displacement: [ ]

[OK] [Cancel]

Fig 4.23: Load application control data form

- In pushover load case for other parameters, to modify the steps at which results needs to be saved click **Modify** the results saved for non-linear static load case form will appear. In this form for each state **Minimum** and **Maximum** number of **saved steps** should be kept **1000** and **5000** in order to avoid solution coverage.

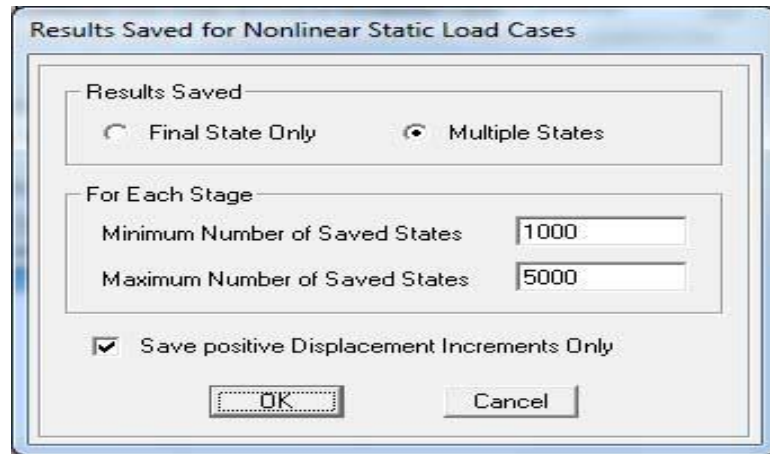


Fig 4.24: Minimum and maximum number of saved states form

- For **unloading the hinge**, **Unload Entire Structure** method should be used as shown non-linear parameter form.

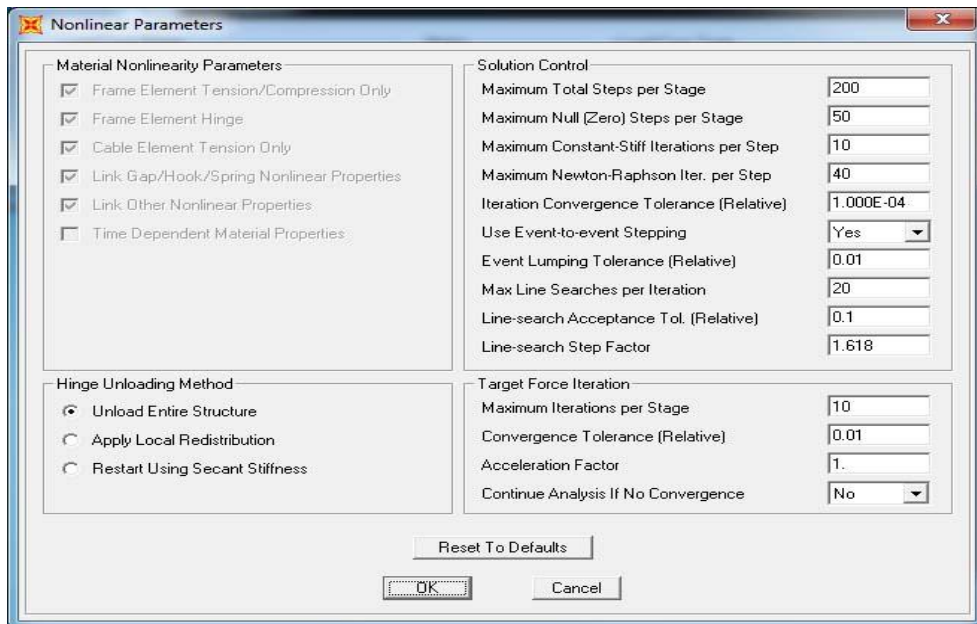


Fig 4.25: Solution control form for nonlinear parameters

#### 4.16 Step 16 Graphically review of the Results

- Go to > Display > Show Static Pushover Curve

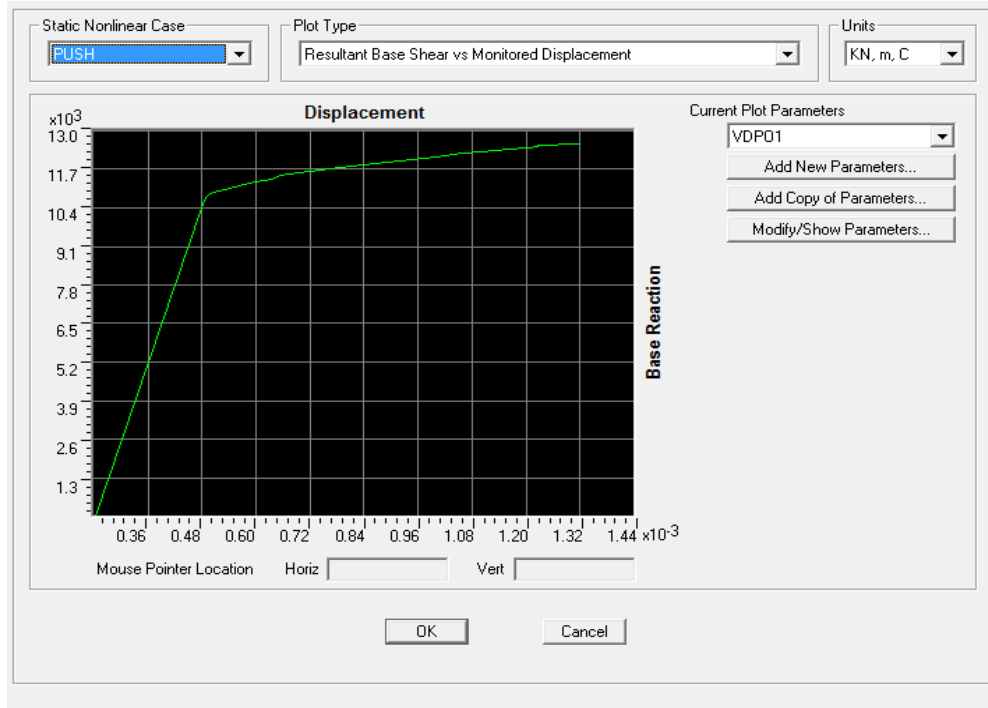


Fig 4.26: Display window for Static pushover curve

- Go to Display > Show Deformed Shape > Select Load Case > PUSH

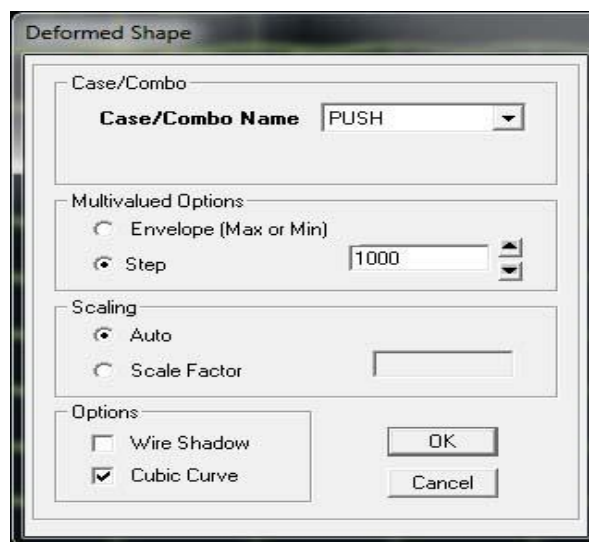


Fig 4.27: Deformed shape data form

### 5.1 General

The present study is intended for simplified analysis procedure to perform seismic evaluation of some symmetric and asymmetric building models. A NSP based analysis is done according to FEMA 356CM, FEMA 440 DM, ATC 40 CSM on G plus four storied building models following same structural gridlines and elevation. Initially pushover analysis is performed on the OMRF skeleton model of the buildings in SAP-2000 platform. The gravity loads are incrementally increased at first in a force controlled manner. Then the lateral pushover subjected separately in X & Y directions in displacement controlled manner. The distribution of the lateral force is assumed to be model adaptive distribution with high mode. Seismic performances of the models are observed along with vulnerability indices.

**5.2 Case Study:** The preliminary design parameters of the numerical models are as follows:

1. Grade of concrete used is M 20 and grade of steel used is Fe 415.
2. Unit weight of R.C.C is  $25 \text{ KN/m}^3$ , unit weight of P.C.C is  $24 \text{ KN/m}^3$  and unit weight of masonry wall is  $20 \text{ KN/m}^3$ .
3. Building frame type is O.M.R.F.
4. Floor to floor height is 3.2 m.
5. Plinth height above G.L is 0.6 m.
6. Depth of foundation is 1.2 m below G.L.
7. Parapet wall height is 1.5 m.
8. Floor slab thickness is 125 mm and roof slab thickness is 140mm.
9. External wall thickness is 250 mm and internal wall thickness is 125 mm.
10. Size of columns are 350mm x450 mm and size of beams are 300 mm x 400 mm.

11. Live load on floor is  $2.5 \text{ KN/m}^3$  and live load on roof is  $1.5 \text{ KN/m}^3$ .
12. Site located in seismic zone III.
13. Building is resting on medium soil.
14. Finishing (floor and plaster) thickness is 35 mm.
15. Finishing (roof treatment and plaster) thickness is 40 mm.
16. Opening for exterior walls is 50% and opening for internal walls is 15%.

### 5.2.1 : Load Calculations:

#### i) Wall load:

External wall load intensity =  $\{0.25 \times 1 \times (3.2-0.4) \times 20 \times 0.5\} \text{ KN/m} = 7 \text{ KN/m}$

Internal wall load intensity =  $\{0.125 \times 1 \times (3.2-0.4) \times 0.85 \times 20\} \text{ KN/m} = 5.95 \text{ KN/m}$

Parapet wall load intensity =  $\{0.125 \times 1 \times 1.5 \times 20\} \text{ KN/m} = 3.75 \text{ KN/m}$

#### ii) Load from floor and roof slabs:

Floor slab D.L intensity =  $(0.125 \times 25 + 0.035 \times 24) \text{ KN/m}^2 = 3.965 \text{ KN/m}^2 = 4 \text{ KN/m}^2$  (approx)

Roof slab D.L intensity =  $(0.14 \times 25 + 0.04 \times 24) \text{ KN/m}^2 = 4.46 \text{ KN/m}^2 = 4.5 \text{ KN/m}^2$  (approx)

**Table 5-1: Slab loading intensity**

Type of load	Type of slab	Shorter span length(m)	Trapezoidal/Triangular load ordinate(max) in KN/m on beam	
			Type of beam	
			Slab on one side	Slab on both sides
D.L	Floor	4	8	16
		3	6	12
	Roof	4	9	18
		3	6.75	13.5
L.L	Floor	4	5	10
		3	3.75	7.5
	Roof	4	3	6
		3	2.25	4.5



The typical gridline plan and Y face elevation of the models as shown in figure 5.1 and 5.2 is considered for case study.

### 5.3 FOUR STORIED O.M.R.F BUILDING

The typical gridline plan and typical Y face elevation of all the models are given below.

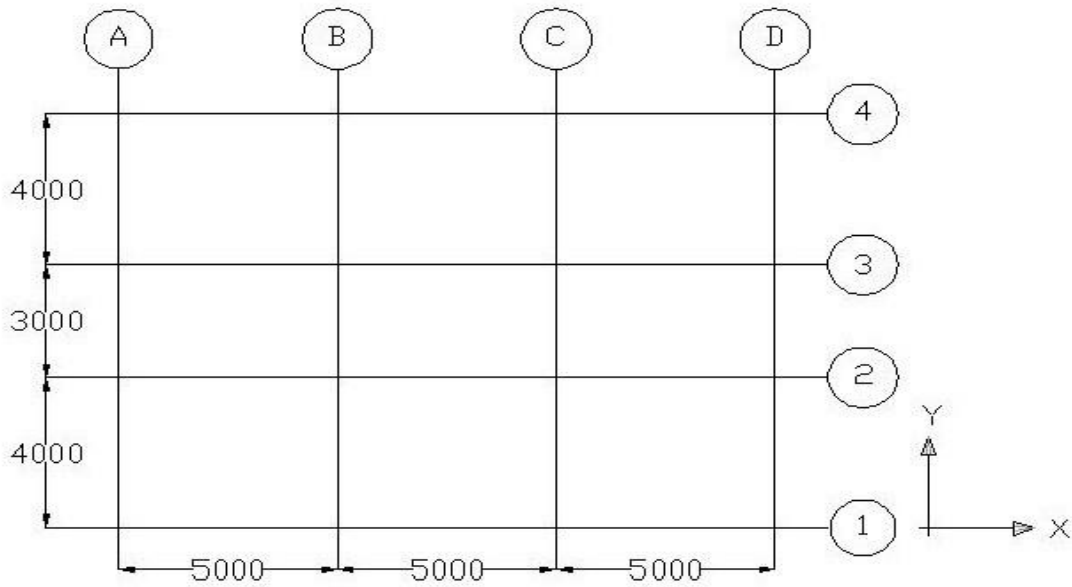


Fig 5.1 TYPICAL GRIDLINE PLAN OF MODELS

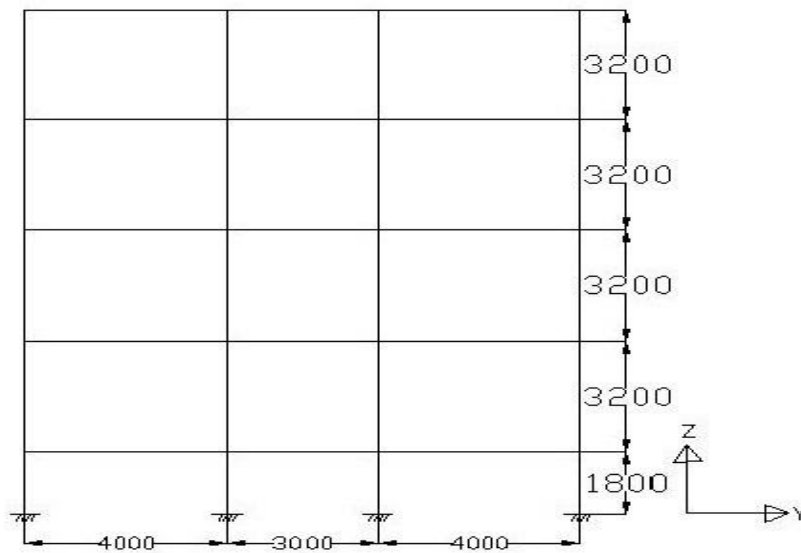


Fig 5.2 TYPICAL Y FACE ELEVATION OF MODELS

## 5.4 MODELS SYMMETRIC ABOUT BOTH X & Y AXES

### 5.4.1 MODEL 1: RECTANGULAR MODEL

The plan and other details of rectangular model are given below.

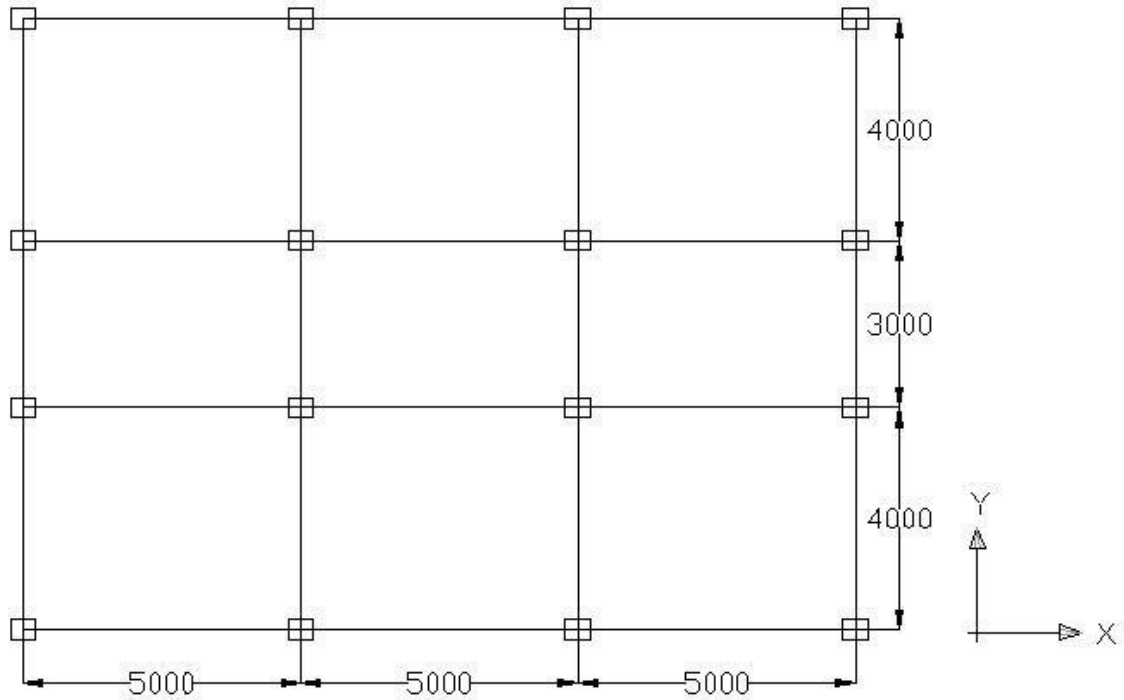


Fig 5.3 PLAN OF RECTANGULAR MODEL

The major axis of the columns are along X axis. The building is regular O.M.R.F type. The sap skeleton model with slab diaphragm and wall diaphragm along with their load distribution pattern are given below separately. The slabs and walls are assumed as rigid diaphragm and the loading (D.L + L.L) are given accordingly.

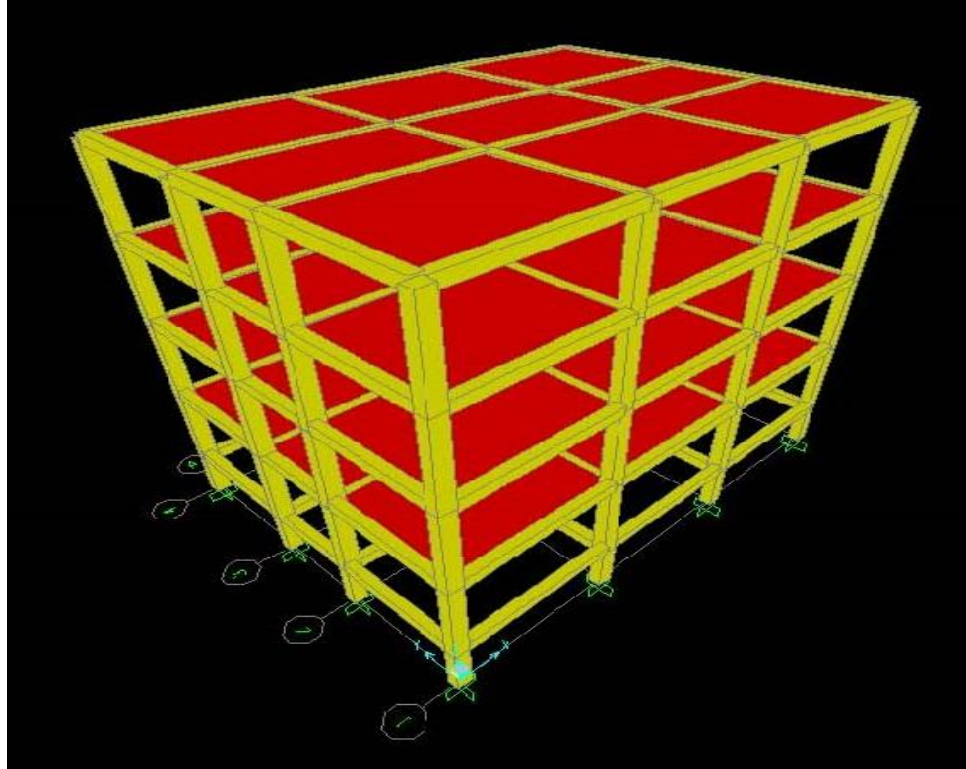


Fig 5.4 : Isometric view of rectangular model with slab diaphragm

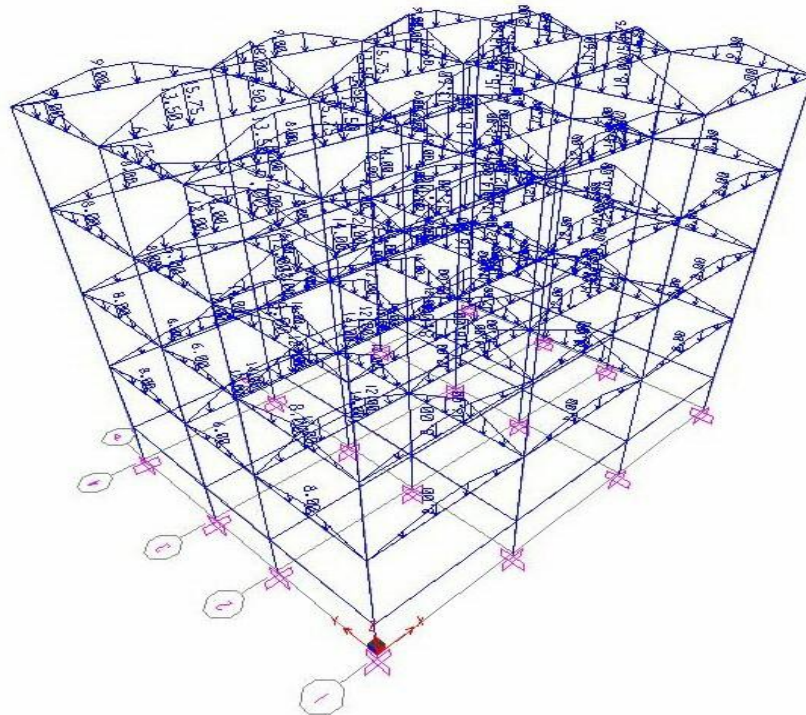


Fig 5.5 Slab loading pattern of rectangular model

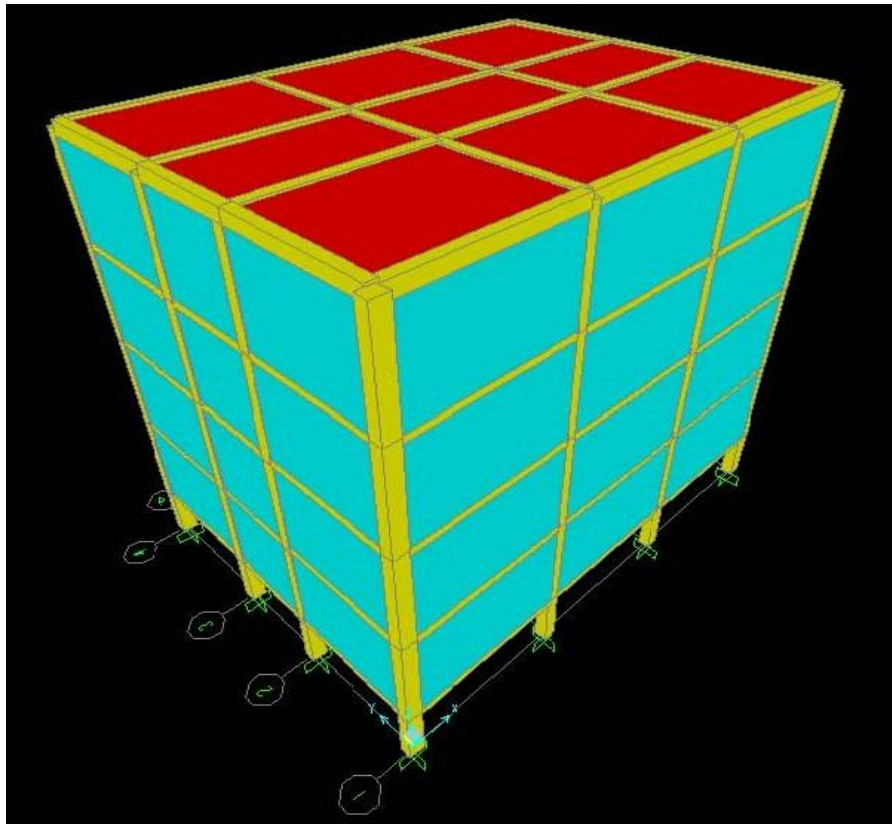


Fig 5.6: Isometric view of rectangular model with wall diaphragm

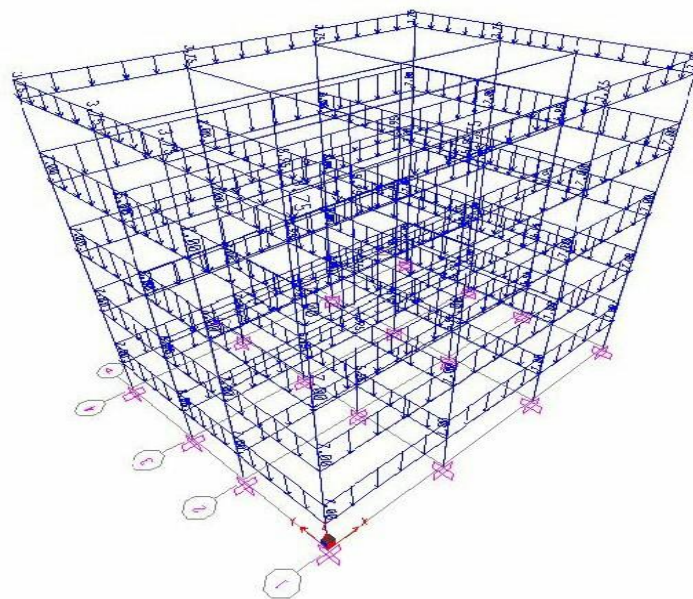
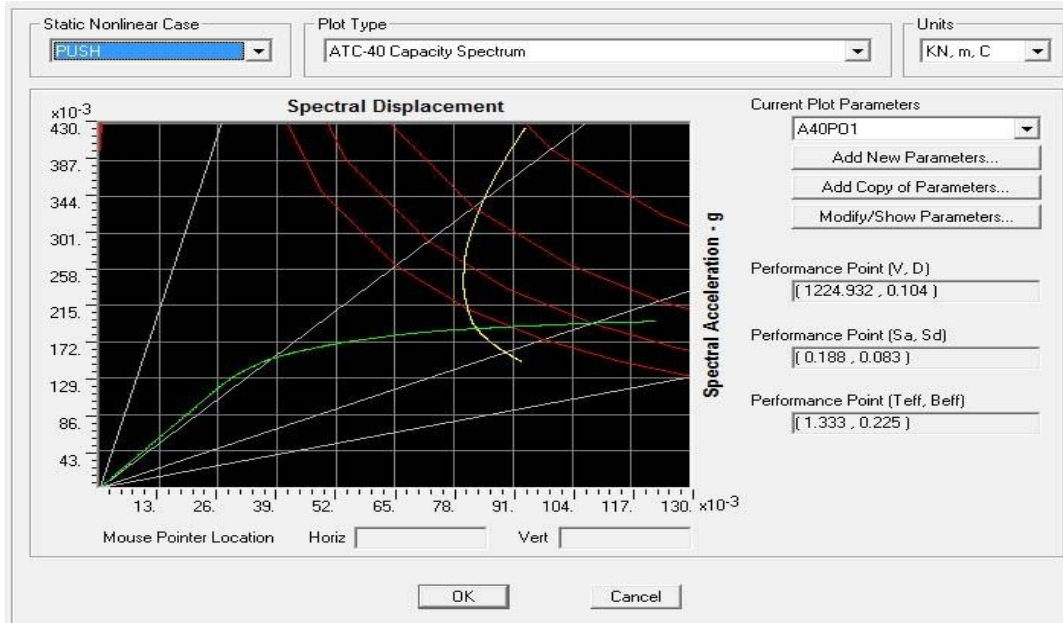
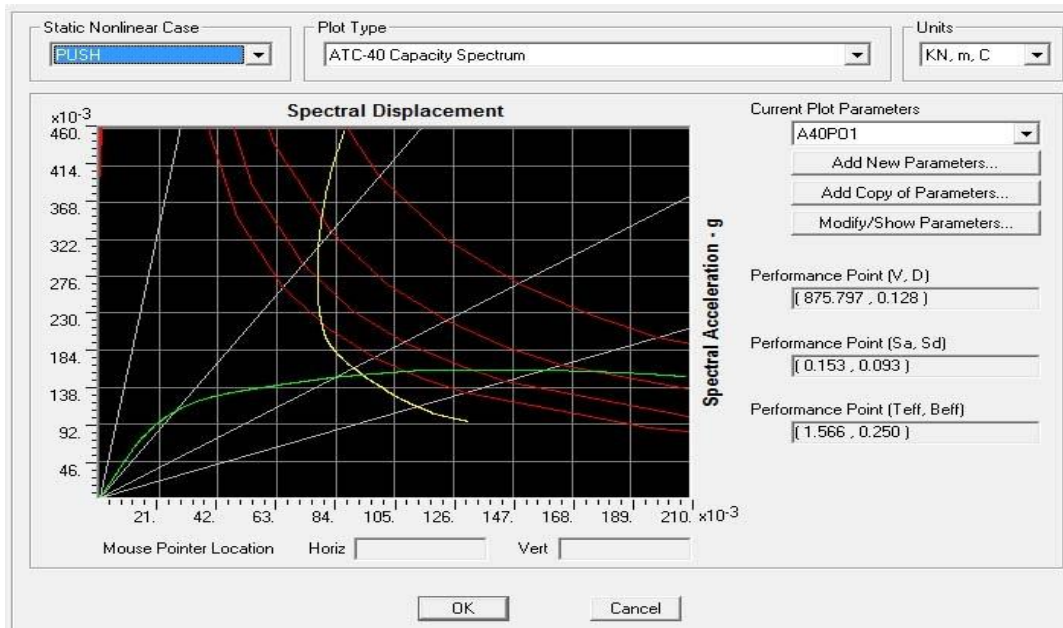


Fig 5.7 Wall loading pattern of rectangular model

Results (Pushover curve, demand and capacity spectrum) from rectangular model in X & Y direction are shown below where green colour indicates the pushover curve in capacity spectrum, yellow colour indicates demand spectrum and performance point shown separately.



**Fig 5.8 Rectangular model ATC 40 (X)**



**Fig 5.9 Rectangular model ATC 40 (Y)**

### 5.4.2 MODEL 2: MODEL H

The plan and other details of model H are given below.

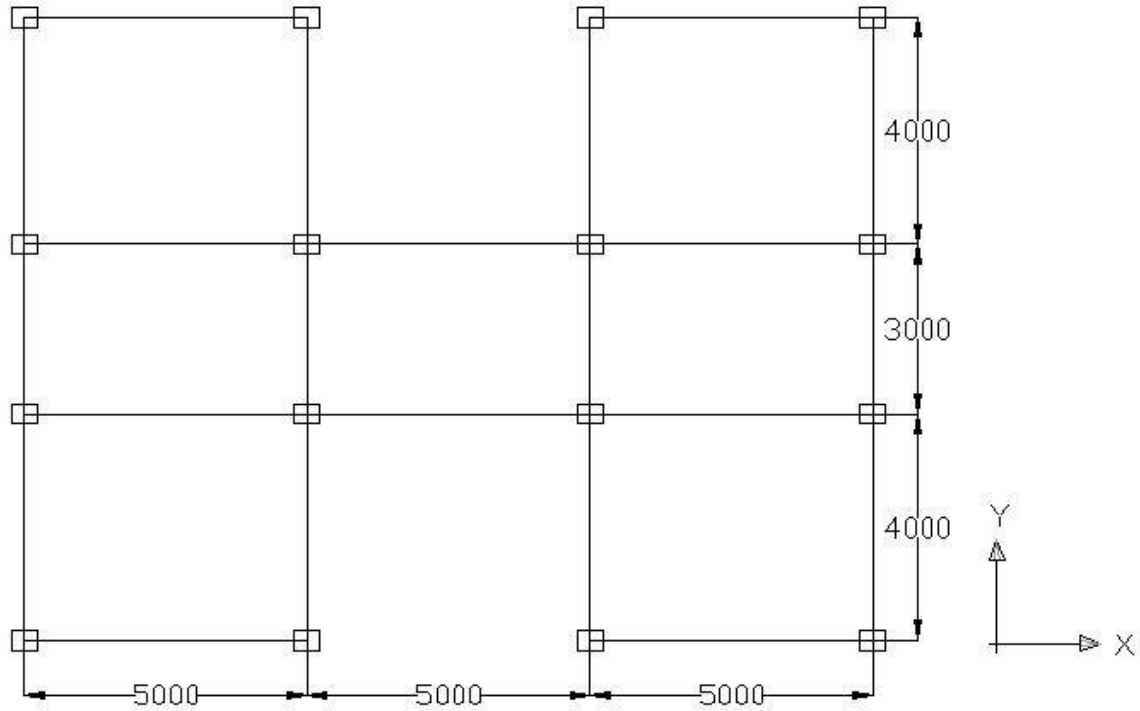


Fig 5.10 PLAN OF MODEL H

The major axis of the columns are along X axis. The building is regular O.M.R.F type. The sap skeleton model with slab diaphragm and wall diaphragm along with their load distribution pattern are given below separately. The slabs and walls are assumed as rigid diaphragm and the loading (D.L + L.L) are given accordingly.

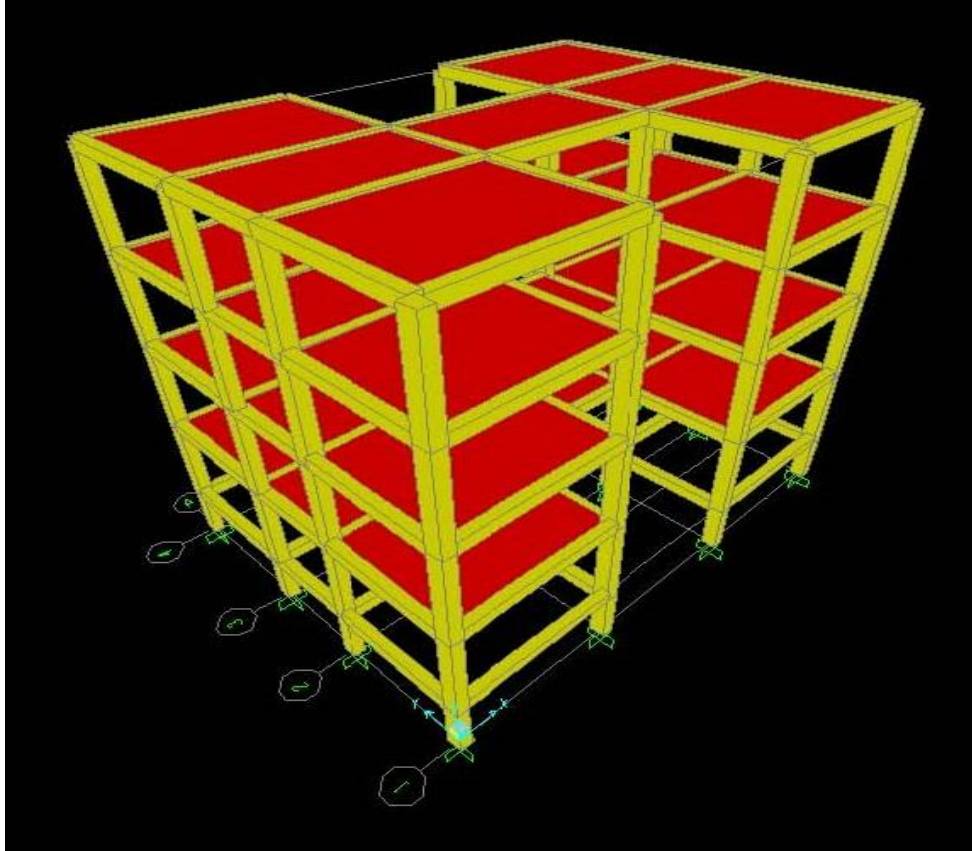


Fig 5.11: Isometric view of model H with slab diaphragm

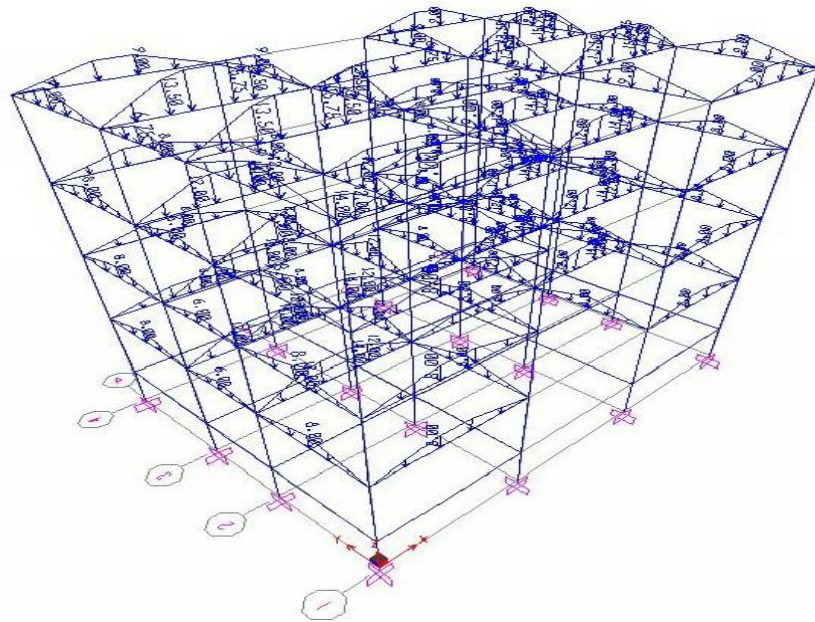


Fig 5.12 Slab loading pattern of model H

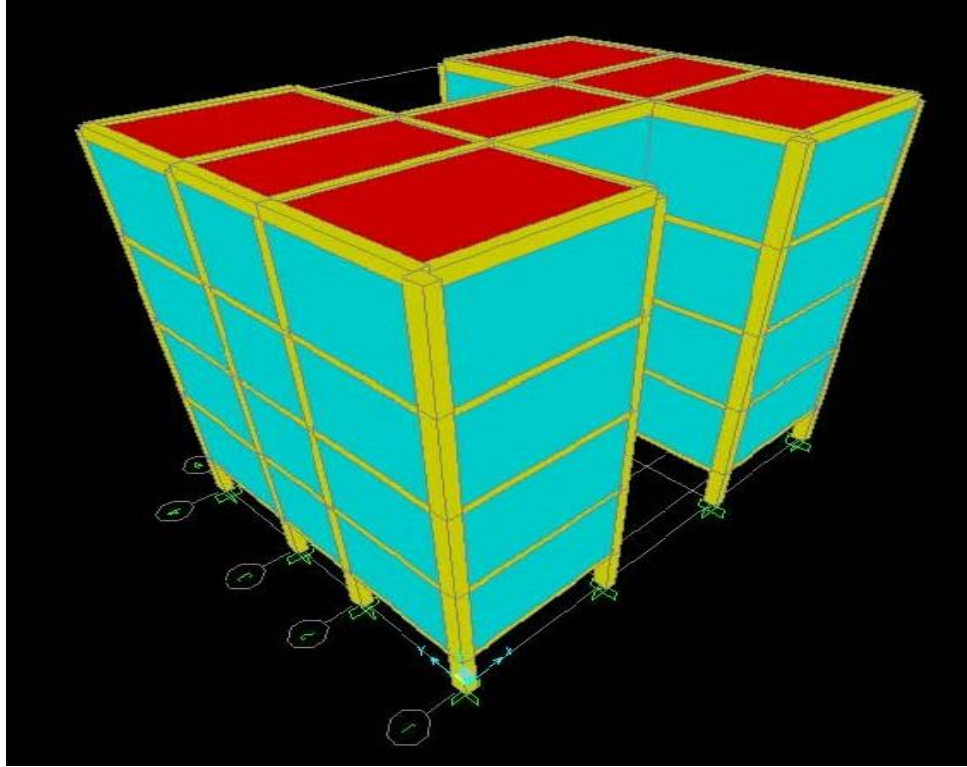


Fig 5.13: Isometric view of model H with wall diaphragm

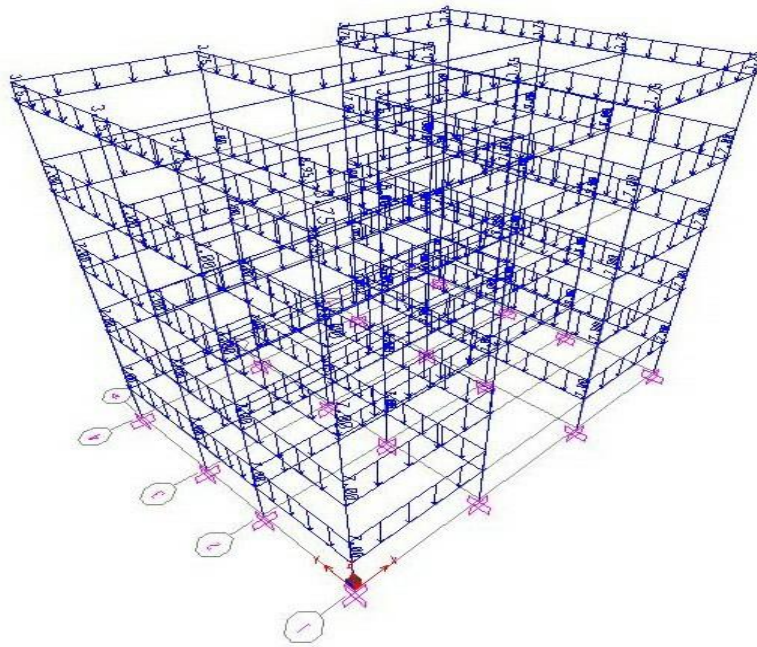
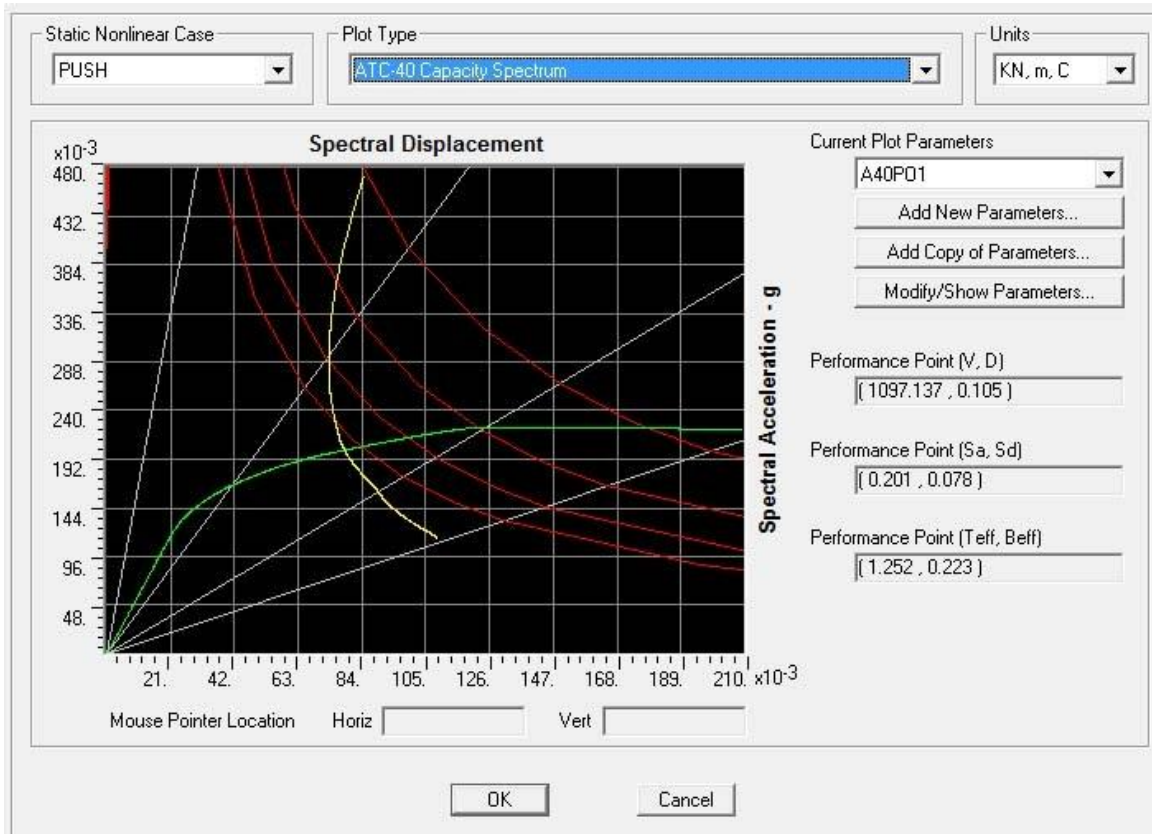


Fig 5.14 Wall loading pattern of model H



Results (Pushover curve, demand and capacity spectrum) from model H in X & Y direction are shown below where green colour indicates the pushover curve in capacity spectrum; yellow colour indicates demand spectrum and performance point shown separately.



**Fig 5.15 Model H ATC 40 (X)**

Due to mass and stiffness irregularity in the second bay of model H in Y direction there was convergence problem while conducting non linear pushover analysis in Y direction. Thus subsequent results such as pushover curve, demand and capacity spectrum were not available in Y direction.

### 5.4.3 MODEL 3: MODEL I

The plan and other details of model I are given below.

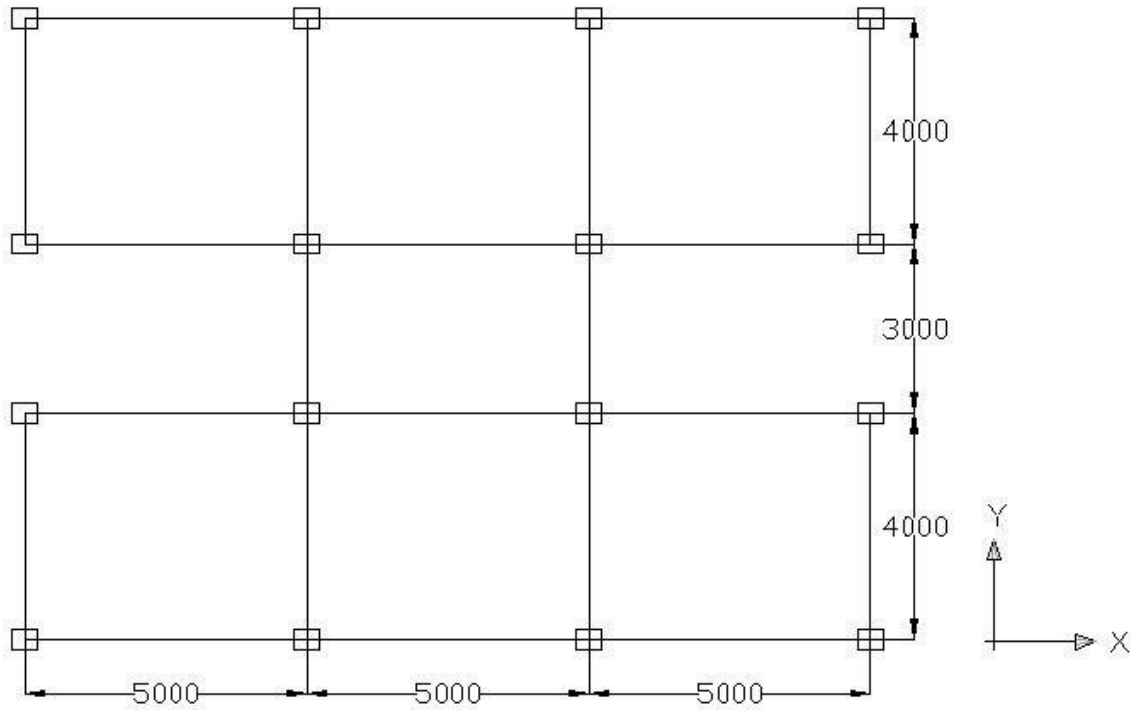


Fig 5.16 PLAN OF MODEL I

The major axis of the columns are along X axis. The building is regular O.M.R.F type. The sap skeleton model with slab diaphragm and wall diaphragm along with their load distribution pattern are given below separately. The slabs and walls are assumed as rigid diaphragm and the loading (D.L + L.L) are given accordingly.

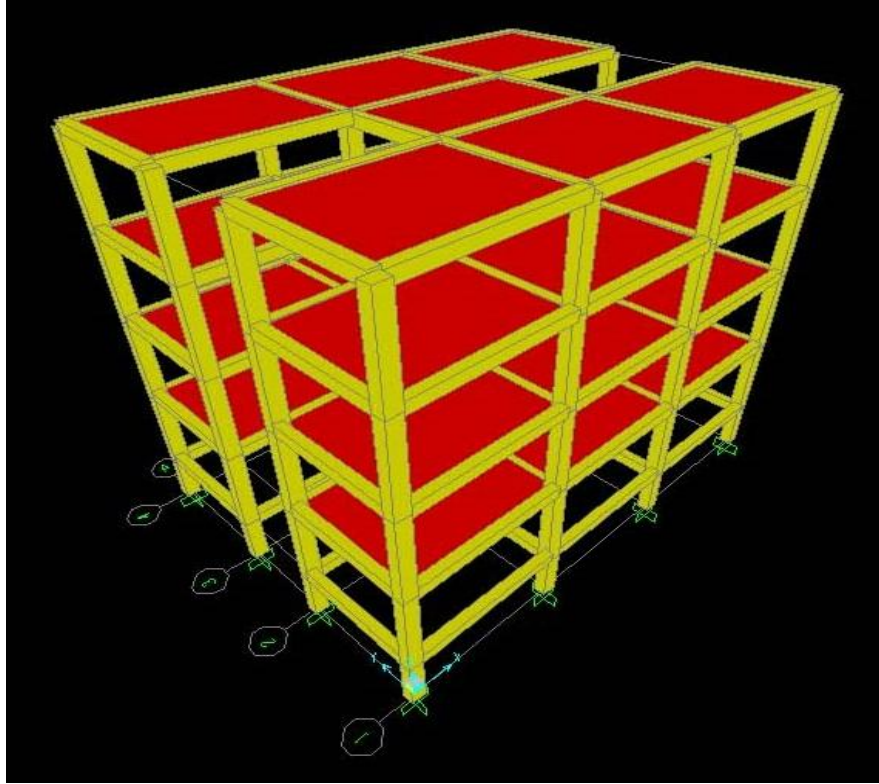


Fig 5.17: Isometric view of model I with slab diaphragm

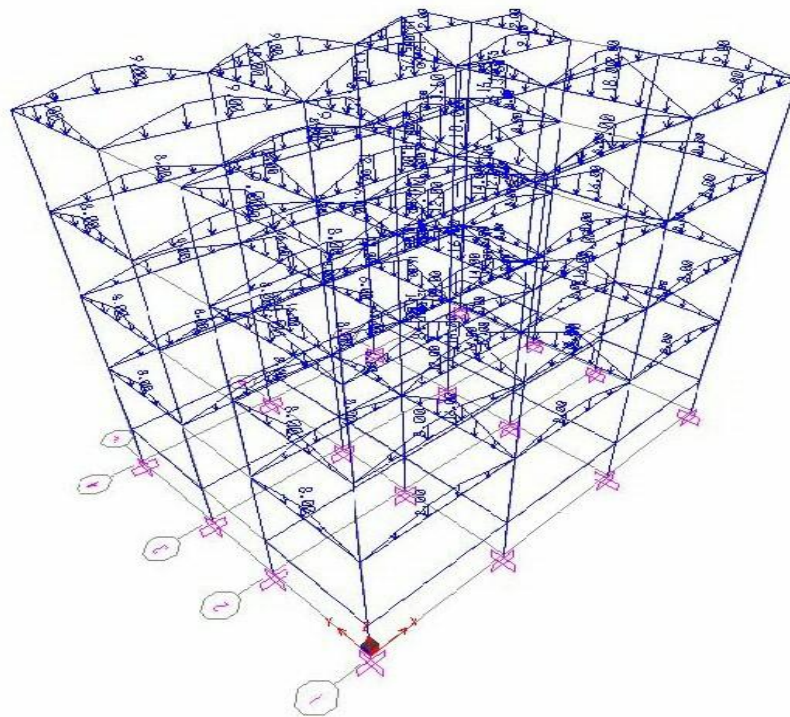


Fig 5.18 Slab loading pattern of model I

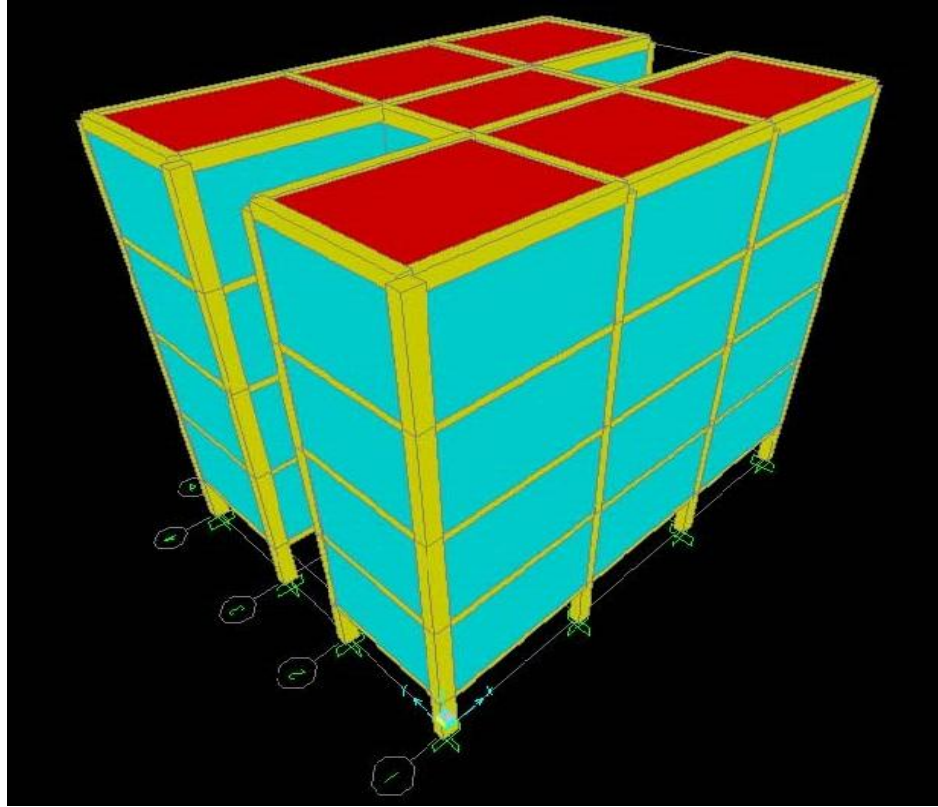


Fig 5.19: Isometric view of model I with wall diaphragm

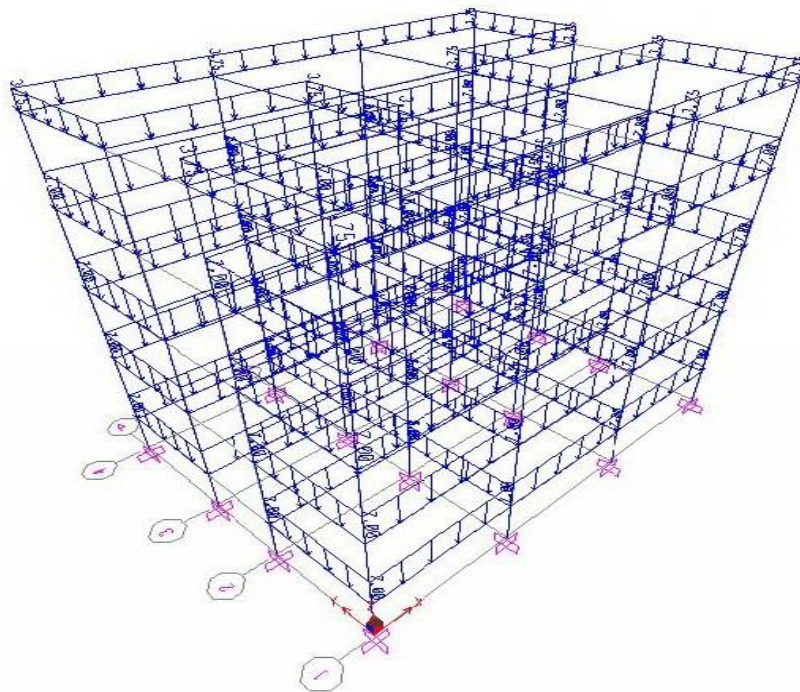
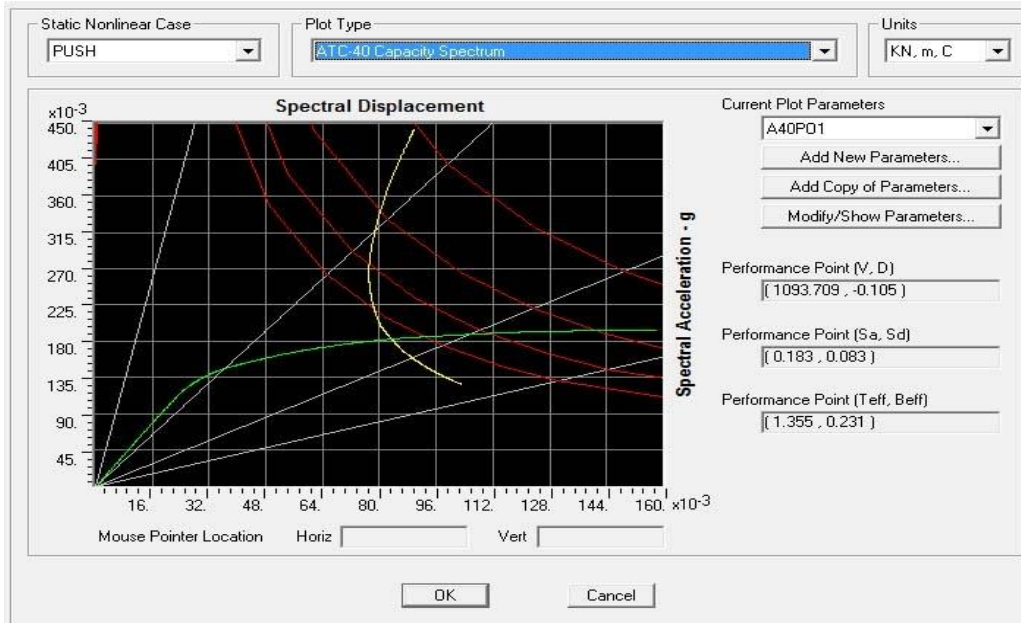
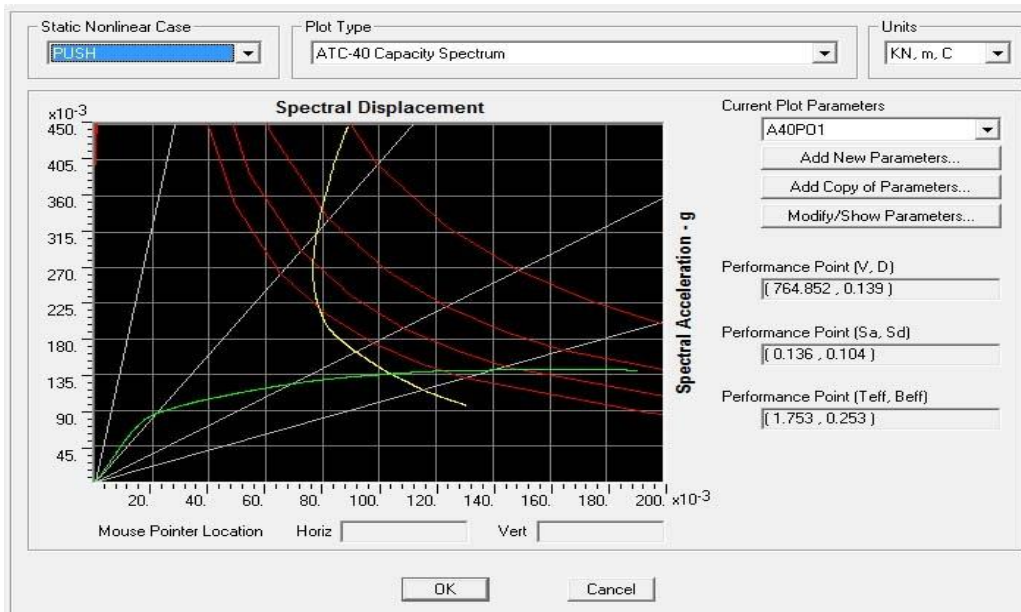


Fig 5.20 Wall loading pattern of model I

Results (Pushover curve, demand and capacity spectrum) from model I in X & Y direction are shown below where green colour indicates the pushover curve in capacity spectrum, yellow colour indicates demand spectrum and performance point shown separately.



**Fig 5.21 Model I ATC 40 (X)**



**Fig 5.22 Model I ATC 40 (Y)**

#### 5.4.4 MODEL 4: MODEL O

The plan and other details of model O are given below.

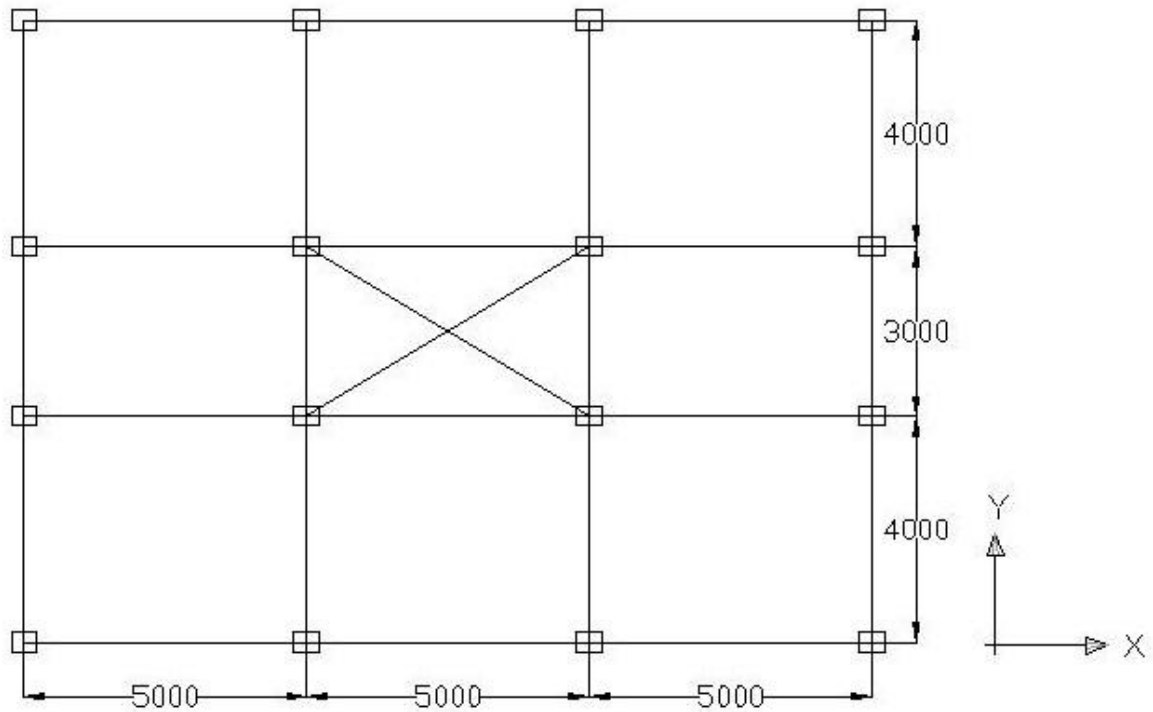


Fig 5.23 PLAN OF MODEL O

The major axis of the columns are along X axis. The building is regular O.M.R.F type. The sap skeleton model with slab diaphragm and wall diaphragm along with their load distribution pattern are given below separately. The slabs and walls are assumed as rigid diaphragm and the loading (D.L + L.L) are given accordingly.

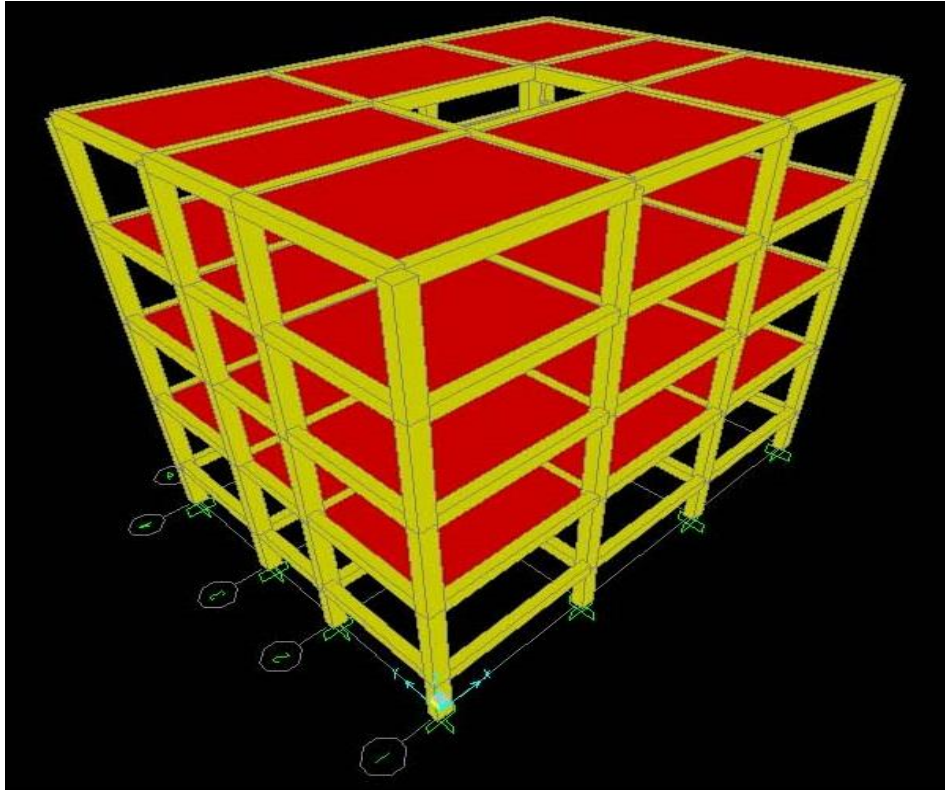


Fig 5.24 : Isometric view of model O with slab diaphragm

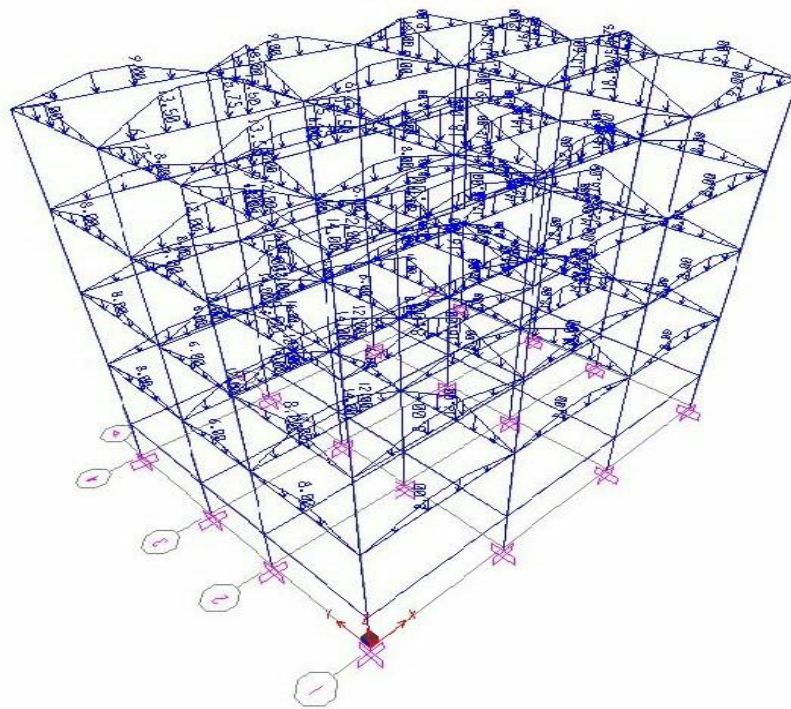


Fig 5.25 Slab loading pattern of model O

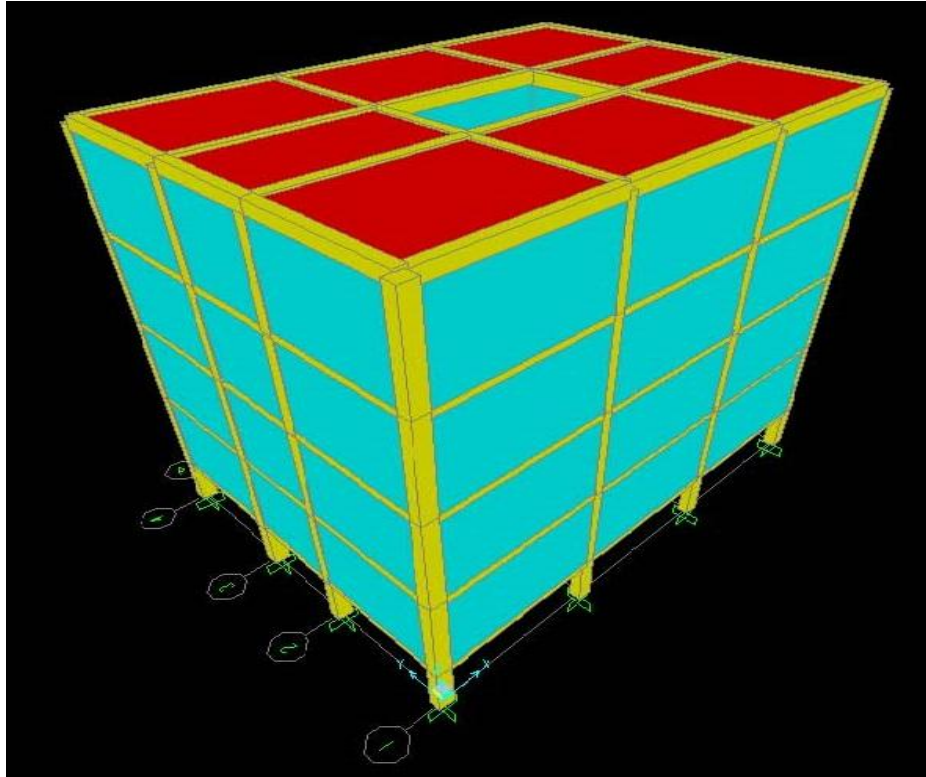


Fig 5.26: Isometric view of model O with wall diaphragm

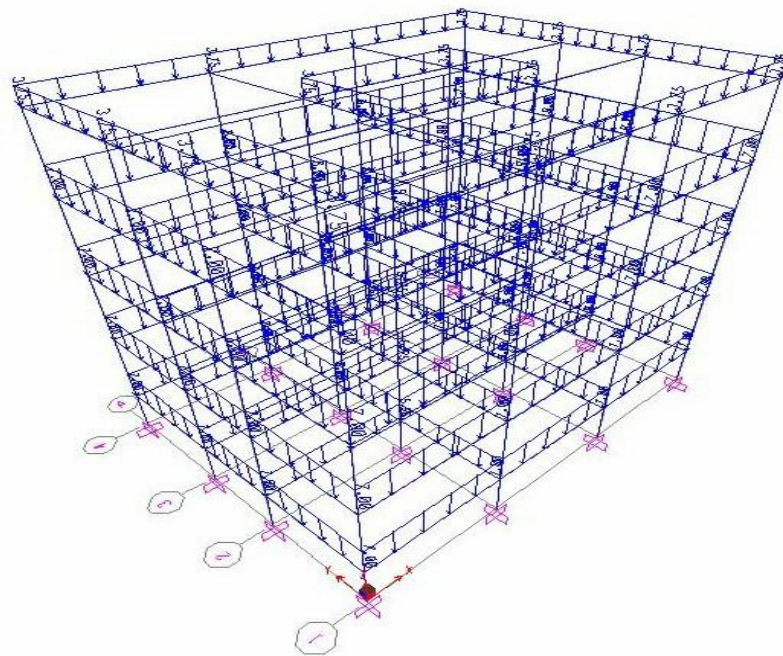
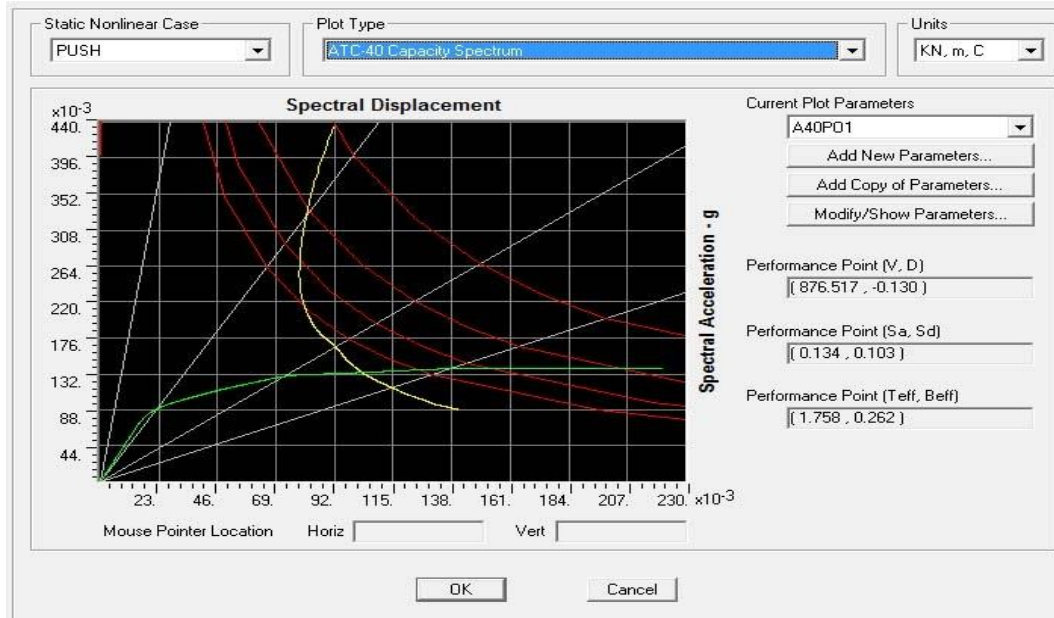


Fig 5.27 Wall loading pattern of model O



Results (Pushover curve, demand and capacity spectrum) from model O in X & Y direction are shown below where green colour indicates the pushover curve in capacity spectrum, yellow colour indicates demand spectrum and performance point shown separately.



**Fig 5.28 Model O ATC 40 (X)**

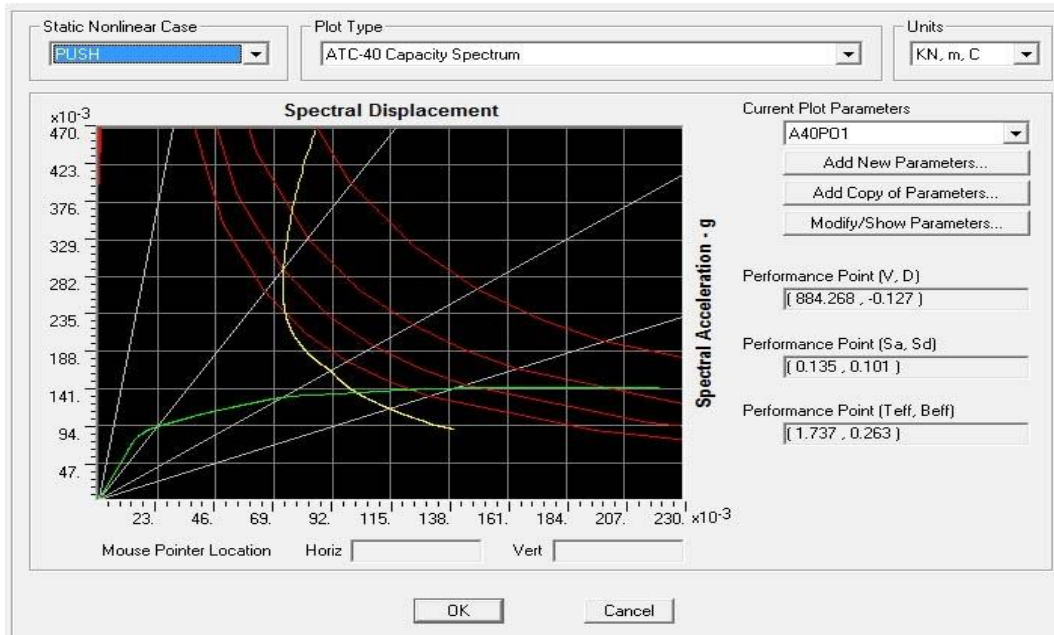


**Fig 5.29 Model O ATC 40 (Y)**

#### 5.4.5 RESULT DISCUSSION OF SYMMETRIC MODELS:

Summary of the results obtained from pushover analysis for model 1 to 4 in X & Y direction are given in table 5-2 and table 5-3 respectively.

**Table5-2 : Comparison of various seismic resisting features of symmetric models along X direction**

MODEL TYPE	DIRCTION	BASE SHEAR (V) in KN	PLAN AREA(m <sup>2</sup> )	BASE SHEAR PER UNIT AREA	ROOF DISPLACEMENT (D) in m	SPECTRAL ACCLERETION (Sa) in m/s <sup>2</sup>	SPECTRAL DISPLACEMENT (Sd) in m	EFFECTIVE PERIOD (Teff) in s	EFFECTIVE DAMPING ( $\beta_{eff}$ )
RECT	X	1224.93	165	7.42383	0.104	0.188	0.083	1.333	0.225
H		1097.14	125	8.7771	0.105	0.201	0.078	1.252	0.223
I		1093.71	135	8.10155	0.105	0.183	0.083	1.355	0.231
O		876.517	150	5.84345	0.13	0.134	0.103	1.758	0.262

**Table5-3 : Comparison of various seismic resisting features of symmetric models along Y direction**

MODEL TYPE	DIRCTION	BASE SHEAR (V) in KN	PLAN AREA(m <sup>2</sup> )	BASE SHEAR PER UNIT AREA (KN/m <sup>2</sup> )	ROOF DISPLACEMENT (D) in m	SPECTRAL ACCLERETION (Sa) in m/s <sup>2</sup>	SPECTRAL DISPLACEMENT (Sd) in m	EFFECTIVE PERIOD (Teff) in s	EFFECTIVE DAMPING ( $\beta_{eff}$ )
RECT	Y	875.797	165	5.30786	0.128	0.153	0.093	1.566	0.25
H		Convergence problem in Y direction							
I		764.852	135	5.66557	0.139	0.136	0.104	1.753	0.253
O		762.547	150	5.08365	0.127	0.135	0.101	1.737	0.263

Comparison of base shear and roof displacement along X & Y direction are given in Fig 5.30 and 5.31 respectively for better understanding.

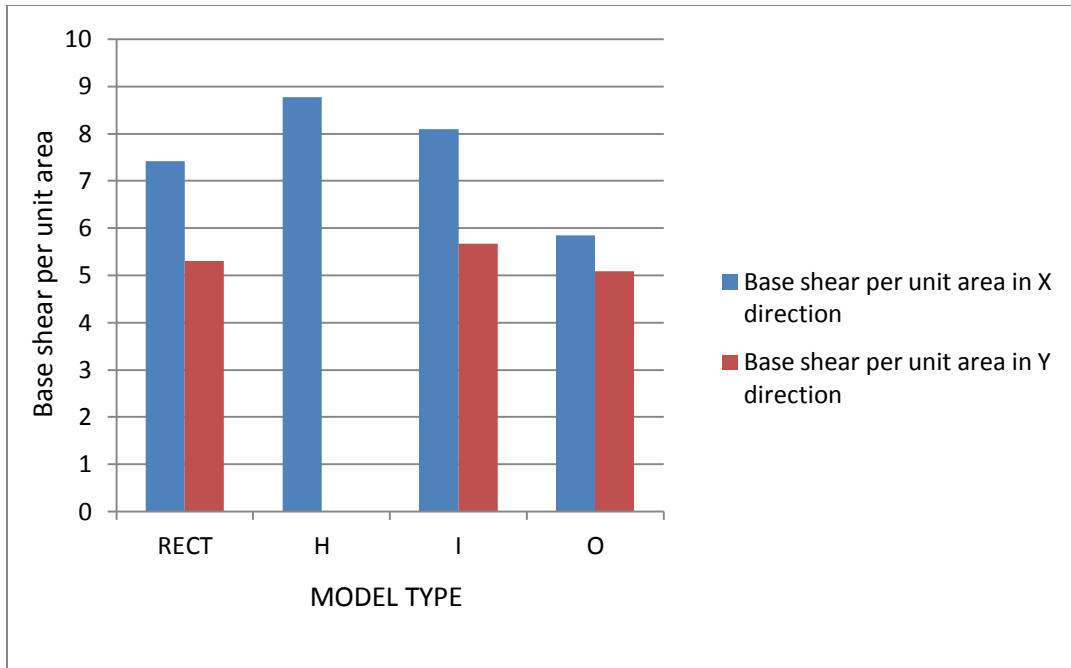


Fig 5.30: BASE SHEAR (V) of symmetric models in X & Y Direction

It is observed that the base shear capacity per unit area of rectangular model, model H and model I are higher than those of the model O in both X and Y directions as model O has got a void space in the central region of its plan area. At the same time base shear capacity in Y direction of all the models are considerably lower than base shear capacity in X direction. This happens as the base dimension in X direction is more than that of Y direction.

In case of model H there was a convergence problem while performing non-linear analysis in Y direction as in the second bay there is a sudden reduction of mass and stiffness resulting in irregularity in Y direction.

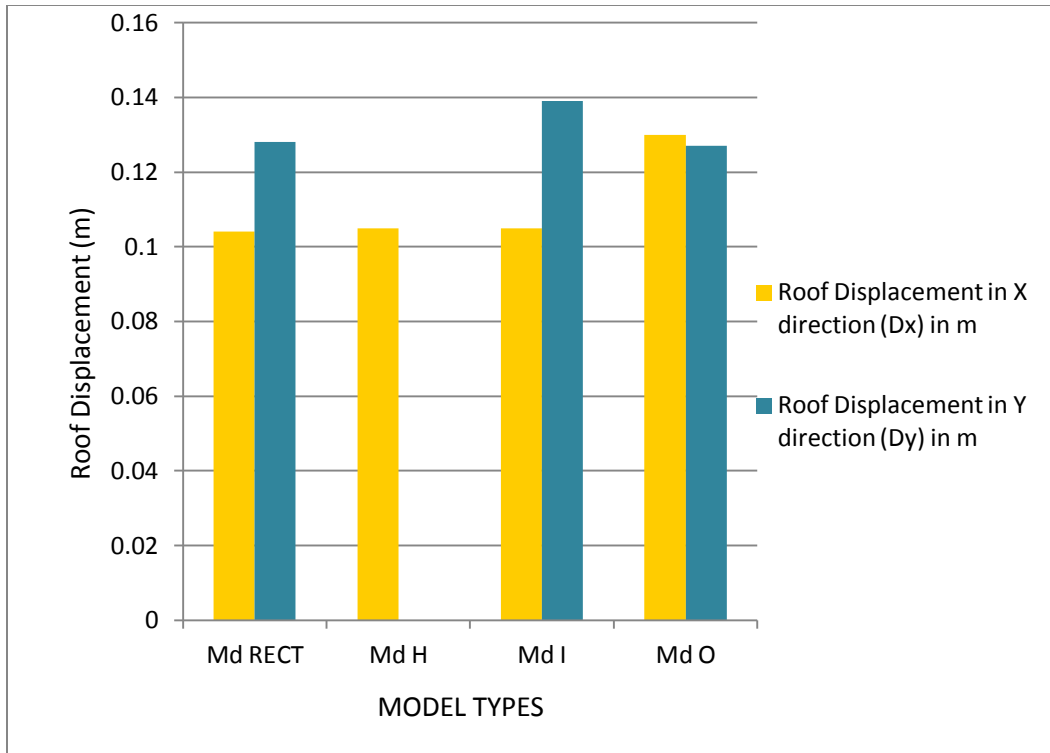


Fig 5.31: ROOF DISPLACEMENT ( $D_{rf}$ ) of symmetric models in X & Y Direction

Roof displacement in Y direction is higher than roof displacement in X direction in general because of the higher rigidity in X direction. Roof displacement in X direction of model O is higher than those of the other models as the diaphragm rigidity of model O is minimum among the symmetric models.

Roof displacement of model I in Y direction is significantly higher due to reduced stiffness in the 1<sup>st</sup> and 3<sup>rd</sup> bay in Y direction. For model O roof displacements in both the directions are more or less same as the base shear capacity for this particular model are nearby in both the directions.

Comparison of Spectral Acceleration and Spectral displacement along X & Y direction of the symmetric models considered are shown in Fig 5.32 & 5.33 respectively.

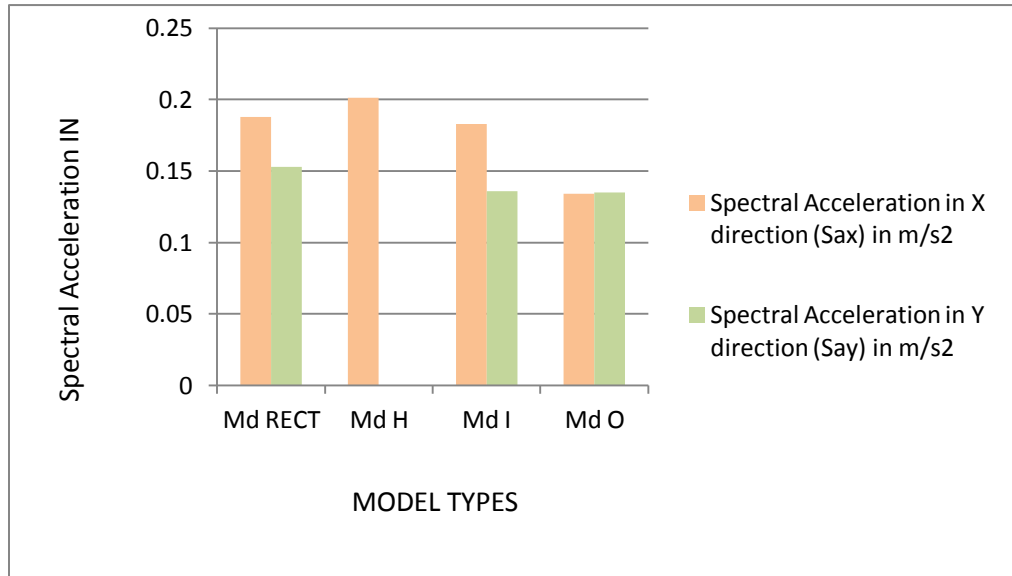


Fig 5.32: Spectral Acceleration of symmetric models ( $S_a$ ) in X & Y Direction

Spectral acceleration in rectangular model, model H, I are in tune in X direction due to similar lateral stiffness and mass distribution. For models rectangle and I spectral accelerations are lower in Y direction than that in X direction but for model O spectral acceleration in X and Y direction are more or less same and lower than spectral accelerations of other models in X direction.

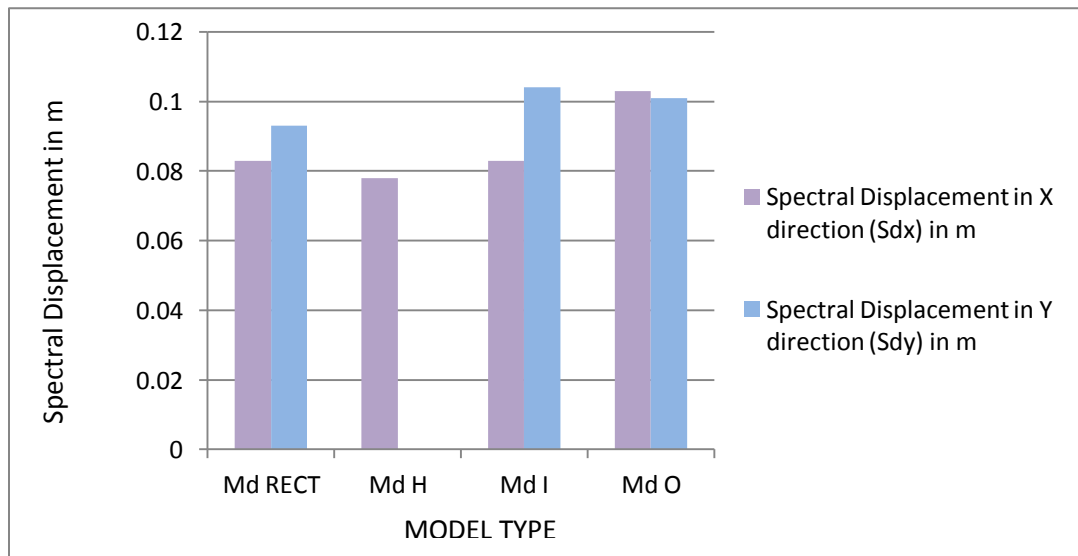


Fig 5.33: Spectral Displacement ( $S_d$ ) of symmetric models in X & Y Direction

Spectral displacement in Y direction is higher than spectral displacement in X direction in general. Spectral displacement of model O is higher than those of the other models in X direction. For the other models spectral displacements in X direction are more or less similar. Spectral displacement of model I in Y direction is significantly higher. These observations are of similar nature as those of roof displacements.

Comparison of Global Stiffness of different symmetric models is shown in Fig 5.34

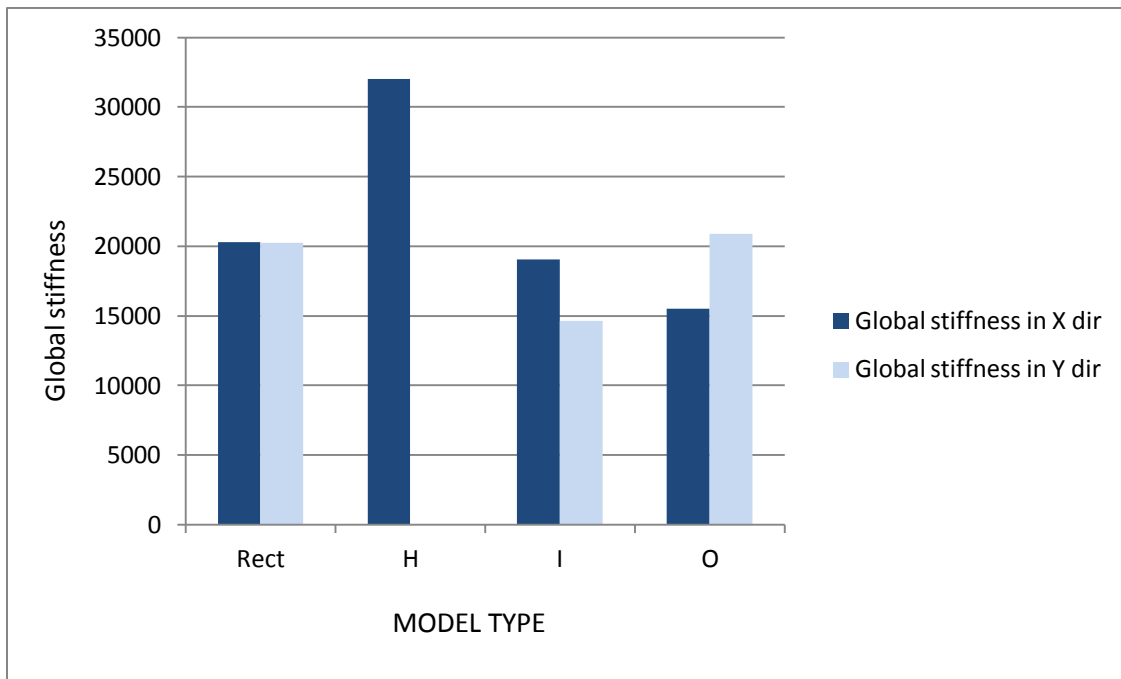


Fig 5.34: Global Stiffness of symmetric models in X & Y Direction

Global stiffness is more or less similar for rectangular model and model I in X direction. For model H it is significantly higher in X direction and for model O it is slightly lower than model 1 and model 3. This happened due to orientation of mass along X direction.

For rectangular model global stiffness in both the directions are same. For model I it is a bit higher in X direction and for model O scenario is opposite. In I model there is a discontinuity of mass in the 1<sup>st</sup> and 3<sup>rd</sup> bay in Y direction. For the same reason global

stiffness of model O is lower in X direction but for Y direction removal of mass from the unequally spaced grid gave advantage contributing higher global stiffness in Y direction.

**Table 5-4:  $VI_{\text{bdg}}$  in both direction for Symmetric models**

Type of Model	Direction	$VI_{\text{bdg}}$
RECT	X	0.41754
H		0.625
I		0.41888
O		0.6525
RECT	Y	0.46875
H		
I		0.56406
O		0.54167

Comparison of Building Vulnerability of different symmetric models is shown in Fig 5.35:

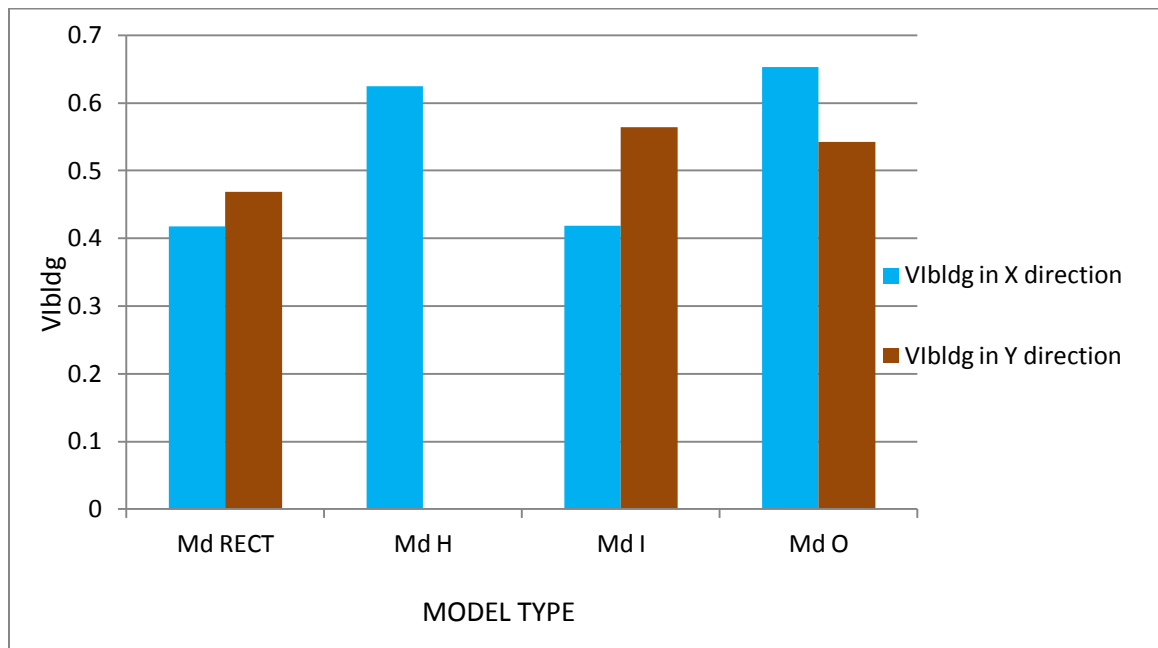


**Fig 5.35: Building Vulnerability ( $VI_{\text{bdg}}$ ) of symmetric models in X & Y Direction**

Building vulnerability of models H and O are on higher side than in X direction which may be due to discontinuous diaphragm action. However, the Vulnerability Index of model I has not properly manifested by the above result.

Building vulnerability of models I and O are on higher side compared to rectangular model due to the disturbed diaphragm action in Y direction.

**Table 5-5:  $VI_{storey}$  in both direction for Symmetric models at all levels**

Vistorey in both direction for Symmetric models					
Storey Height(m)	Direction	MODEL TYPE			
		RECT	H	I	O
0	X	0.125	0.25	0.125	1
1.8		0.78125	0.25	0.78125	0.125
5		0	0	0	0
8.2		0.125	0	0	0
11.4		0.125	0	0.125	0
14.6		0	0	0	0
0	Y	0	Converge nce problem in Y direction	0.125	1
1.8		1		0.64063	0.125
5		0.125		0	0
8.2		0		0	0
11.4		0		0	0.125
14.6		0		0	0

Comparison of Storey Vulnerability at level 1.8 m of different symmetric models is shown in Fig 5.36:



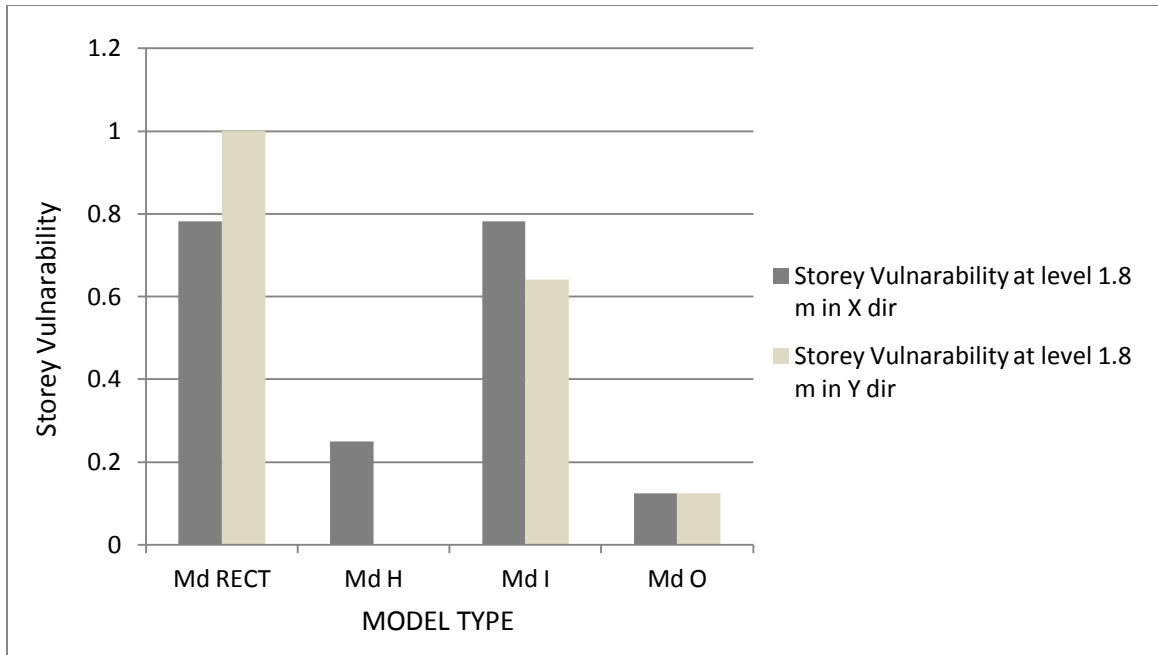


Fig 5.36: Storey Vulnerability ( $VI_{storey}$ ) of symmetric models at 1.8 m level in X & Y Direction

Storey vulnerability of rectangular model and model I are similar in X direction whereas storey vulnerability for model H and O are significantly lower in X direction. The value of storey vulnerability is highest for rectangular model in Y direction. For model I this value is a bit lower in Y direction and for model O it is the lowest.

In case of model O storey vulnerabilities in both the directions are same and lowest of the lot.

## 5.5 MODELS ASYMMETRIC ABOUT BOTH X & Y AXES OR SYMMETRIC ABOUT ONE OF THE AXES

The gridline plan and elevation of the asymmetric models are same as the symmetric models and given earlier.

### 5.5.1 MODEL 5: MODEL C

Plan and other details of model C are given below.

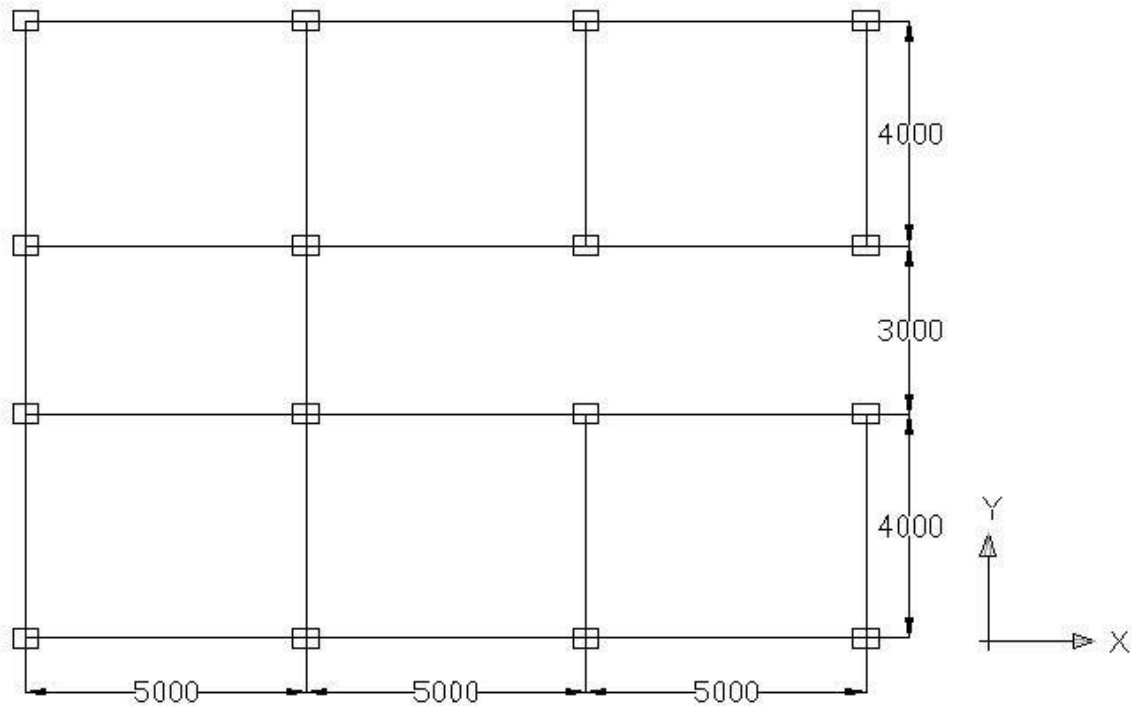


Fig 5.37 PLAN OF MODEL C

The major axis of the columns are along X axis. The building is regular O.M.R.F type. The sap skeleton model with slab diaphragm and wall diaphragm along with their load distribution pattern are given below separately. The slabs and walls are assumed as rigid diaphragm and the loading (D.L + L.L) are given accordingly.

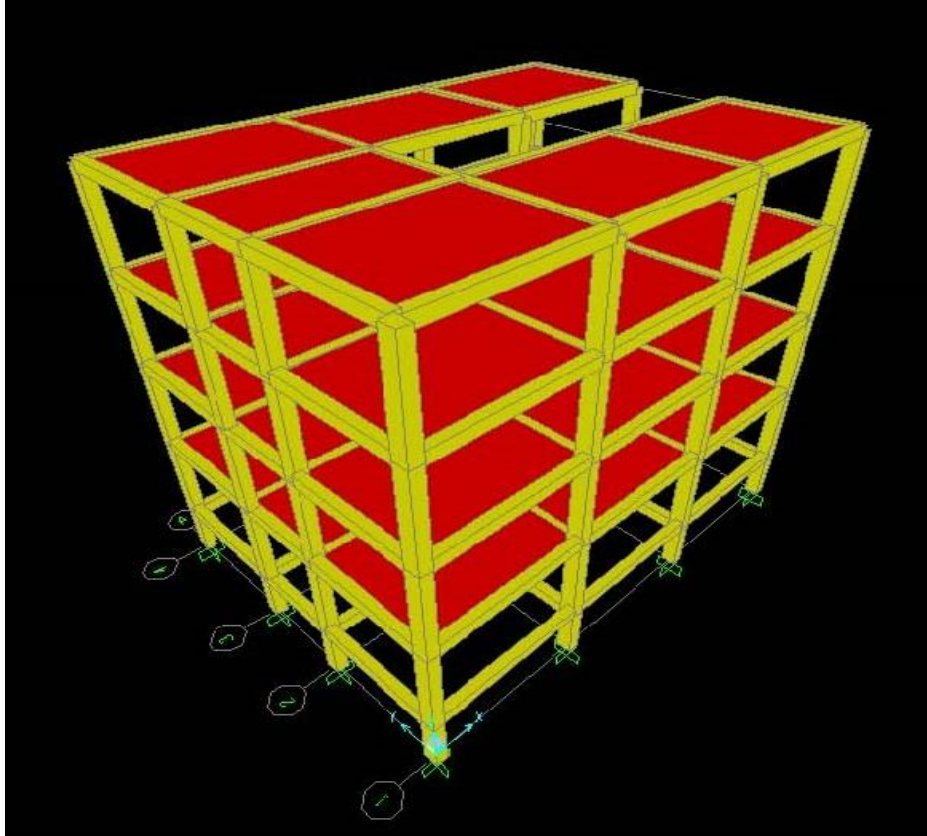


Fig 5.38: Isometric view of model C with slab diaphragm

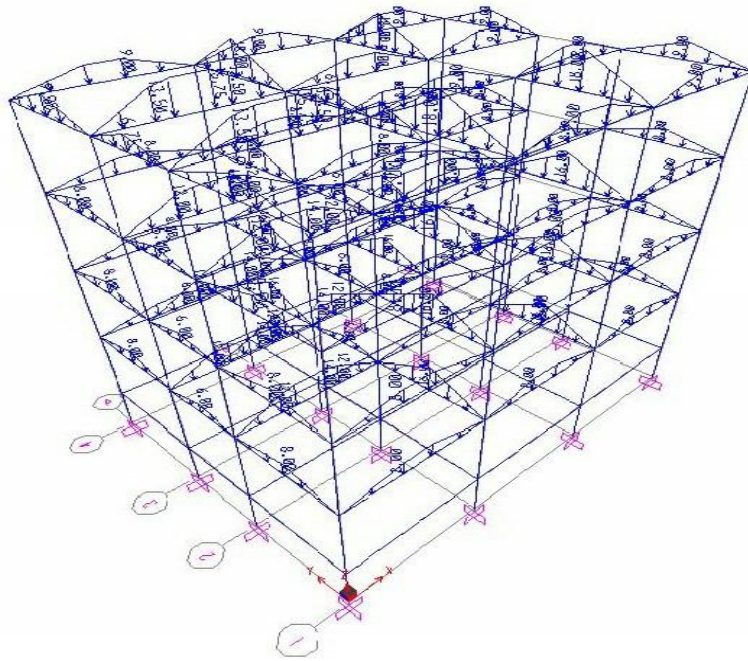


Fig 5.39 Slab loading pattern of model C

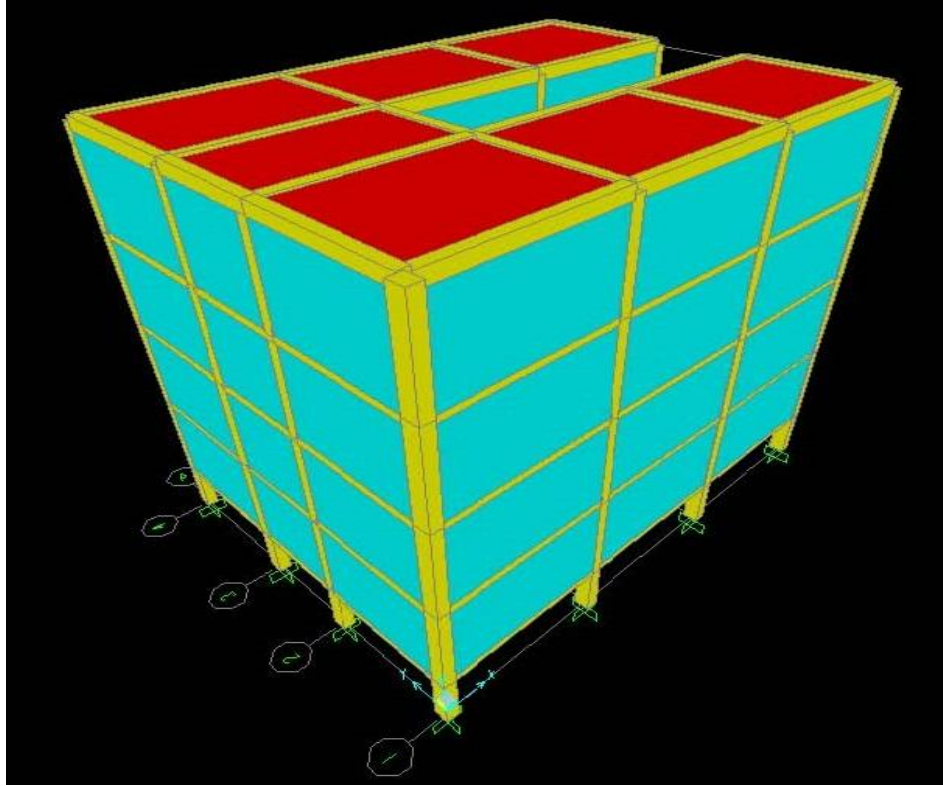


Fig 5.40: Isometric view of model C with wall diaphragm

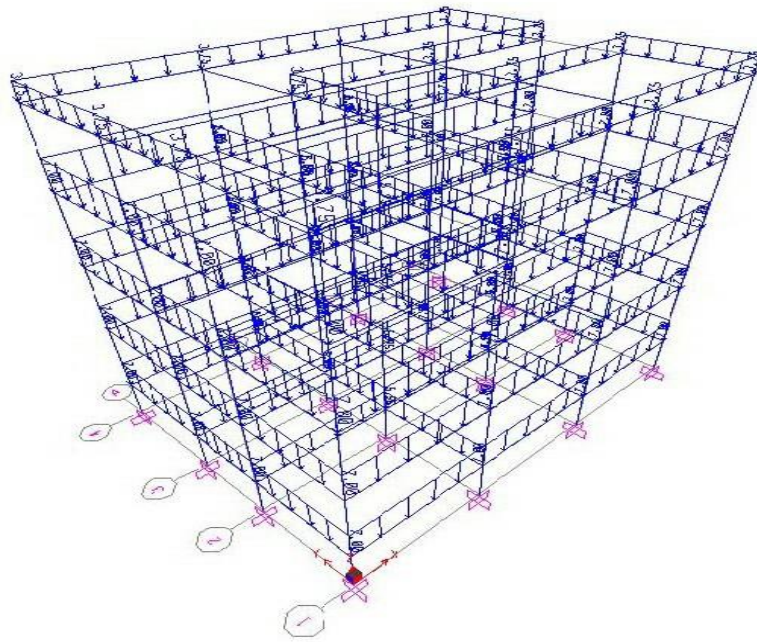
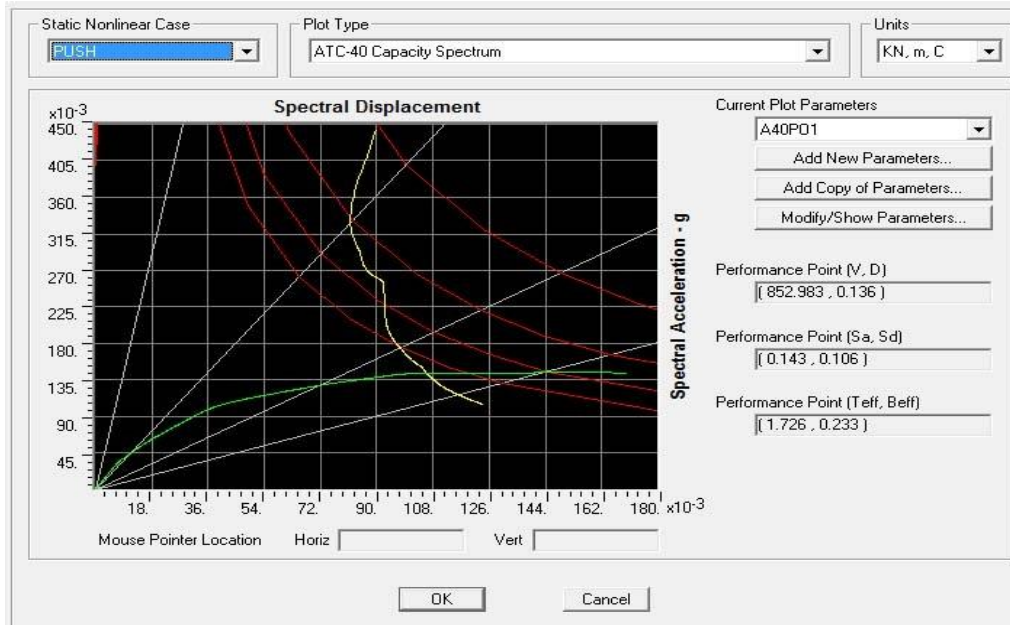
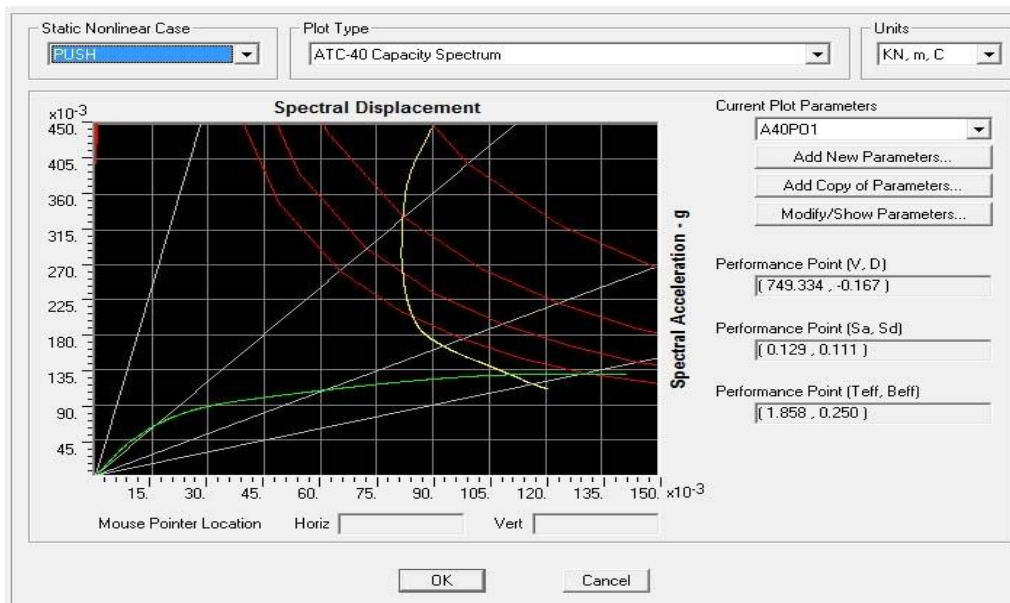


Fig 5.41 Wall loading pattern of model C

Results (Pushover curve, demand and capacity spectrum) from model C in X & Y direction are shown below where green colour indicates the pushover curve in capacity spectrum; yellow colour indicates demand spectrum and performance point shown separately.



**Fig 5.42 Model C ATC 40 (X)**



**Fig 5.43 Model C ATC 40 (Y)**

### 5.5.2 MODEL 6: MODEL L

Plan and other details of model L are given below.

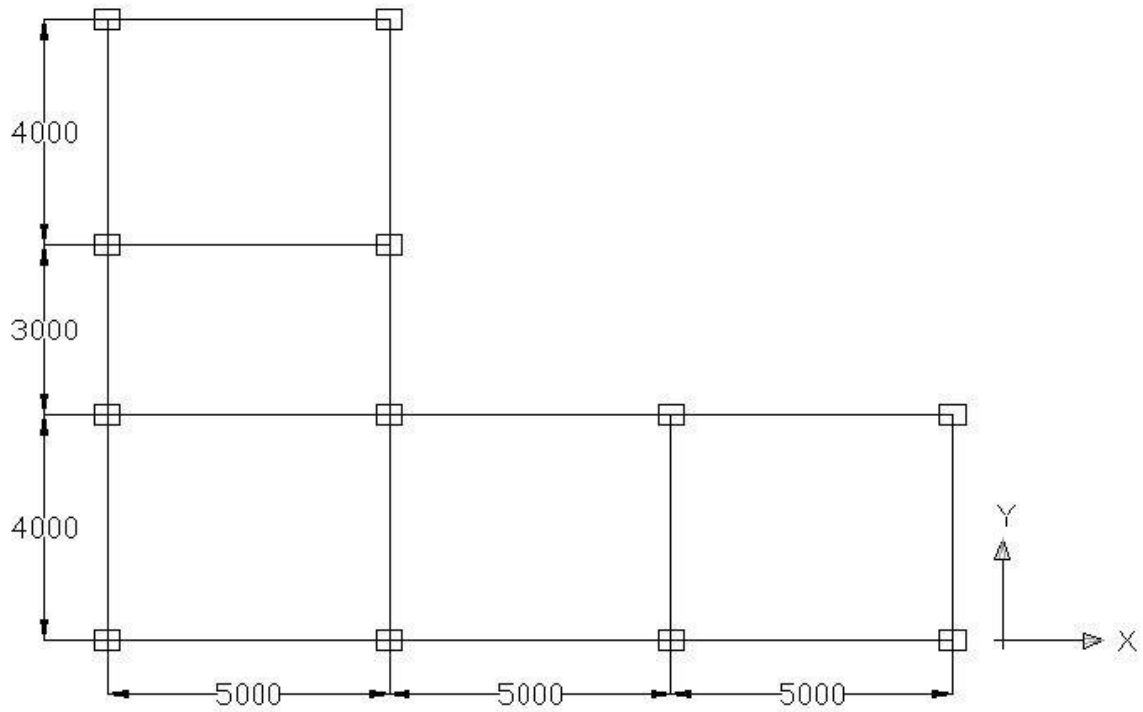


Fig 5.44 PLAN OF MODEL L

The major axis of the columns are along X axis. The building is regular O.M.R.F type. The sap skeleton model with slab diaphragm and wall diaphragm along with their load distribution pattern are given below separately. The slabs and walls are assumed as rigid diaphragm and the loading (D.L + L.L) are given accordingly.

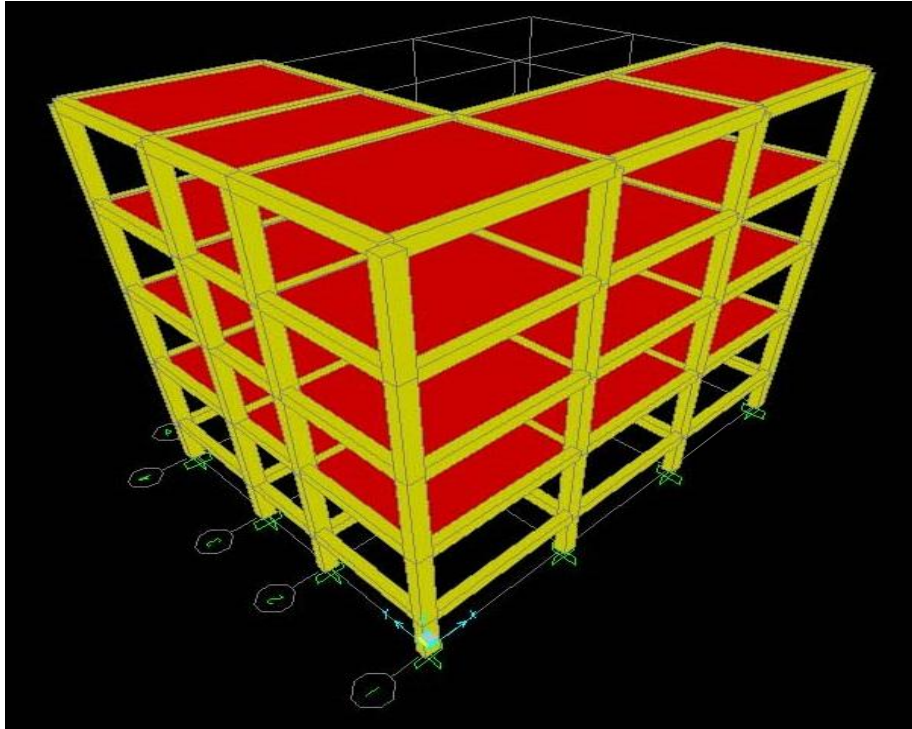


Fig 5.45: Isometric view of model L with slab diaphragm

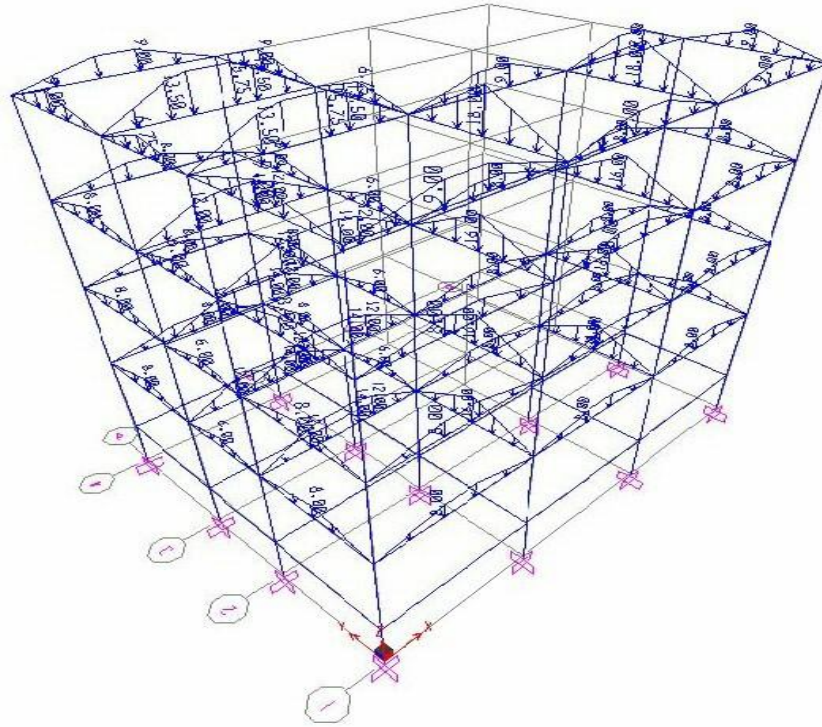


Fig 5.46 Slab loading pattern of model L

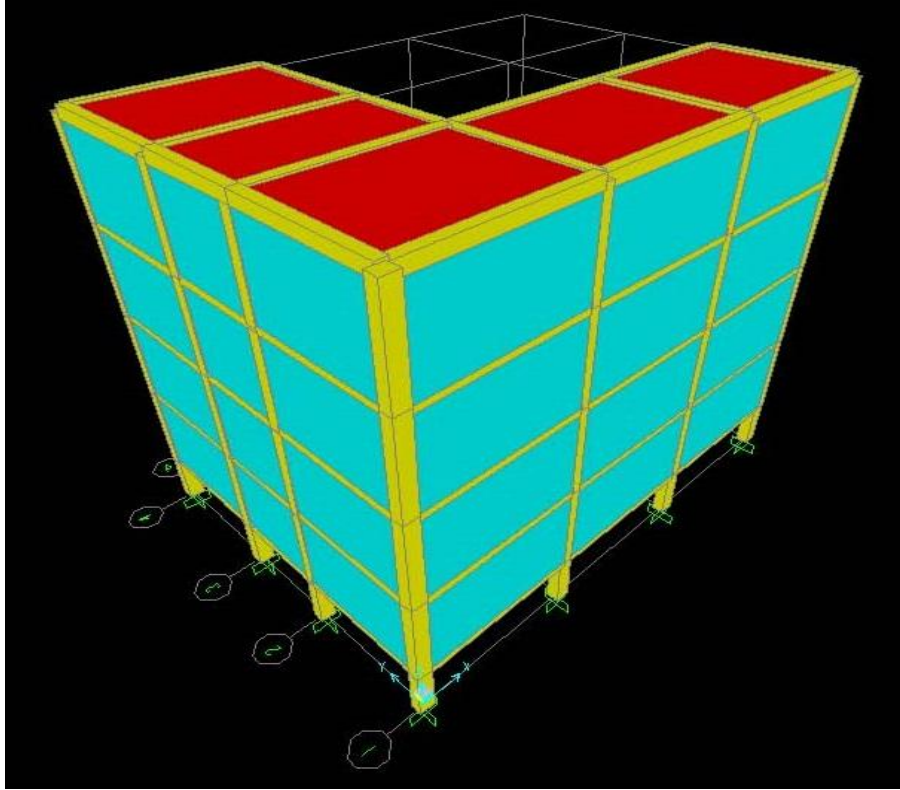


Fig 5.47: Isometric view of model L with wall diaphragm

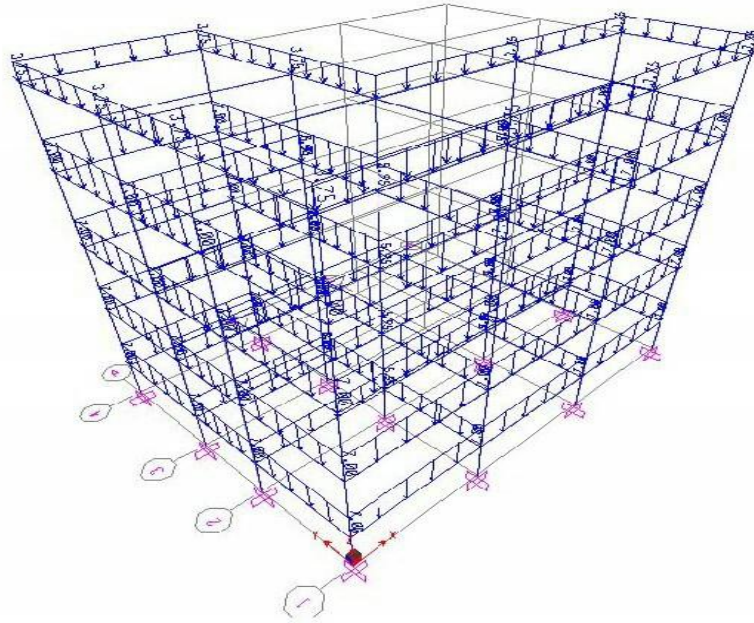
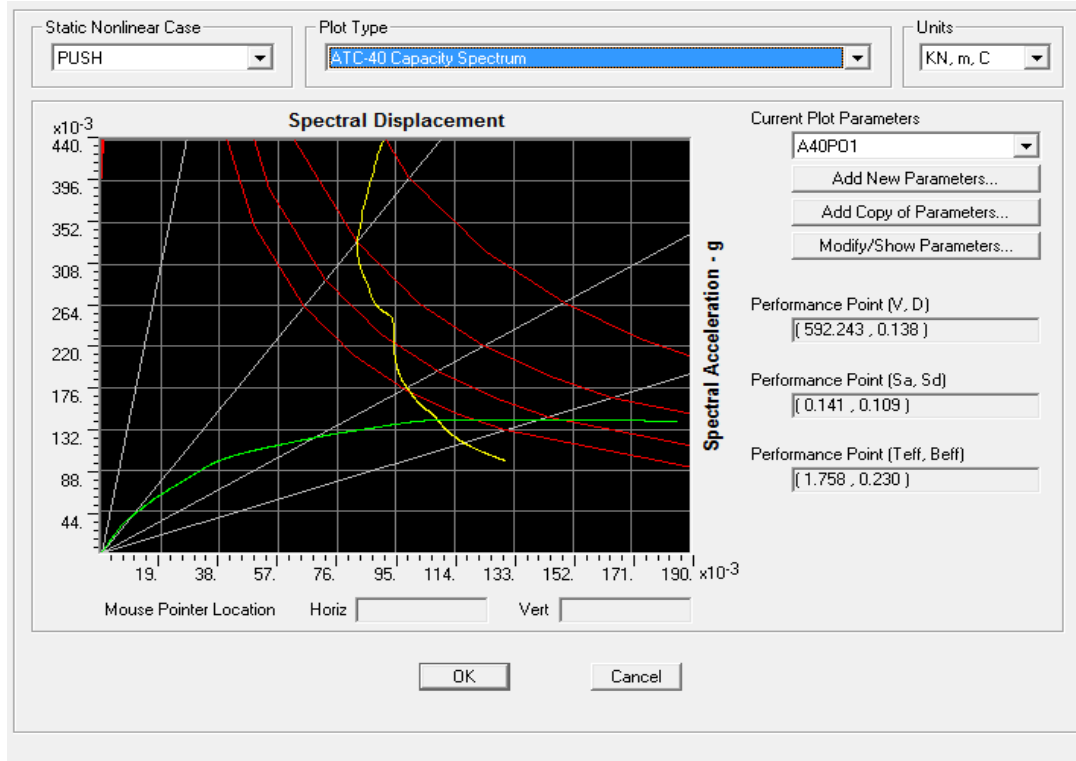


Fig 5.48 Wall loading pattern of model L



Results (Pushover curve, demand and capacity spectrum) from model L in X & Y direction are shown below where green colour indicates the pushover curve in capacity spectrum, yellow colour indicates demand spectrum and performance point shown separately.



**Fig 5.49 Model L ATC 40 (X)**

Mass and Stiffness in the first bay of model L in Y direction are considerably larger than those in second and third bays in Y direction, as well as base shear due to gravity load is higher in Y direction compared to the base shear in the X direction. Due to these reasons there was convergence problem while conducting non linear pushover analysis in Y direction. Thus subsequent results such as pushover curve, demand and capacity spectrum were not available in Y direction. Thus a new model broader L is introduced eliminating mass and stiffness irregularity in both X & Y directions to nullify the convergence problem and the results observed whether there is any improvement in base shear capacity.

### 5.5.3 MODEL 7: MODEL BROADER L

Plan and other details of model Broader L are given below.

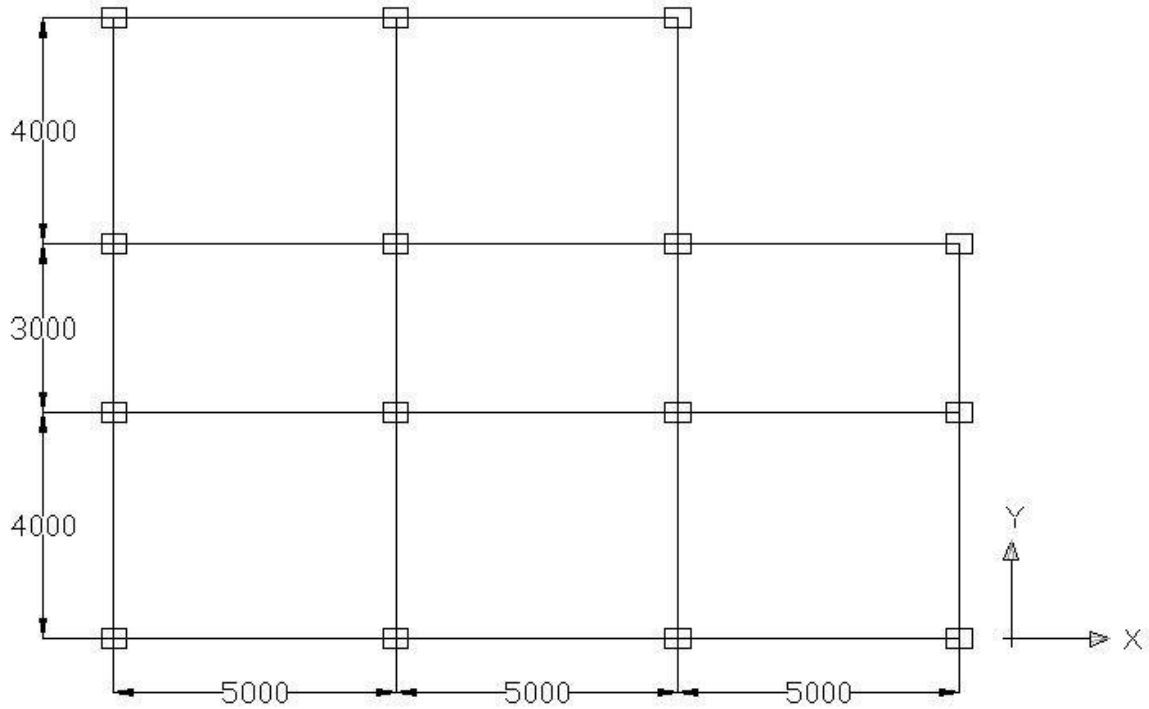


Fig 5.50 PLAN OF MODEL BROADER L

The major axis of the columns are along X axis. The building is regular O.M.R.F type. The sap skeleton model with slab diaphragm and wall diaphragm along with their load distribution pattern are given below separately. The slabs and walls are assumed as rigid diaphragm and the loading (D.L + L.L) are given accordingly.

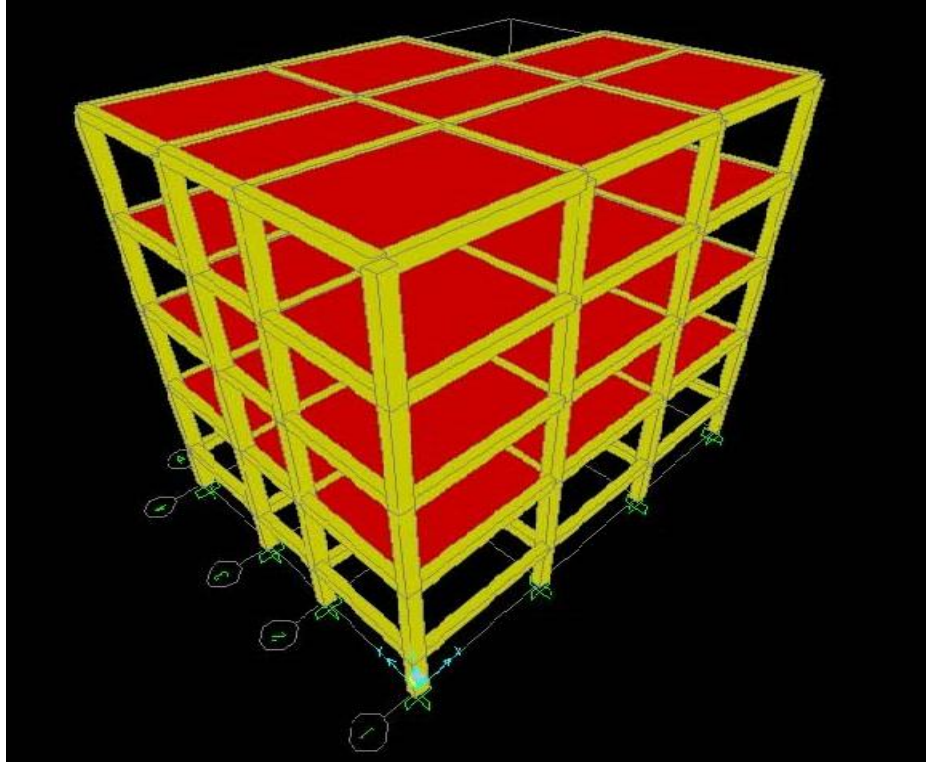


Fig 5.51: Isometric view of model Broader L with slab diaphragm

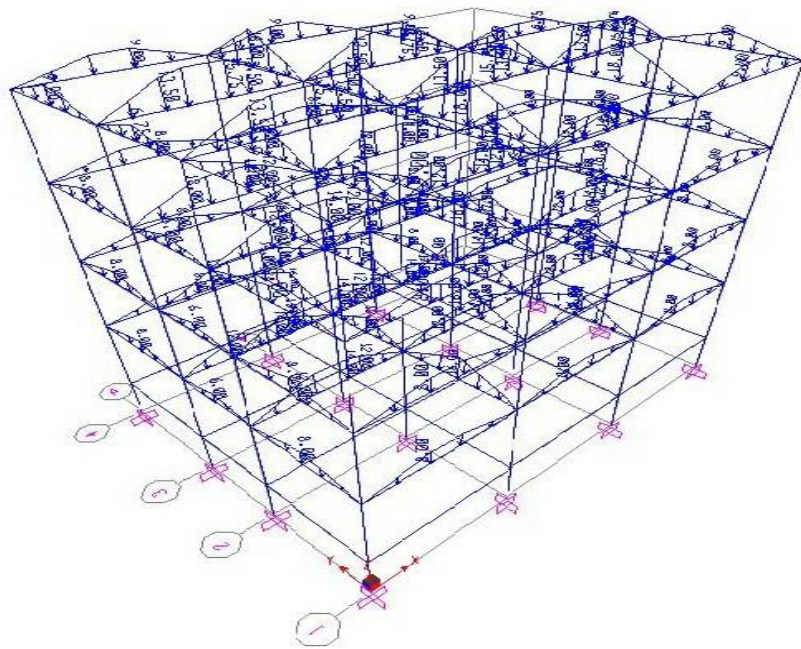


Fig 5.52 Slab loading pattern of model Broader L

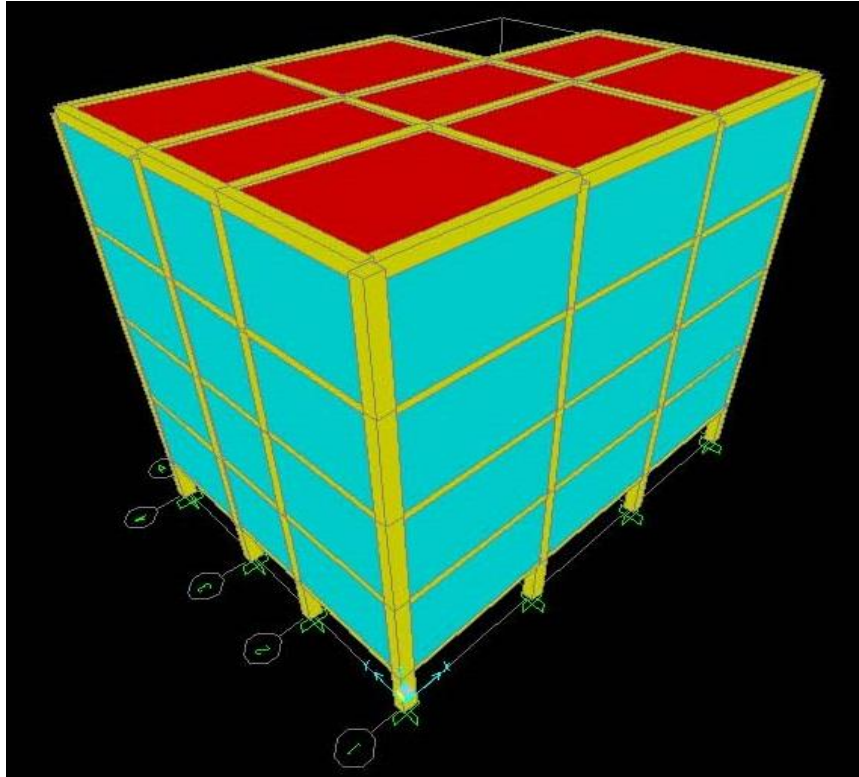


Fig 5.53: Isometric view of model Broader L with wall diaphragm

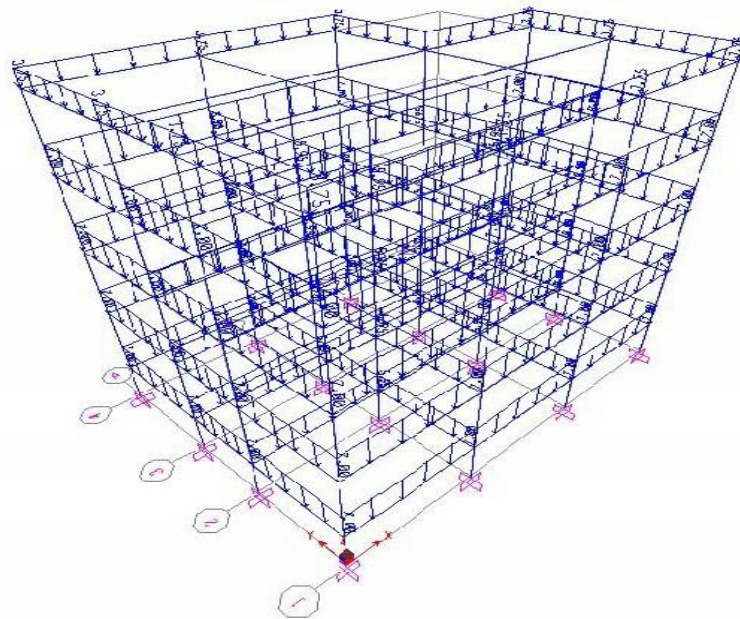
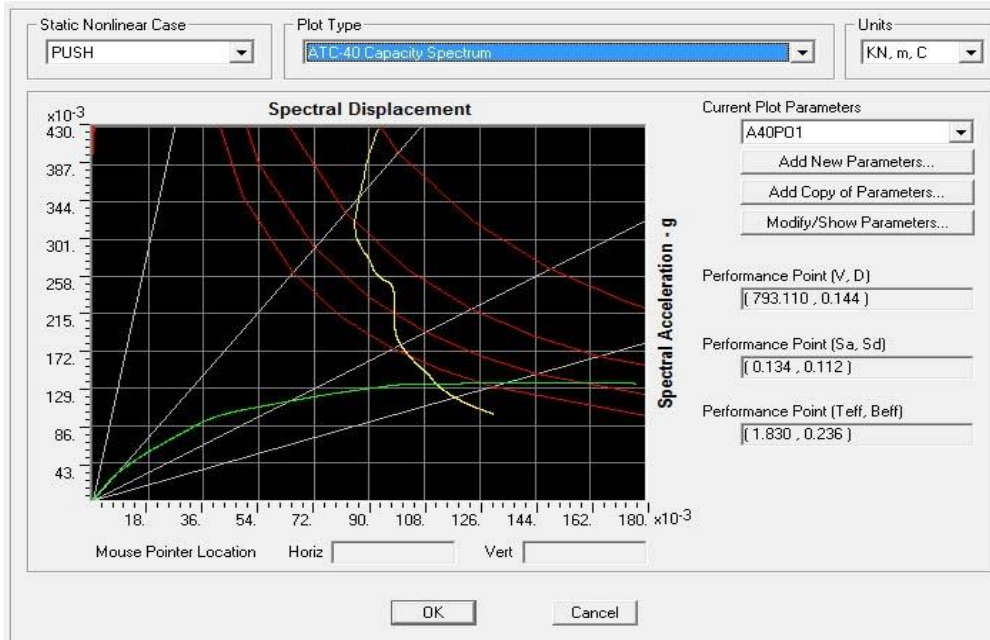
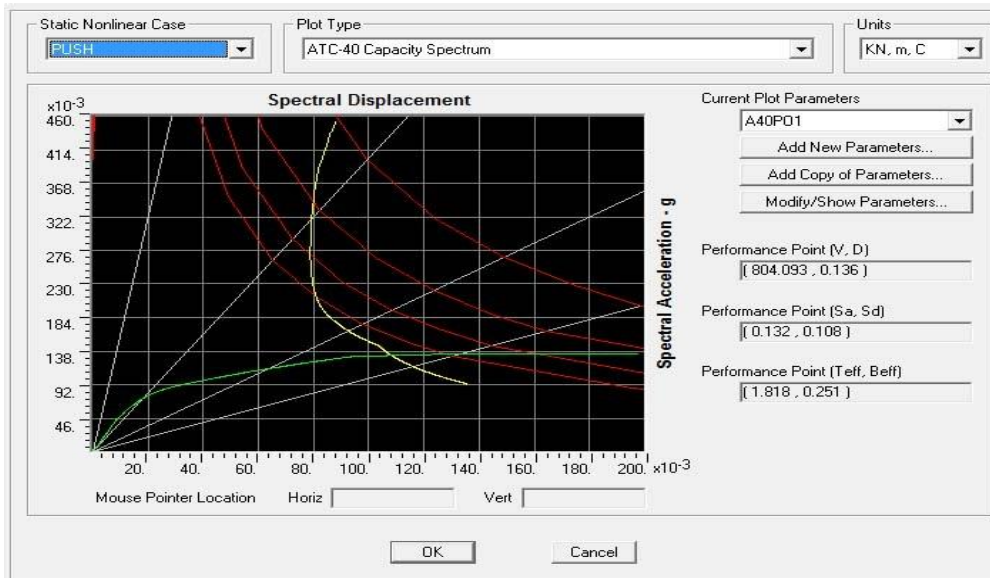


Fig 5.54 Wall loading pattern of model Broader L

Results (Pushover curve, demand and capacity spectrum) from model Broader L in X & Y direction are shown below where green colour indicates the pushover curve in capacity spectrum; yellow colour indicates demand spectrum and performance point shown separately.



**Fig 5.55 Model Broader L ATC 40 (X)**



**Fig 5.56 Model Broader L ATC 40 (Y)**

#### 5.5.4 MODEL 8: MODEL T

Plan and other details of model T are given below.

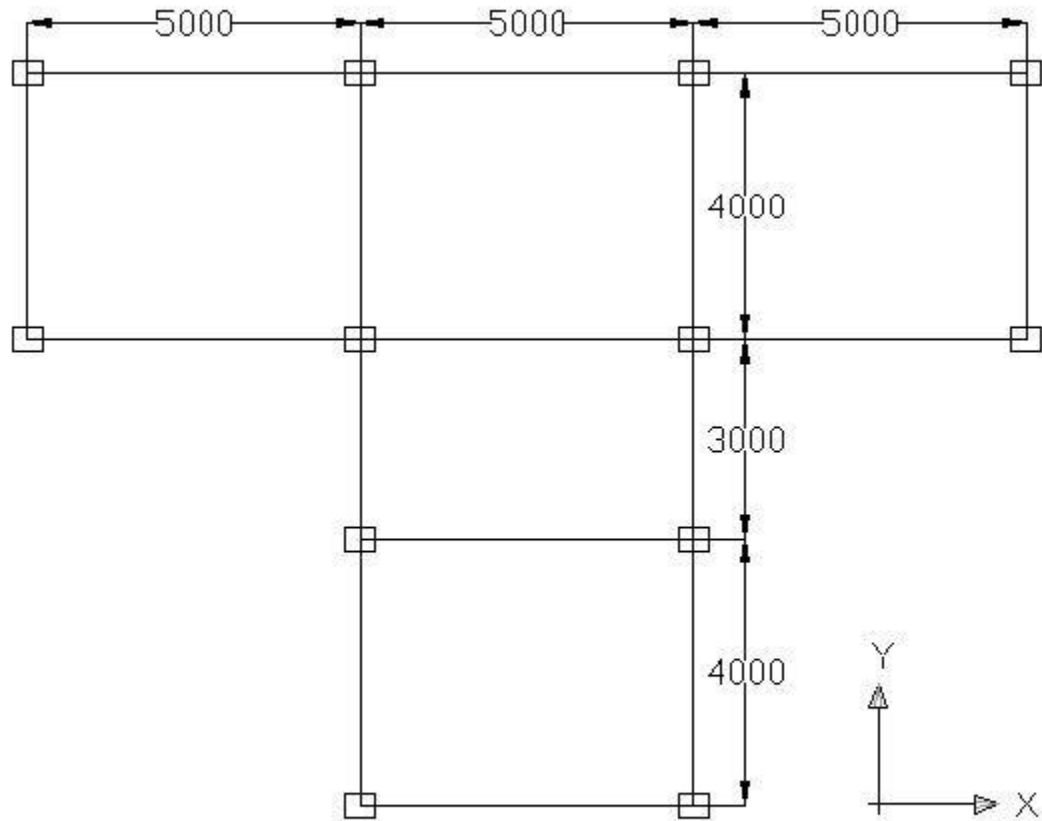


Fig 5.57 PLAN OF MODEL T

The major axis of the columns are along X axis. The building is regular O.M.R.F type. The sap skeleton model with slab diaphragm and wall diaphragm along with their load distribution pattern are given below separately. The slabs and walls are assumed as rigid diaphragm and the loading (D.L + L.L) are given accordingly.

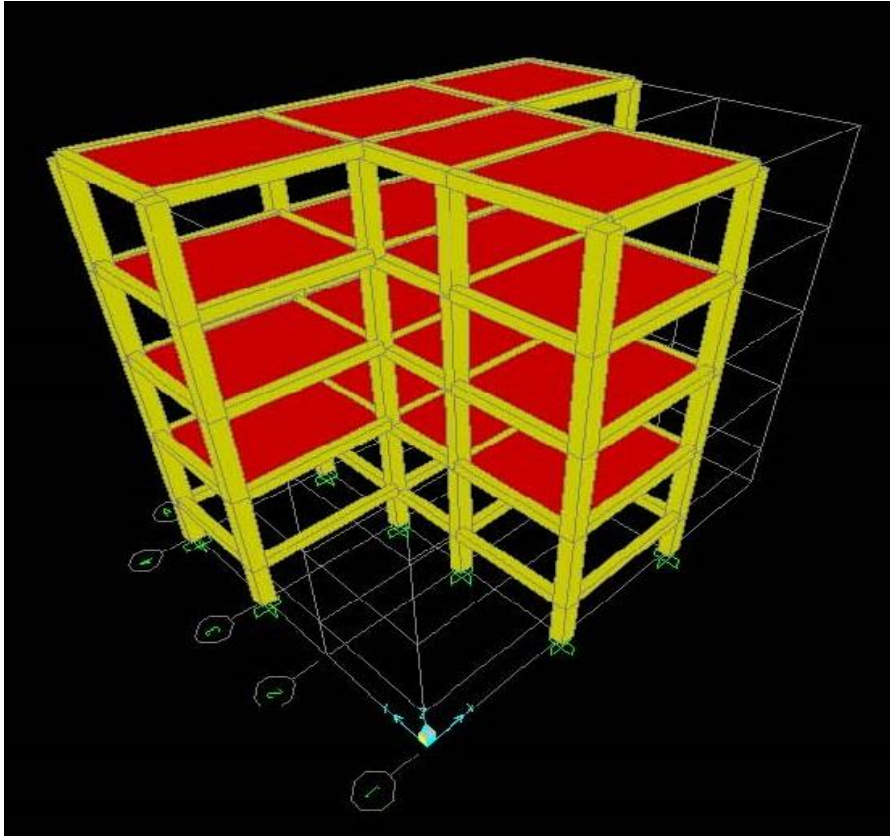


Fig 5.58: Isometric view of model T with slab diaphragm

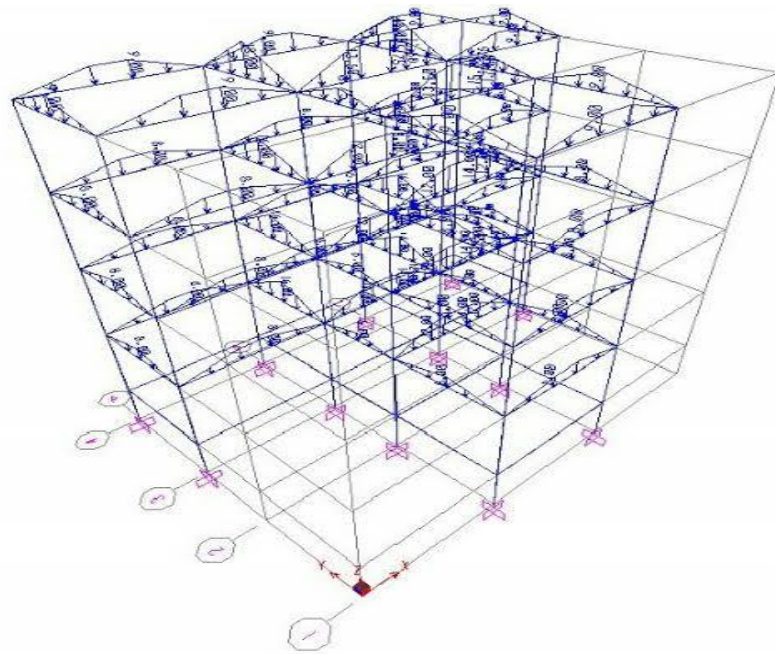


Fig 5.59 Slab loading pattern of model T

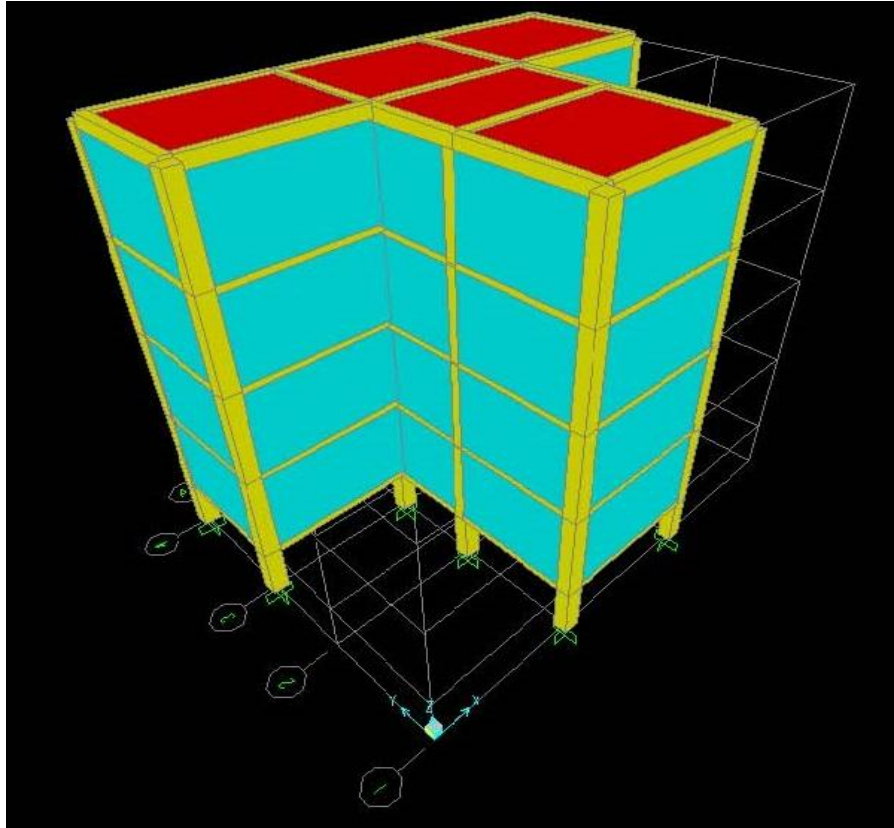


Fig 5.60: Isometric view of model T with wall diaphragm

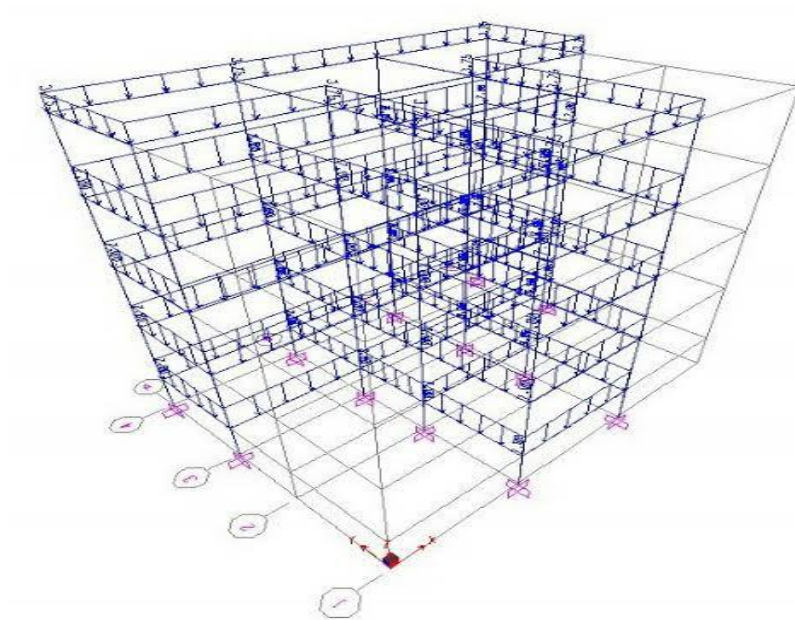
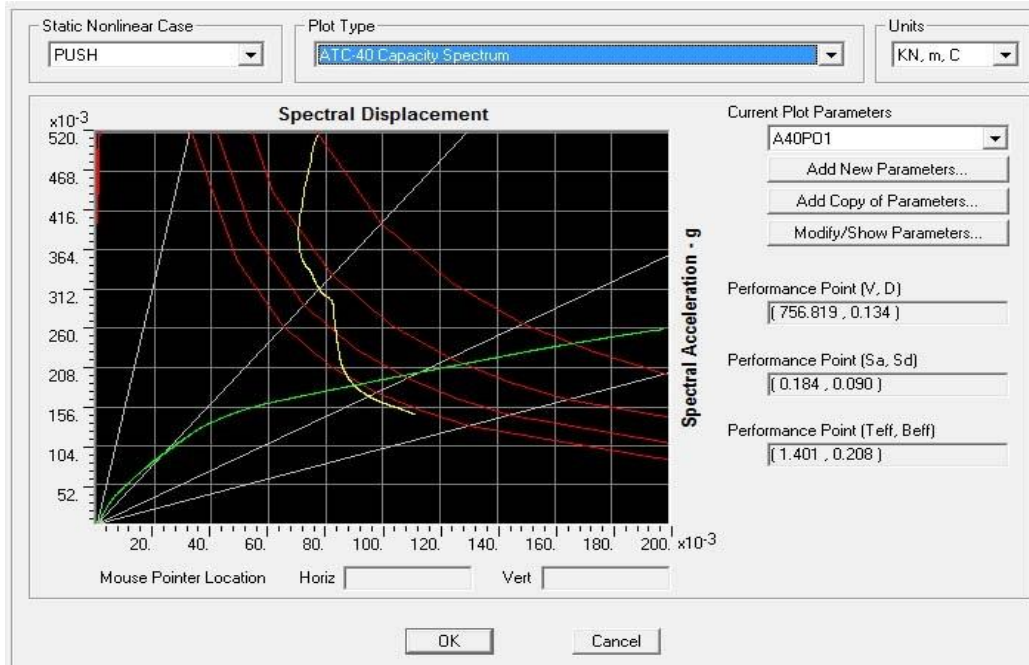


Fig 5.61 Wall loading pattern of model T



Results (Pushover curve, demand and capacity spectrum) from model T in X & Y direction are shown below where green colour indicates the pushover curve in capacity spectrum; yellow colour indicates demand spectrum and performance point shown separately.



**Fig 5.62 Model T ATC 40 (X)**

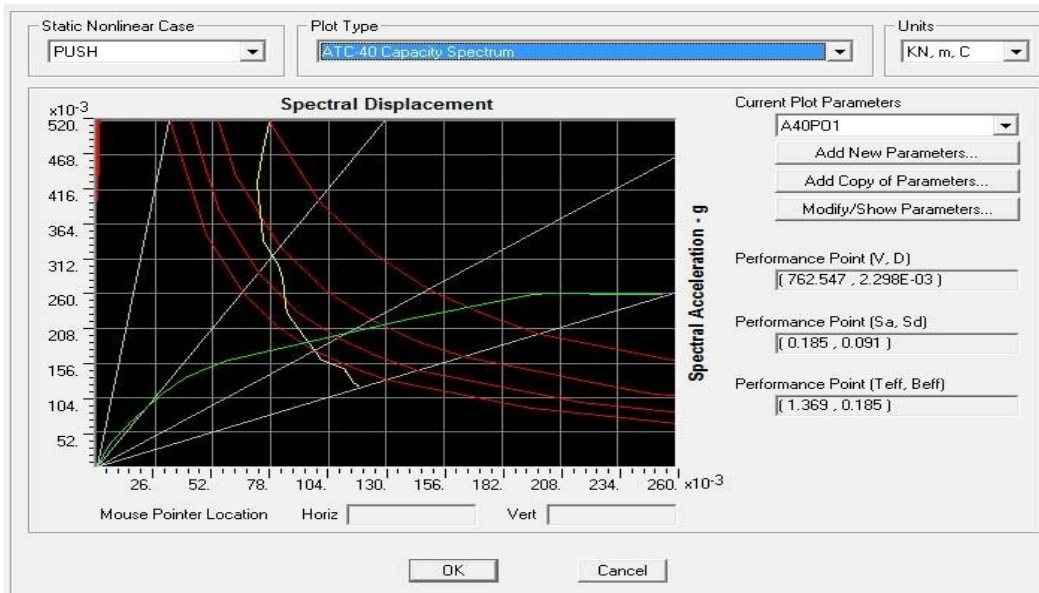


**Fig 5.63 Model T ATC 40 (Y)**

### 5.5.5 MODEL 9: MODEL U

Plan and other details of model U are given below.

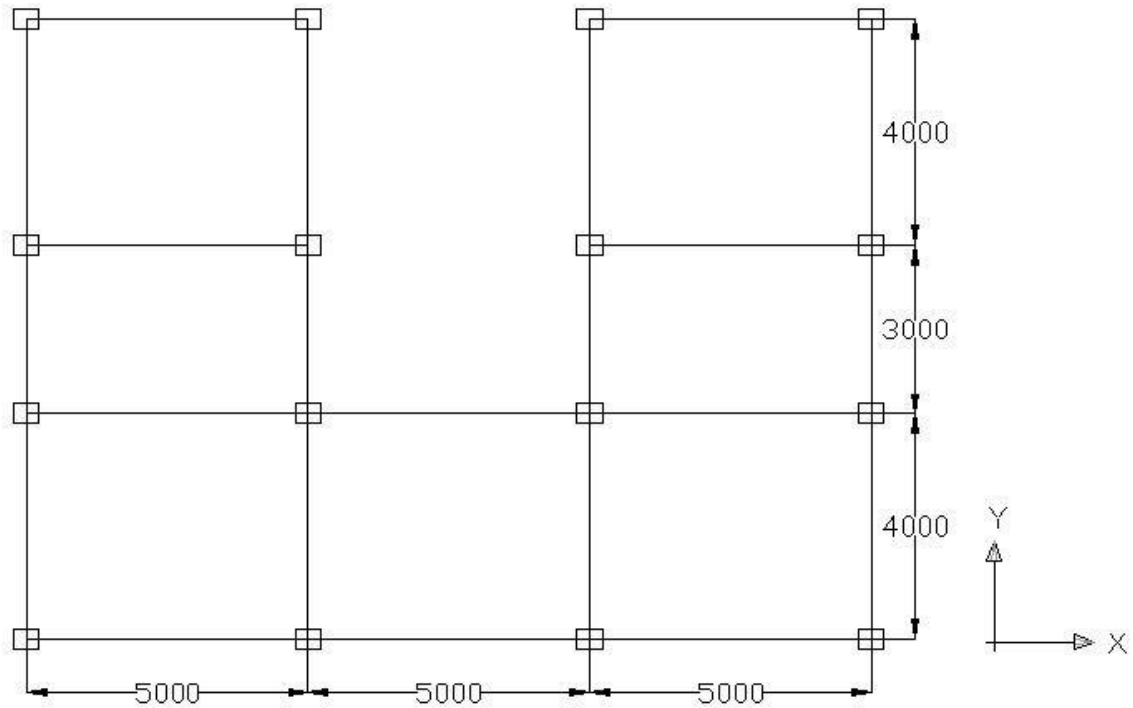


Fig 5.64 PLAN OF MODEL U

The major axis of the columns are along X axis. The building is regular O.M.R.F type. The sap skeleton model with slab diaphragm and wall diaphragm along with their load distribution pattern are given below separately. The slabs and walls are assumed as rigid diaphragm and the loading (D.L + L.L) are given accordingly.

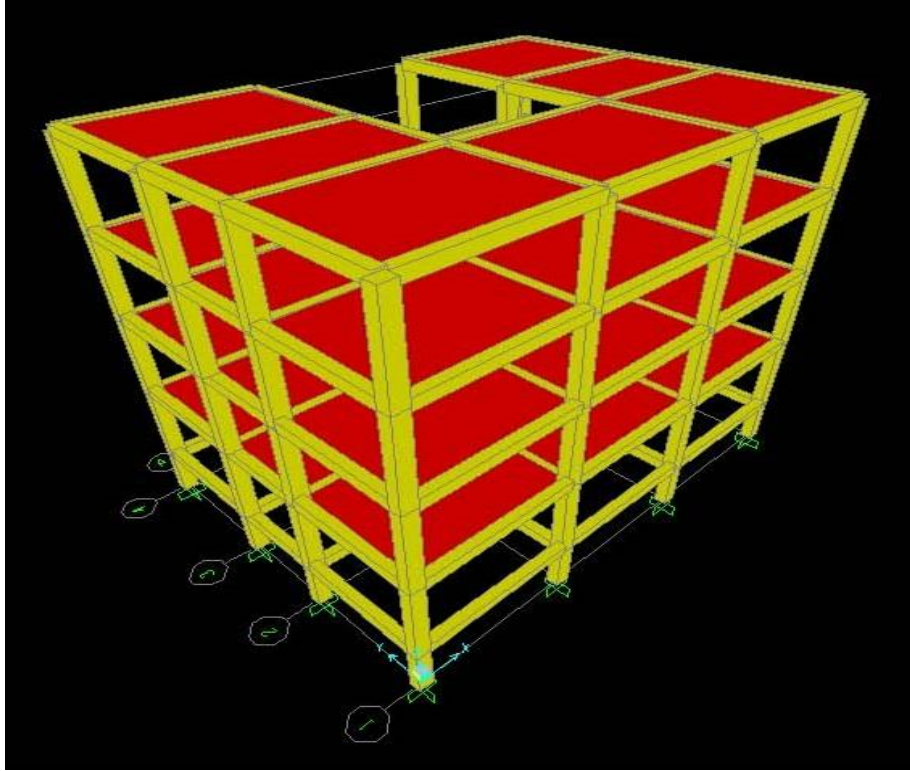


Fig 5.65: Isometric view of model U with slab diaphragm

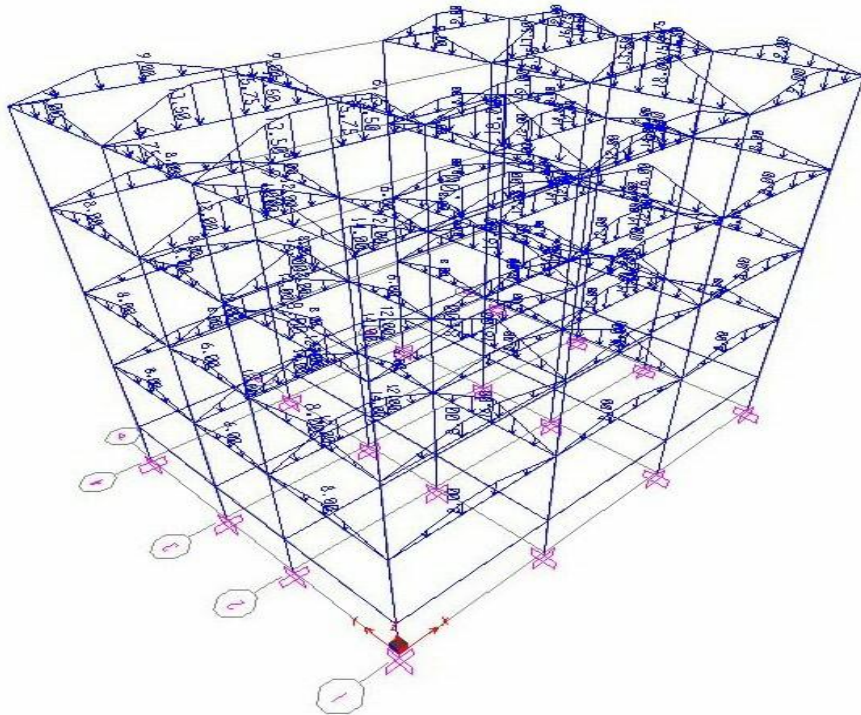


Fig 5.66 Slab loading pattern of model U

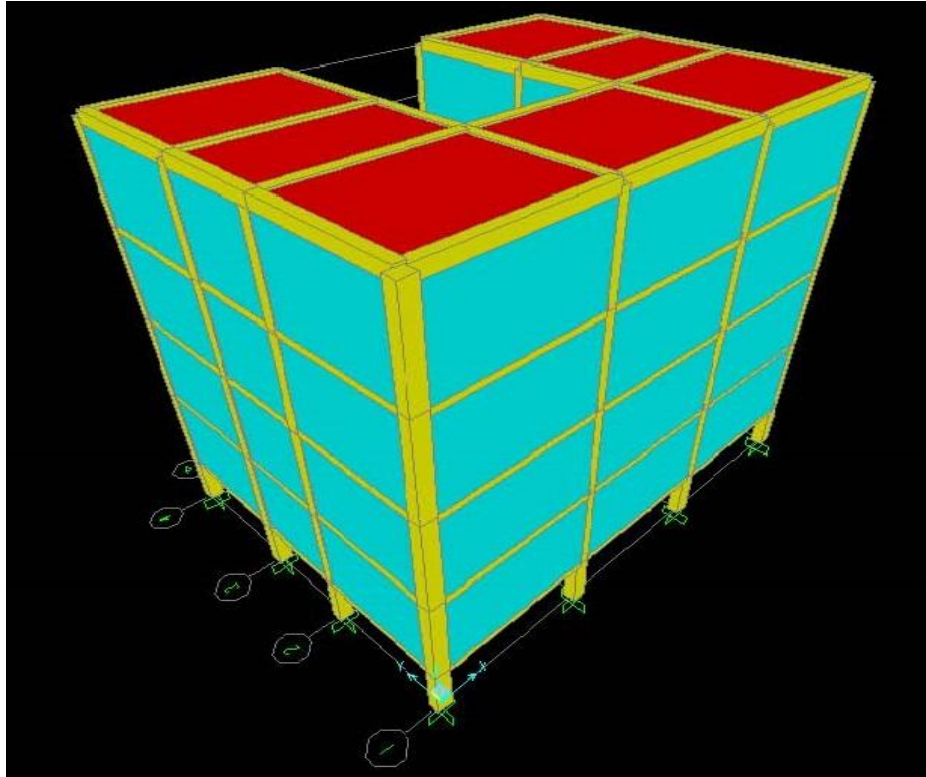


Fig 5.67: Isometric view of model U with wall diaphragm

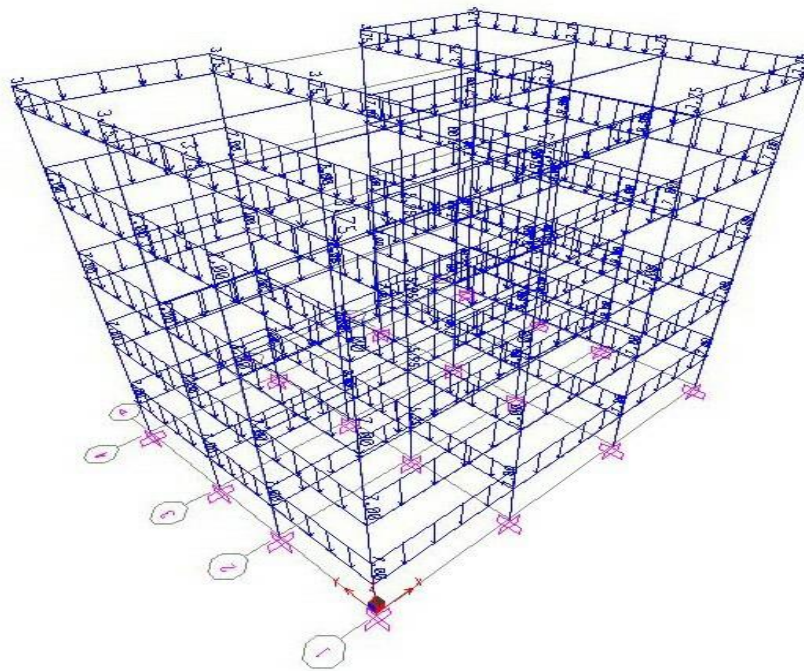
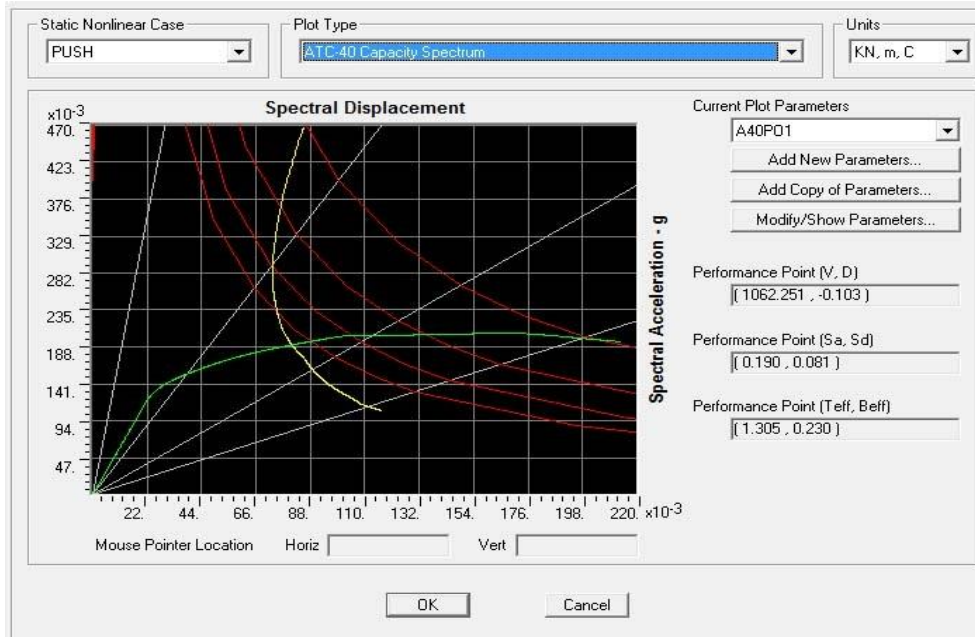
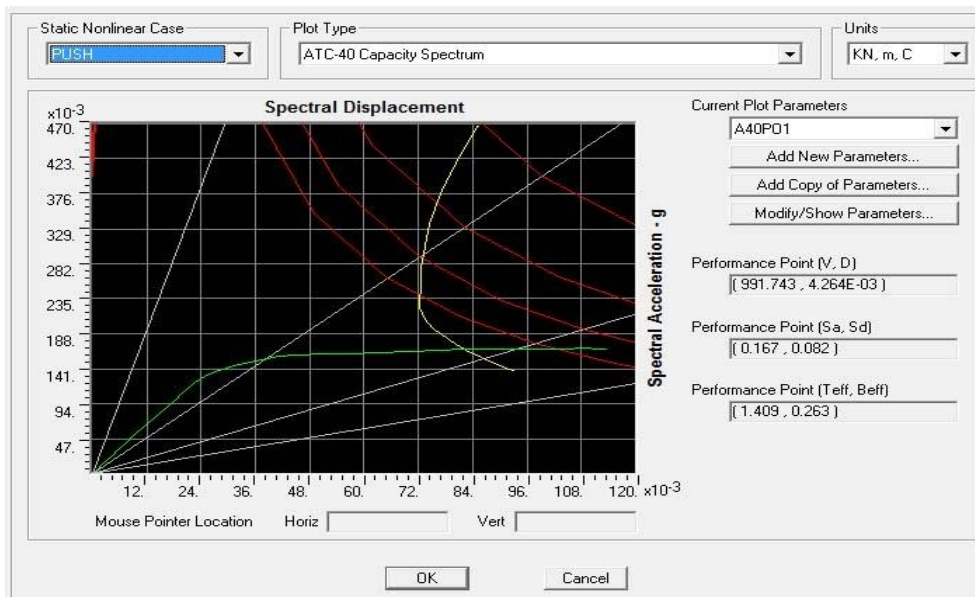


Fig 5.68 Wall loading pattern of model U

Results (Pushover curve, demand and capacity spectrum) from model U in X & Y direction are shown below where green colour indicates the pushover curve in capacity spectrum; yellow colour indicates demand spectrum and performance point shown separately.



**Fig 5.69 Model U ATC 40 (X)**



**Fig 5.70 Model U ATC 40 (Y)**

### 5.5.6 RESULT DISCUSSION OF ASYMMETRIC MODELS:

Summary of the results obtained from pushover analysis for model 5 to 9 in X & Y direction are given in table 5-4 and table 5-5 respectively.

**Table5-6: Comparison of various seismic resisting features of asymmetric models along X direction**

MODEL TYPE	DIRCTION	BASE SHEAR (V) in KN	PLAN AREA(m <sup>2</sup> )	BASE SHEAR PER UNIT AREA (KN/m <sup>2</sup> )	ROOF DISPLACEMENT (D) in m	SPECTRAL ACCLERETION (Sa) in m/s <sup>2</sup>	SPECTRAL DISPLACEMENT (Sd) in m	EFFECTIVE PERIOD (Teff) in s	EFFECTIVE DAMPING (Beff)
C	X	852.983	135	6.31839	0.136	0.143	0.106	1.726	0.233
L		592.243	95	6.23414	0.138	0.141	0.109	1.758	0.23
BrL		793.11	145	5.46972	0.144	0.134	0.112	1.83	0.236
T		756.819	95	7.96652	0.134	0.184	0.09	1.401	0.208
U		1062.25	130	8.17116	0.103	0.19	0.081	1.305	0.23

**Table5-7: Comparison of various seismic resisting features of asymmetric models along Y direction**

MODEL TYPE	DIRCTION	BASE SHEAR (V) in KN	PLAN AREA(m <sup>2</sup> )	BASE SHEAR PER UNIT AREA (KN/m <sup>2</sup> )	ROOF DISPLACEMENT (D) in m	SPECTRAL ACCLERETION (Sa) in m/s <sup>2</sup>	SPECTRAL DISPLACEMENT (Sd) in m	EFFECTIVE PERIOD (Teff) in s	EFFECTIVE DAMPING (Beff)
C	Y	749.334	135	5.55062	0.167	0.129	0.111	1.858	0.25
L		Convergence problem in Y direction							
BrL		804.093	145	5.54547	0.136	0.132	0.108	1.818	0.251
T		762.547	95	8.02681	0.002	0.185	0.091	1.369	0.185
U		991.743	130	7.62879	0.004	0.167	0.082	1.409	0.263

Comparison of base shear and roof displacement along X & Y direction are given in Fig 5.71 and 5.72 respectively for better understanding.

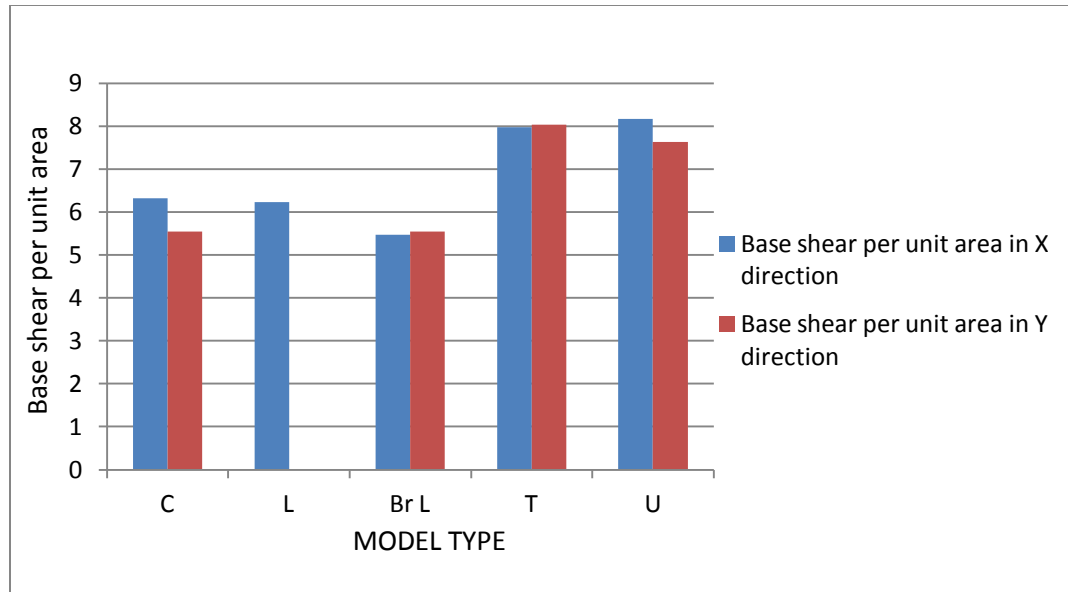


Fig 5.71: BASE SHEAR (V) of asymmetric models in X & Y Direction

From the above figure it is clearly observed base shear capacity per unit area of model Br L is lowest among all the models. Base shear capacity of model L is lowest due to its asymmetric plan area about both the axes and mass and stiffness of the end bay becomes huge compared to other two bays in both the directions, along the Y direction gridline spacing is also unequal with this mass and stiffness irregularity, thus the non linear analysis becomes non convergent and results in Y direction could not be obtained.

To overcome this plan irregularity as in model L, another model broader L is introduced and from the above figure it is seen that there is an improvement of base shear capacity in both the directions as well as convergence problem could be overcome. But base shear per unit area has been decreased than model L meant the ratio of base shear increase is much lower than the area increase in Br L compared to model L.

For model C and model U base shear capacity is on the higher side about X axis. For model T they are almost same, though the model is symmetric about Y axis but irregularity of mass and stiffness in the second bay compared to first and third one reduces the base shear capacity along Y direction to some extent.

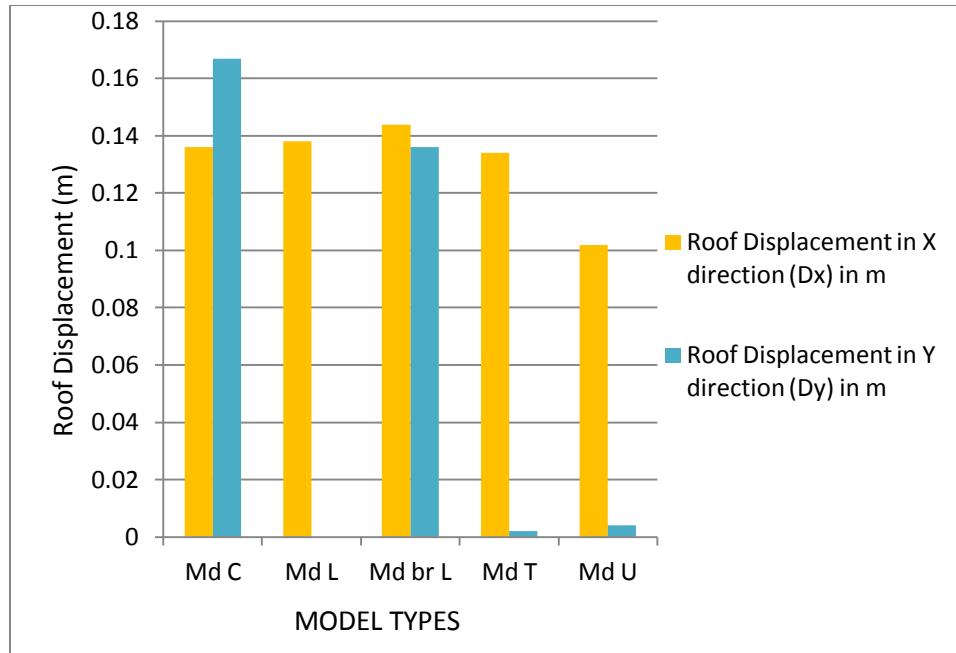


Fig 5.72: ROOF DISPLACEMENT ( $D_{rf}$ ) of asymmetric models in X & Y Direction

Roof displacements of model T and U in Y direction are significantly small than the all other displacements because of the plan irregularity along Y direction. Mass and stiffness in the second bay in Y direction becomes huge compared to the other two in case of model T and in case of model U the scenario is reverse. Not only that, due to this irregularity after a certain percentage of analysis collapse mechanism becomes global and no further analysis could be done along Y direction for these two models.

Roof displacements of all the models are on the higher side due to non symmetric behaviour of the models. With close observation it could be seen that the results of roof displacements are in tune with the corresponding base shear capacities of the models.



Comparison of Spectral Acceleration and Spectral displacement along X & Y direction of the asymmetric models considered are shown in Fig 5.73 & 5.74 respectively.

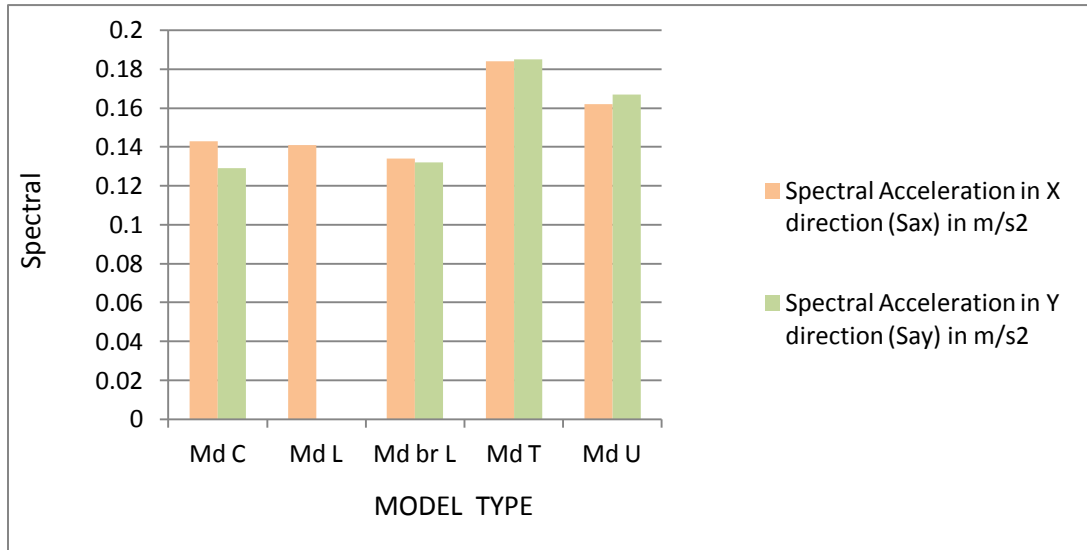


Fig 5.73: Spectral Acceleration ( $S_a$ ) of asymmetric models in X & Y Direction

Spectral accelerations of first three models are lower in both the directions compared to model 8 & 9. The value of spectral accelerations are highest for model T in both the directions. If compared to the figure below it could be clearly observed that in models where the spectral acceleration value is high spectral displacement is on the lesser side.

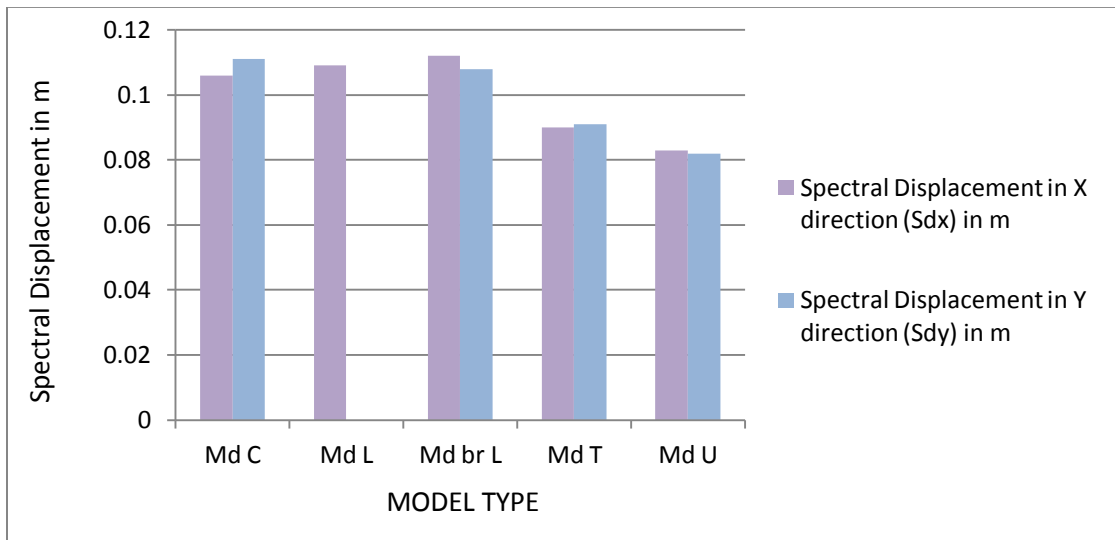


Fig 5.74: Spectral Displacement ( $S_d$ ) of asymmetric models in X & Y Direction

It is noted that the trend of roof displacement has been carried over for spectral displacement too. For model T and U spectral displacements are lesser than the other models in both directions. For the other models they are more or less comparable.

Comparison of Global Stiffness of different asymmetric models is shown in Fig 5.75

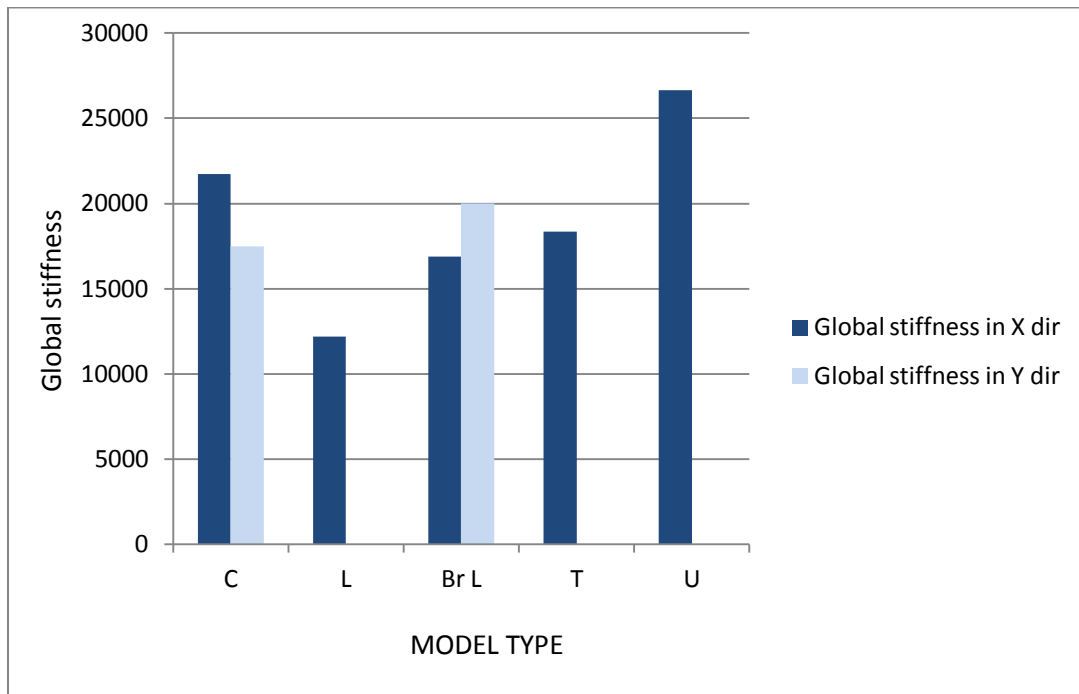


Fig 5.75: Global Stiffness of asymmetric models in X & Y Direction

For model T and model U global stiffness could not be calculated properly along Y direction as because non linear analysis in Y direction could only be performed to a certain percentage due to plan irregularity in Y direction. Thus the global stiffness which is represented by the initial slope of the pushover curve could not be drawn accurately. Rather it gives a very steeper slope resulting in very high global stiffness which is not the proper representation of global stiffness which could have been obtained if the analysis could be completed properly.

Among the models model U has got highest global stiffness along X direction and model L having the lowest. For models C, broader L and T global stiffnesses are in a comparable range.

**Table 5-8:  $VI_{\text{bldg}}$  in both direction for Asymmetric models**

Type of Model	Direction	$VI_{\text{bldg}}$
C	X	0.56339
L		0.5625
Br L		0.55052
T		0.47236
U		0.67986
C	Y	0.42655
L		
Br L		0.63942
T		
U		0.4835

Comparison of Building Vulnerability of different symmetric models is shown in Fig 5.76:

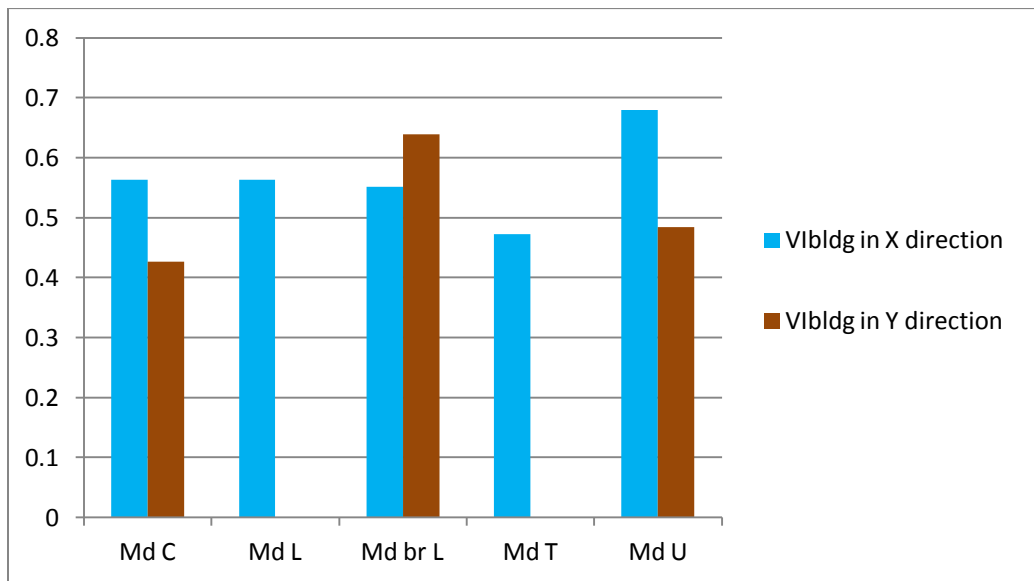


Fig 5.76: Building Vulnerability ( $VI_{\text{bldg}}$ ) of asymmetric models in X Direction

Building Vulnerability of model T is lowest and model U is highest in X direction. For models C, L and Br L the values are more or less same in X direction.

In Y direction building Vulnerability of model C is lowest and model broader L is highest due to its plan irregularity. For model L and T building Vulnerability could not be calculated due to non convergence and early development of collapse mechanism (hinge formation was not proper).

**Table 5-9:  $VI_{storey}$  in both direction for Asymmetric models at all levels**

Vistorey in both direction for Asymmetric models						
Storey Height(m)	Direction	MODEL TYPE				
		C	L	Br L	T	U
0	X	0.95313	0.96875	0.9	0.125	1
1.8		0.125	0.125	0.125	0	0
5		0	0	0	0	0
8.2		0	0	0	0	0
11.4		0	0	0	0	0.125
14.6		0	0	0	0	0.125
0	Y	0.125	Convergence problem in Y direction	0.975	0	1
1.8		0.125		0.125	0	0
5		0		0	0	0
8.2		0		0	0	0
11.4		0		0	0	0.125
14.6		0		0	0	0.125

Comparison of Storey Vulnerability of different symmetric models at level 1.8 m is shown in Fig 5.77:

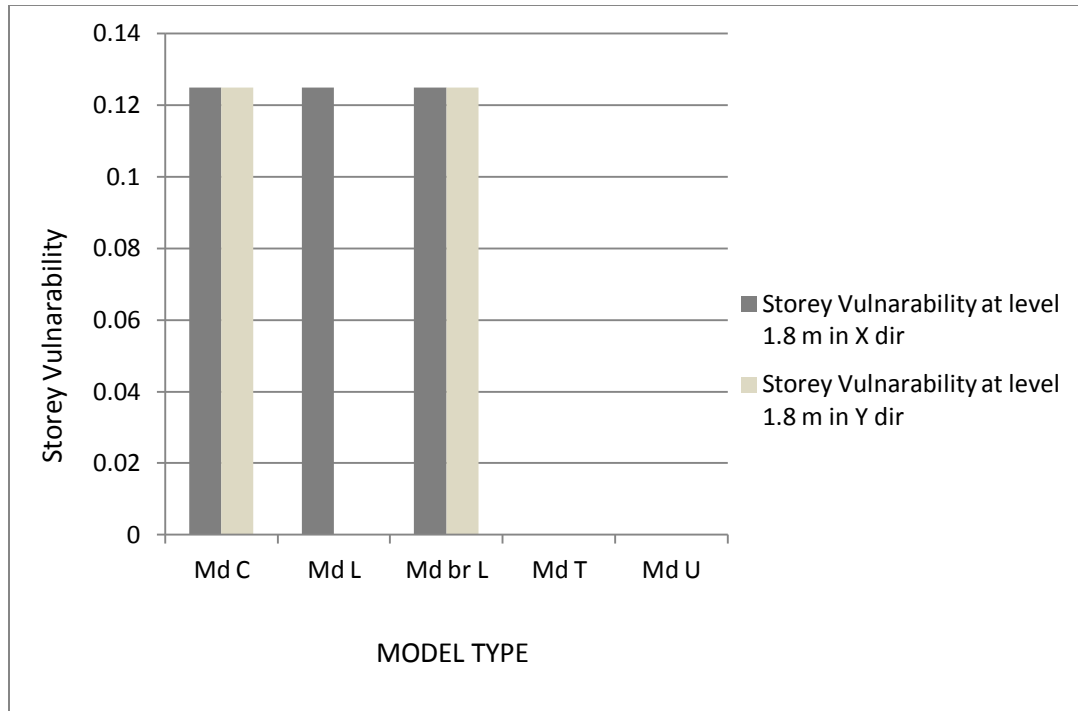


Fig 5.77: Storey Vulnerability ( $VI_{storey}$ ) of asymmetric models at 1.8 m level in X & Y Direction

Storey Vulnerability of Model C, L and Broader L are more or less same at level 1.8 m in both X and Y directions and the values are 0.125 which is comparatively lower. But Storey Vulnerability of all these models show higher values at ground floor level due to inadequacy of strength and stiffness at that level and attributed overall higher values for building vulnerability for the models mentioned above. At a particular level the values may be on lower side according to the formulation.

## 5.6: RESULT DISCUSSION OF ALL MODELS

**Table5-10: Comparison of various seismic resisting features of all models along X direction**

MODEL TYPE	DIRCTION	BASE SHEAR (V) in KN	PLAN AREA(m <sup>2</sup> )	BASE SHEAR PER UNIT AREA (KN/m <sup>2</sup> )	ROOF DISPLACEMENT (D) in m	SPECTRAL ACCLERETION (Sa) in m/s <sup>2</sup>	SPECTRAL DISPLACEMENT (Sd) in m	EFFECTIVE PERIOD (Teff) in s	EFFECTIVE DAMPING (Beff)
RECT	X	1224.93	165	7.42383	0.104	0.188	0.083	1.333	0.225
C		852.983	135	6.31839	0.136	0.143	0.106	1.726	0.233
H		1097.14	125	8.7771	0.105	0.201	0.078	1.252	0.223
I		1093.71	135	8.10155	0.105	0.183	0.083	1.355	0.231
L		592.243	95	6.23414	0.138	0.141	0.109	1.758	0.23
BrL		793.11	145	5.46972	0.144	0.134	0.112	1.83	0.236
O		876.517	150	5.84345	0.13	0.134	0.103	1.758	0.262
T		756.819	95	7.96652	0.134	0.184	0.09	1.401	0.208
U		1062.25	130	8.17116	0.103	0.19	0.081	1.305	0.23

**Table5-11: Comparison of various seismic resisting features of all models along Y direction**

MODEL TYPE	DIRCTION	BASE SHEAR (V) in KN	PLAN AREA(m <sup>2</sup> )	BASE SHEAR PER UNIT AREA (KN/m <sup>2</sup> )	ROOF DISPLACEMENT (D) in m	SPECTRAL ACCLERETION (Sa) in m/s <sup>2</sup>	SPECTRAL DISPLACEMENT (Sd) in m	EFFECTIVE PERIOD (Teff) in s	EFFECTIVE DAMPING (Beff)
RECT	Y	875.797	165	5.30786	0.128	0.153	0.093	1.566	0.25
C		749.334	135	5.55062	0.167	0.129	0.111	1.858	0.25
H		Convergence problem in Y direction							
I		764.852	135	5.66557	0.139	0.136	0.104	1.753	0.253
L		Convergence problem in Y direction							
BrL		804.093	145	5.54547	0.136	0.132	0.108	1.818	0.251
O		762.547	150	5.08365	0.127	0.135	0.101	1.737	0.263
T		762.547	95	8.02681	0.002	0.185	0.091	1.369	0.185
U		991.743	130	7.62879	0.004	0.167	0.082	1.409	0.263

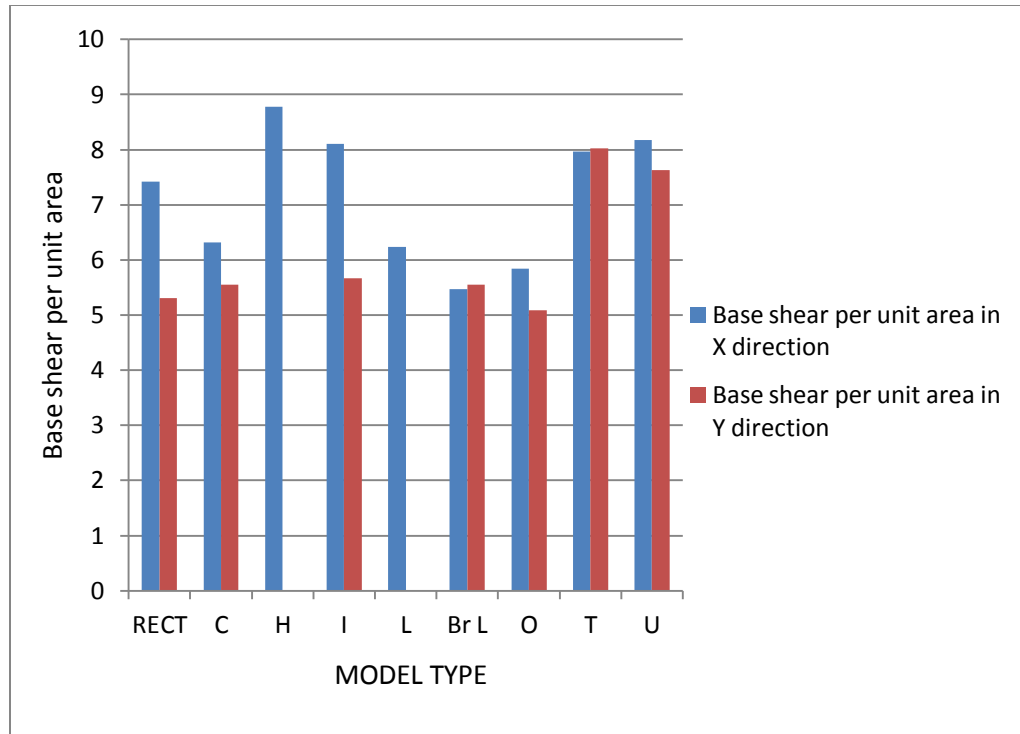


Fig 5.78: BASE SHEAR (V) in X & Y Direction for all models

With close observation it could be seen that the base shear capacities of the models symmetric about both the axes are higher than the base shear capacities of the models asymmetric about both the axes or symmetric about one of the axes only. Although base shear per unit area of model T and U are on higher side.

Among all the models base shear capacity per unit area of model H is highest in X direction. Among the asymmetric models model U has got higher base shear capacity per unit area and model L and Br L being asymmetric about both the axes and maximum plan irregularity has got lower values. Among the symmetric models model O has got lower base shear per unit area due to its disturbed diaphragm action at centre.

For model I base shear capacity along Y direction is a bit lower because of the reentrant corner of the model along Y direction.

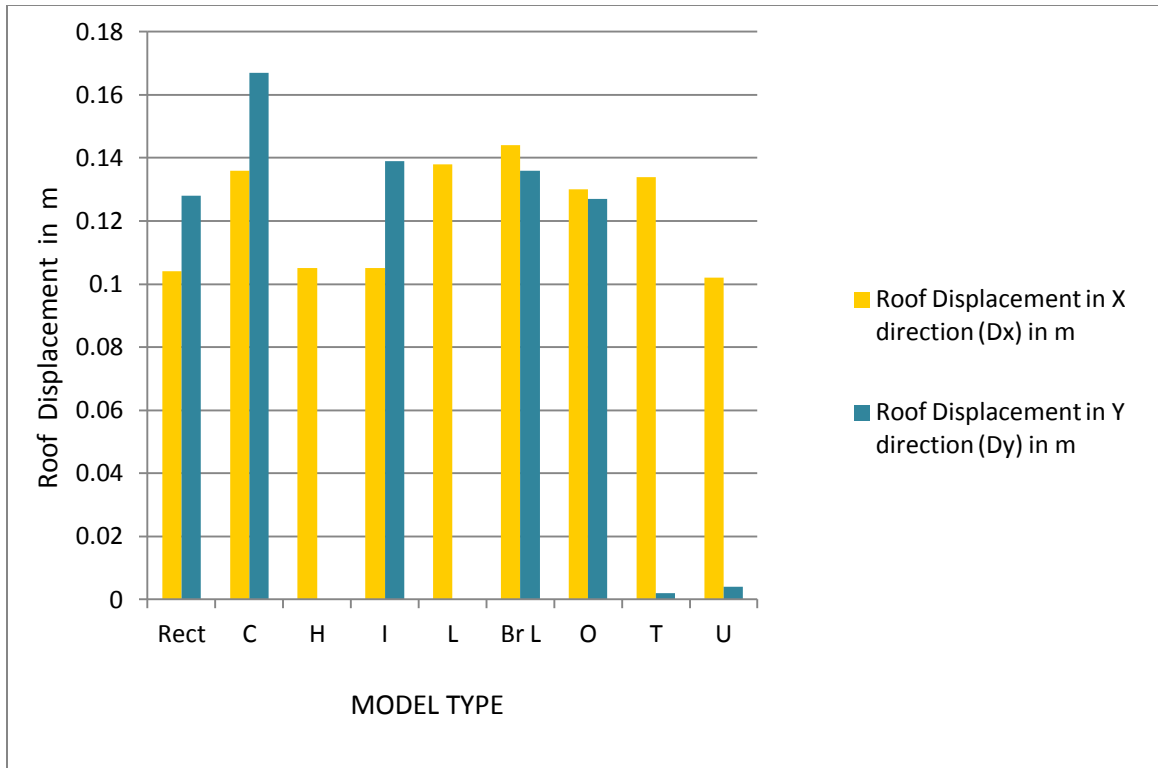


Fig 5.79: ROOF DISPLACEMENT ( $D_{rf}$ ) in X & Y Direction for all models

In general roof displacements of the symmetric models are lesser than that of the asymmetric models and having parity with the base shear capacities of the corresponding models.

Roof displacement of model C along Y direction is the highest among all the models and roof displacements of rectangular model, model H and model I are on the lower side compared to other models because of getting advantage of their plan symmetry.

Roof displacement of model U is lesser among the asymmetric models due to its higher base shear capacity and target displacement has been taken on a node situated in the bay of significantly higher mass and stiffness compared to other two bays.



**Table 5-12: Global Ductility & Global Stiffness in X direction of all models**

Model type	Direction	Vy in X(KN)	0.6 Vy(KN)	$\Delta_v$ (m)	$\Delta_t$ (m)	$\Delta = (\Delta_t - \Delta_v)$ in m	Global Ductility $= (\Delta_t / \Delta_v)$	I.O = $(\Delta_v + 0.2\Delta)$	L.S = $(\Delta_v + 0.5\Delta)$	C.P = $(\Delta_v + 0.9\Delta)$	Global stiffness in X dir
Rect	X	1092	655.2	0.045	0.2	0.155	4.444444444	0.076	0.1225	0.1845	20312.5
C		756.8	454.08	0.053	0.266	0.213	5.018867925	0.0956	0.1595	0.2447	21728.4
H		1568	940.8	0.024	0.125	0.101	5.208333333	0.0442	0.0745	0.1149	32000
I		968	580.8	0.042	0.173	0.131	4.119047619	0.0682	0.1075	0.1599	19047.6
L		536.8	322.08	0.054	0.241	0.187	4.462962963	0.0914	0.1475	0.2223	12200
Br L		720.9	432.54	0.055	0.309	0.254	5.618181818	0.1058	0.182	0.2836	16875
O		716.1	429.66	0.03	0.186	0.156	6.2	0.0612	0.108	0.1704	15500
T		577.5	346.5	0.047	0.234	0.187	4.978723404	0.0844	0.1405	0.2153	18333.3
U		954	572.4	0.039	0.17	0.131	4.358974359	0.0652	0.1045	0.1569	26666.7

**Table 5-13: Global Ductility & Global Stiffness in Y direction of all models**

Model type	Direction	Vy in Y dir(KN)	0.6 Vy(KN)	$\Delta_v$ (m)	$\Delta_t$ (m)	$\Delta = (\Delta_t - \Delta_v)$ in m	Global Ductility $= (\Delta_t / \Delta_v)$	I.O = $(\Delta_v + 0.2\Delta)$	L.S = $(\Delta_v + 0.5\Delta)$	C.P = $(\Delta_v + 0.9\Delta)$	Global stiffness in Y dir	
Rect	Y	764.4	458.64	0.029	0.192	0.163	6.620689655	0.0616	0.1105	0.1757	20222.2	
C		577.5	346.5	0.037	0.191	0.1544	5.172972973	0.06788	0.1142	0.17596	17500	
H		Convergence problem in Y direction										
I		616.2	369.72	0.026	0.184	0.158	7.076923077	0.0576	0.105	0.1682	14629.6	
L			0	0.054	0.241	0.187	4.462962963	0.0914	0.1475	0.2223	12200	
Br L		705.2	423.12	0.032	0.26	0.228	8.125	0.0776	0.146	0.2372	20000	
O		695.6	417.36	0.026	0.172	0.146	6.615384615	0.0552	0.099	0.1574	20888.9	
T		Incomplete analysis in Y direction										
U		Incomplete analysis in Y direction										

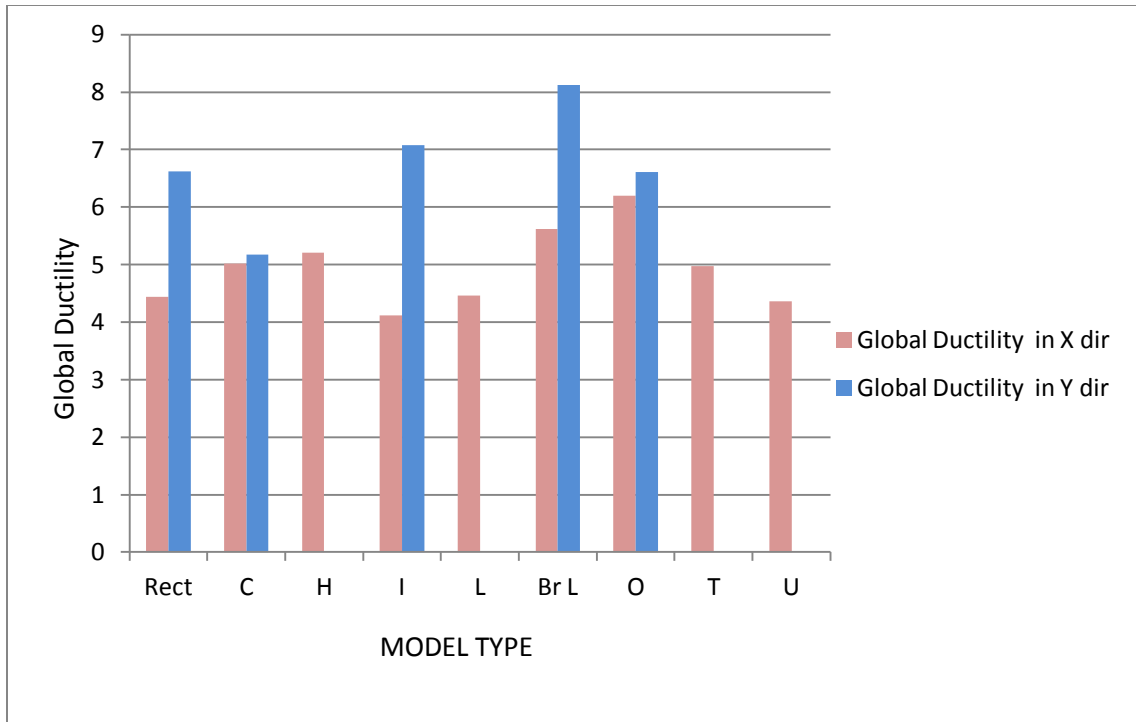


Fig 5.80: Global Ductility in X & Y Direction for all models

Global ductilities of model T and model U in Y direction could not be calculated properly as non linear analysis in Y direction could only be performed to a certain percentage due to plan irregularity in Y direction. For model L and model H results not available in Y direction due to convergence problem.

Global ductilities of all the models have higher values in Y direction compared to X direction. As along Y direction seismic masses and stiffnesses are lesser due to shorter span length. Global ductility of model broader L is highest in Y direction and lowest in model I in X direction. In general Global ductilities of symmetric models are on higher side than those of asymmetric models thus giving better seismic performance.

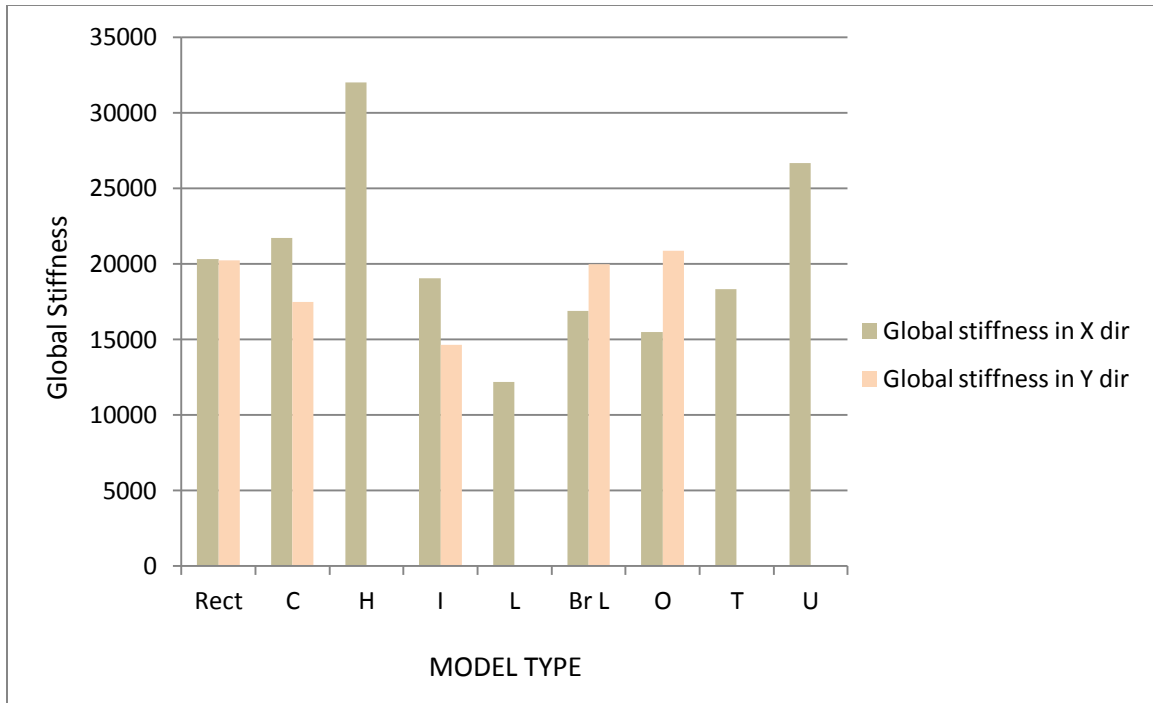


Fig 5.81: Global Stiffness in X & Y Direction for all models

For models having higher global ductilities have lower global stiffness. This feature is reflected in the above graph. Rectangular model has more or less similar global stiffness along both the directions. Model H having lower global ductility in X direction has higher global stiffness along X direction. Same conclusion could be drawn for model U.

Symmetric models show lesser global stiffness than asymmetric models specially in X direction. Model H has got highest global stiffness whereas model L has got lower global stiffness due to its lesser seismic mass though it has got moderate global ductility. Model C has got higher global stiffness along X direction as it showed lesser global ductility along X direction.

**Table 5-14: VI<sub>bldg</sub> & VI<sub>storey</sub> of all models in details in both X and Y direction**

TYPE OF MODEL	LEVEL	B		I.O		L.S		C.P		C		VI <sub>bldg</sub>	VI <sub>storey</sub>
		COL	BM	COL	BM	COL	BM	COL	BM	COL	BM		
RECT X	0.00	8										0.41754	0.125
	1.80	4	20							12			0.78125
	5.00						24						
	8.20	4			4		20						0.125
	11.40	10	20		4								0.125
	14.60		14										
			26	54	0	8	0	44	0	0	12		0
RECT Y	0.00											0.46875	
	1.80		4							16			1
	5.00	10					18				6		0.125
	8.20										24		
	11.40										24		
	14.60										24		
		10	0	0	0	0	18	0	0	0	78		
MD C X	0.00					2				14		0.563393	0.953125
	1.80	16			10		14						0.125
	5.00						12				12		
	8.20						24						
	11.40				12		12						
	14.60		12		12								
		16	12	0	34	2	62	0	0	14	12		
MD C Y	0.00	16										0.426546	0.125
	1.80	10			18		2						0.125
	5.00		6				20						
	8.20		6				20						
	11.40		5		12		8						
	14.60		11		9								
		0	28	0	21	0	48	0	0	0	0		
MD H X	0.00	12				4						0.625	0.25
	1.80	12			20	4							0.25
	5.00						10				10		
	8.20										20		
	11.40						10				10		
	14.60						14				6		
		0	0	0	0	0	34	0	0	0	46		

TYPE OF MODEL	LEVEL	B		I.O		L.S		C.P		C		VI <sub>bidg</sub>	VI <sub>storey</sub>
		COL	BM	COL	BM	COL	BM	COL	BM	COL	BM		
MD H Y	0.00											0.418883	
	1.80												
	5.00												
	8.20												
	11.40												
	14.60												
			0	0	0	0	0	0	0	0	0		0
MD I X	0.00	16										0.418883	0.125
	1.80	4	14		10					12			0.78125
	5.00						12				12		
	8.20						24						
	11.40	10			24								0.125
	14.60		12		12								
		10	12	0	36	0	36	0	0	0	12		
MD I Y	0.00	4										0.564063	0.125
	1.80	4	14		6	6				6			0.640625
	5.00						10				10		
	8.20										20		
	11.40						10				10		
	14.60						20						
		8	14	0	6	6	40	0	0	6	40		
MD L X	0.00					1				11		0.5625	0.96875
	1.80	10			4		12						0.125
	5.00						8				8		
	8.20						8				8		
	11.40						16						
	14.60				12		4						
		0	0	0	12	0	36	0	0	0	16		
MD L Y	0.00												
	1.80												
	5.00												
	8.20												
	11.40												
	14.60												
			0	0	0	0	0	0	0	0			

TYPE OF MODEL	LEVEL	B		I.O		L.S		C.P		C		VI <sub>bdg</sub>	VI <sub>storey</sub>
		COL	BM	COL	BM	COL	BM	COL	BM	COL	BM		
MD Br L X	0.00					4				11		0.550521	0.9
	1.80	15			10		12						0.125
	5.00						11				11		
	8.20						13				9		
	11.40				11		11						
	14.60		10		12								
			15	10	0	33	4	47	0	0	11		20
MD Br L Y	0.00					1				14		0.639423	0.975
	1.80	15					22						0.125
	5.00										22		
	8.20						8				14		
	11.40						22						
	14.60				18		4						
		15	0	0	18	1	56	0	0	14	36		
MD O X	0.00									16		0.6525	1
	1.80	12					24						0.125
	5.00										24		
	8.20										24		
	11.40						24						
	14.60				24								
		12	0	0	24	0	48	0	0	16	48		
MD O Y	0.00									16		0.541667	1
	1.80	16					24						0.125
	5.00										24		
	8.20										24		
	11.40	2					24						0.125
	14.60				24								
			0	0	24	0	48	0	0	0	48		
MD T X	0.00	9										0.472356	0.125
	1.80				16								
	5.00						11				5		
	8.20						6				10		
	11.40						4				12		
	14.60						6				10		
		9	0	0	16	0	27	0	0	0	37		

TYPE OF MODEL	LEVEL	B		I.O		L.S		C.P		C		VI <sub>bidg</sub>	VI <sub>storey</sub>	
		COL	BM	COL	BM	COL	BM	COL	BM	COL	BM			
MD T Y	0.00													
	1.80													
	5.00													
	8.20													
	11.40													
	14.60													
			0	0	0	0	0	0	0	0	0			0
MD U X	0.00									16		0.679861	1	
	1.80						3				17			
	5.00						2				18			
	8.20						10				10			
	11.40	15					20							0.125
	14.60	4			3		17							0.125
		19	0	0	3	0	52	0	0	16	45			
MD U Y	0.00									16		0.4835	1	
	1.80				20									
	5.00				15		5							
	8.20				20									
	11.40	8	4		16									0.125
	14.60	1	12		8									0.125
		9	16	0	79	0	5	0	0	16	0			

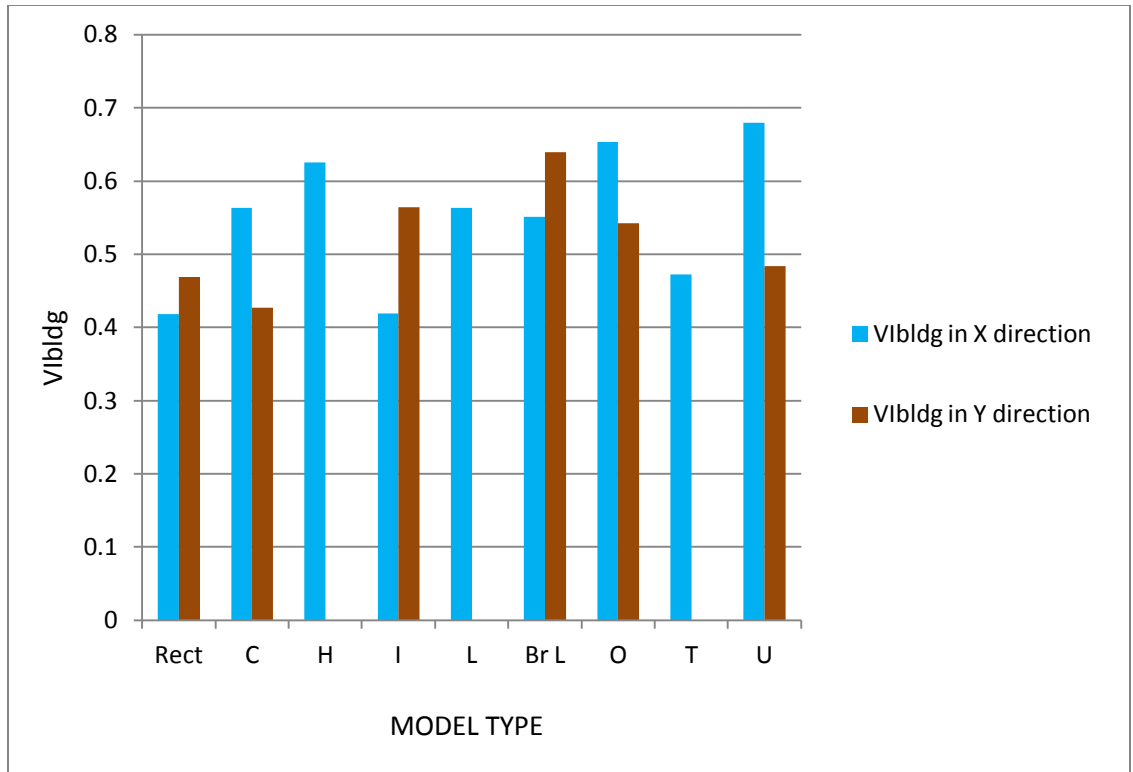


Fig 5.82: Building Vulnerability ( $VI_{bldg}$ ) in X & Y Direction for all models

Among the symmetric models rectangular model and model I are less vulnerable whereas model H and O are on the higher side of vulnerability. All the asymmetric models are more or less highly vulnerable to earthquake. Model U has got the highest vulnerability index among all the models in X direction.

For models H and L there was convergence problem in Y direction and results could not be obtained whereas for model T due to early development of collapse mechanism(hinge formation was not proper) results not available. In case of rectangular model, model C and model U building vulnerabilities are lower and for the other models they are on higher side.



**Table 5-15:  $VI_{storey}$  in both directions for all models in all levels**

		Vistorey in both dir								
Storey Height(m)	Direction	MODEL TYPE								
		RECT	C	H	I	L	Br L	O	T	U
0	X	0.125	0.95313	0.25	0.125	0.96875	0.9	1	0.125	1
	Y	0	0.125		0.125		0.975	1	0	1
1.8	X	0.78125	0.125	0.25	0.78125	0.125	0.125	0.125	0	0
	Y	1	0.125		0.64063		0.125	0.125	0	0
5	X	0	0	0	0	0	0	0	0	0
	Y	0.125	0		0		0	0	0	0
8.2	X	0.125	0	0	0	0	0	0	0	0
	Y	0	0		0		0	0	0	0
11.4	X	0.125	0	0	0.125	0	0	0	0	0.125
	Y	0	0		0		0	0.125	0	0.125
14.6	X	0	0	0	0	0	0	0	0	0.125
	Y	0	0		0		0	0	0	0.125

The higher value of  $VI_{storey}$  of Rectangular and I model at 1.8 m level clearly indicates the formation of soft storey due to absence of slab at 1.8 m level. However, the higher values of  $VI_{storey}$  for L, Br L, O, U at ground level indicates the inadequacy of stiffness and strength at that level.

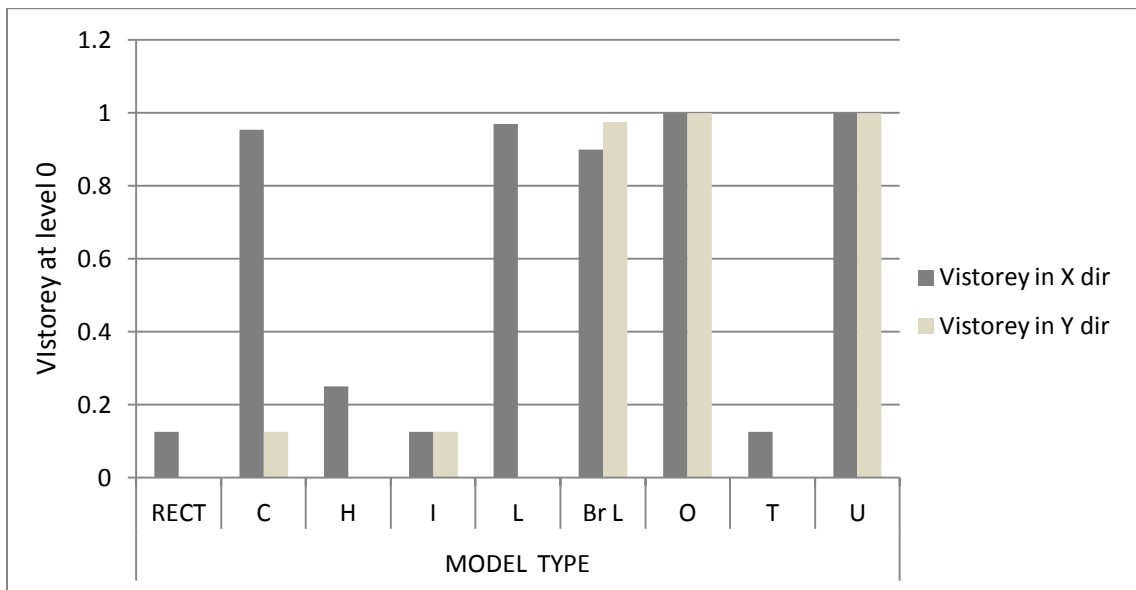


Fig 5.83: Storey Vulnerability ( $VI_{storey}$ ) at 0 m level in X & Y Direction for all models

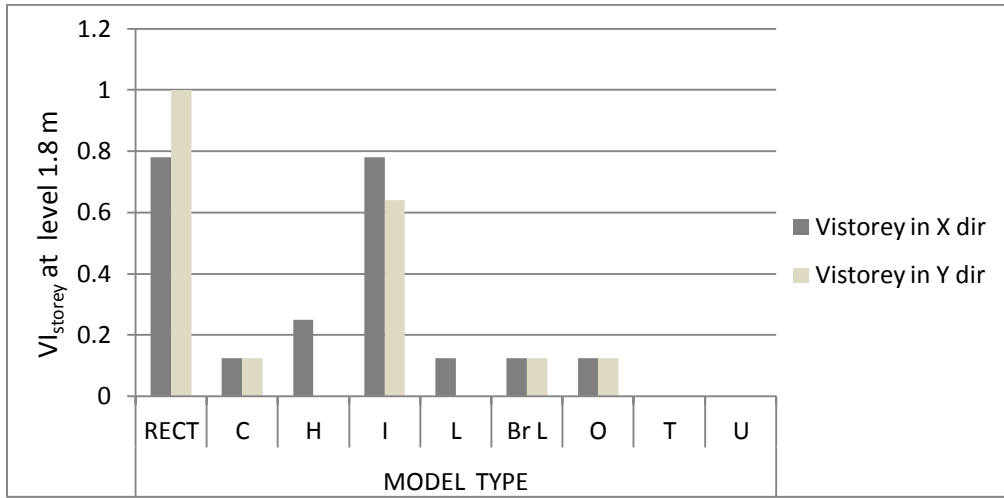


Fig 5.84: Storey Vulnerability ( $VI_{storey}$ ) at 1.8 m level in X & Y Direction for all models

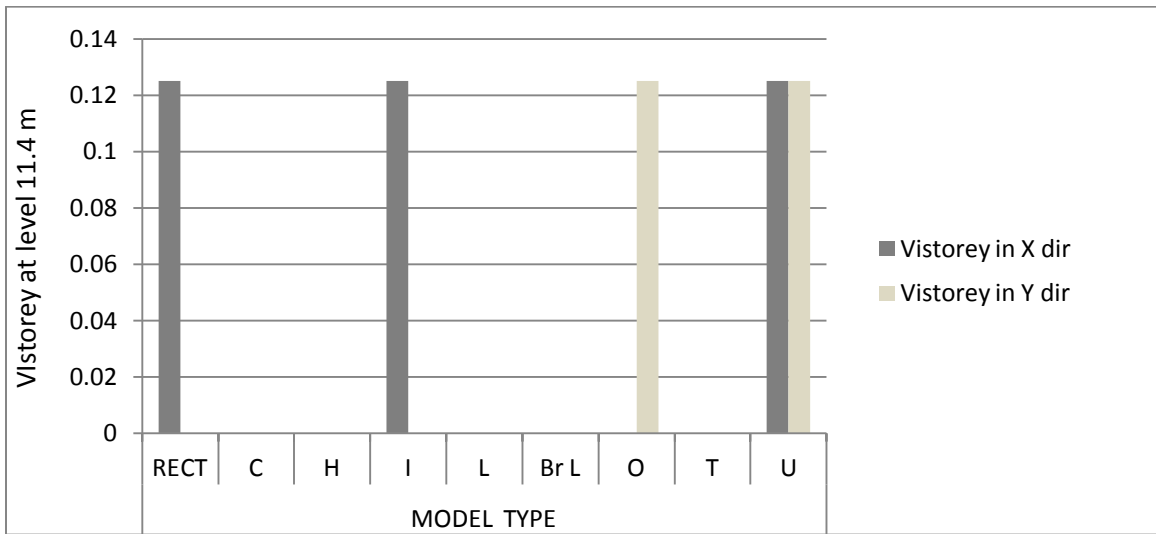


Fig 5.87: Storey Vulnerability ( $VI_{storey}$ ) at 11.4 m level in X & Y Direction for all models

## 6.1 General

The present study deals with seismic analysis of symmetric and asymmetric building models with same gridline plans and elevations. Only the building configurations has been changed and a NSP based analysis is done according to FEMA 356CM, FEMA 440 DM, ATC 40 CSM on G plus four storied building models. Pushover analysis is performed on the OMRF skeleton model of the buildings in SAP-2000 platform and the performance point, demand and capacity spectra, seismic vulnerability, global stiffness of the models are evaluated. Overall seismic performances of the models are observed along with vulnerability indices.

**6.2 Observation and conclusion:** Based on the detailed study of the results of pushover analysis and subsequent discussion the following may be concluded:

- i) The symmetric building configurations manifested better seismic performances in general as evident from the study of models considered.
- ii) The Rectangular building model exhibit better seismic features in both directions compared to other symmetrical models. It has relatively higher base shear capacity, lower roof displacement and less vulnerability index. However, the presence of soft storey due to absence of infill walls at ground level is clearly indicated by the higher value of storey vulnerability at that level. Spectral accelerations and spectral displacements of the models are in tune with their base shear capacities and roof displacement values. Similarly, the global stiffness of different models in X and Y direction depends on the distribution of rigidity including diaphragm action.
- iii) The seismic performance of uni-axial uniformity of building configuration like H,I etc. shows better behaviour along their symmetric axis of stiffness

compared to the other axis as expected. The vulnerability index of building of model I along X direction(0.419) is less than those value along Y direction(0.564) strongly establish the above statement.

- iv) Asymmetric models having high plan irregularities in one or both directions perform relatively poor under seismic load. In many cases analyses could not be completed or collapse mechanism develops at a very early stage for these kind of building configurations. Similar to the symmetric models Spectral accelerations and spectral displacements of the asymmetric models also are in tune with their base shear capacities and roof displacement values. Global stiffness of models C, Br L and T are in the same range.
- v) The seismic performances of asymmetric building models are complex in nature and depend on degree of asymmetry in general. The  $VI_{\text{bldg}}$  in X direction of L model reduces from 0.563 to 0.550, when the plan irregularity decreases. Similarly, the  $VI_{\text{bldg}}$  in Y direction of the broader L model is much more than that of X direction for greater asymmetry in Y direction. The  $VI_{\text{bldg}}$  may be adopted as a good indicator of seismic performance in general.
- vi) Pushover analysis seems to provide a global understanding of various seismic performances of different building configuration. The base shear capacity along with roof displacement may provide the strength and ductility capacity with respect to seismic performance.
- vii) The vulnerability index of the different building models is able to quantify the seismic performance of most of the building models in general manner.

**6.3 : Future scope of work :** The study has been made for a four storied O.M.R.F building with adequate size of beams and columns having the same structural gridline plan. Further study may include the effects of

- a) Changing the building configurations having same plan area.
- b) Buildings with different size of column and beam.

- c) Comparative study with present work introducing the soft storey effect.
- d) Development of vulnerability index formulation based on present study.
- e) Comparative study of different seismic load resisting features for different storied buildings.
- f) Comparative study with S.M.R.F type building models.
- g) Variation of infill dimension and properties.

## APPENDIX

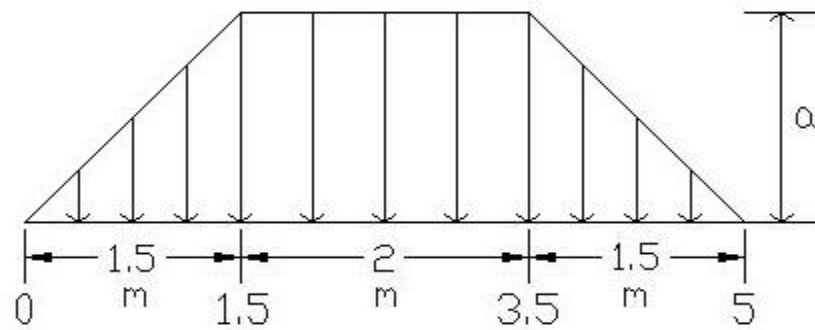


Fig A.1: Trapezoidal loading with shorter span length of slab 3 m

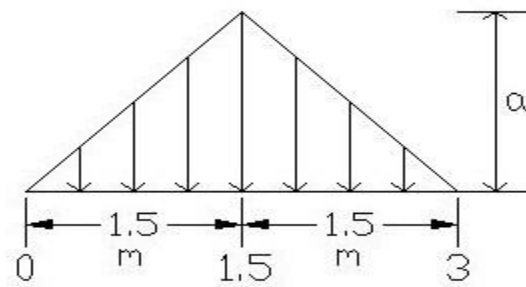


Fig A.2: Triangular loading with shorter span length of slab 3 m

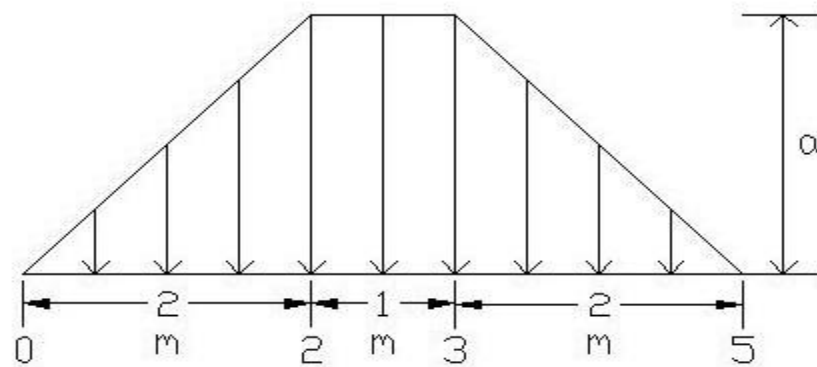


Fig A.3: Trapezoidal loading with shorter span length of slab 4 m

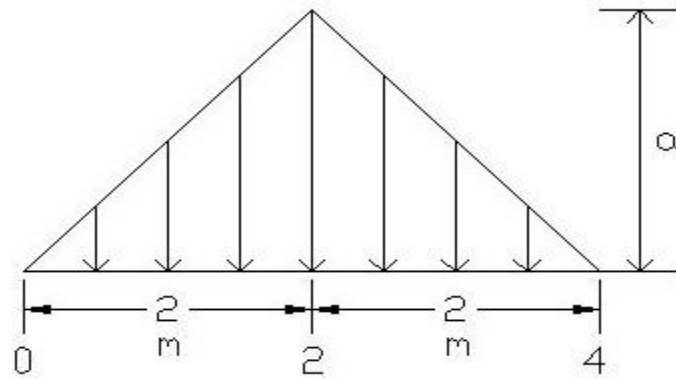


Fig A.4: Triangular loading with shorter span length of slab 4 m

**Table A-1: Load calculations**

Type of load	Type of slab	Type of beam	Slab load case			
			Trapezoidal with shorter span length of slab		Triangular with shorter span length of slab	
			3 m	4 m	3 m	4 m
			Reference Fig A.1	Reference Fig A.3	Reference Fig A.2	Reference Fig A.4
DL	Floor	Slab on one side	$a = (4 \times 1.5) = 6$	$a = (4 \times 2) = 8$	$a = (4 \times 1.5) = 6$	$a = (4 \times 2) = 8$
		Slab on both sides	$a = (4 \times 1.5 \times 2) = 12$	$a = (4 \times 2 \times 2) = 16$	$a = (4 \times 1.5 \times 2) = 12$	$a = (4 \times 2 \times 2) = 16$
	Roof	Slab on one side	$a = (4.5 \times 1.5) = 6.75$	$a = (4.5 \times 2) = 9$	$a = (4.5 \times 1.5) = 6.75$	$a = (4.5 \times 2) = 9$
		Slab on both sides	$a = (4.5 \times 1.5 \times 2) = 13.5$	$a = (4.5 \times 2 \times 2) = 18$	$a = (4.5 \times 1.5 \times 2) = 13.5$	$a = (4.5 \times 2 \times 2) = 18$

Type of load	Type of slab	Type of beam	Slab load case			
			Trapezoidal with shorter span length of slab		Triangular with shorter span length of slab	
			3 m	4 m	3 m	4 m
			Reference Fig A.1	Reference Fig A.3	Reference Fig A.2	Reference Fig A.4
LL	Floor	Slab on one side	a= (2.5x1.5) = 3.75	a= (2.5x2) = 5	a= (2.5x1.5) = 3.75	a= (2.5x2) = 5
		Slab on both sides	a= (2.5x1.5x2) = 7.5	a= (2.5x2x2) = 10	a= (2.5x1.5x2) = 7.5	a= (2.5x2x2) = 10
	Roof	Slab on one side	a= (1.5x1.5) = 2.25	a= (1.5x2) = 3	a= (1.5x1.5) = 2.25	a= (1.5x2) = 3
		Slab on both sides	a= (1.5x1.5x2) = 4.5	a= (1.5x2x2) = 6	a= (1.5x1.5x2) = 4.5	a= (1.5x2x2) = 6

B. Response Spectrum text file:

```

IS 1893:2002 Response Spectra for soil type II (Medium Soil)
Time Period T(sec)    Spectral Acceleration Sa/g
0                    1
0.1                  2.5
0.55                 2.5
0.8                  1.7
1                    1.36
1.2                  1.133333333
1.4                  0.971428571
1.6                  0.85
1.8                  0.755555556
2                    0.68
2.5                  0.544
3                    0.453333333
3.5                  0.388571429
4                    0.34
4.5                  0.302222222
5                    0.272
5.5                  0.247272727
6                    0.226666667
6.5                  0.209230769
7                    0.194285714
7.5                  0.181333333
8                    0.17
8.5                  0.16
9                    0.151111111
9.5                  0.143157895
10                   0.136

```

Fig B.1: Response Spectrum text file



## REFERENCES:

1. A. Kadid and A. Boumrkik(2008), “Pushover analysis of reinforced concrete frame structures”,Paper published in Asian journal of civil engineering (building and housing) vol. 9, no. 1 (2008)
2. A. S. Elnashai and A. M. Mwafy(2002) “Over strength and force reduction factors of multi storey reinforced-concrete buildings”,the structural design of tall buildings
3. A.E. Hassaballa , M. A. Ismaeil, A. N. Alzead & Fathelrahman M. Adam(2014) “Pushover Analysis of Existing 4 Storey RC Flat Slab Building”,International Journal of Sciences: Basic and Applied Research
4. Akshay V. Raut, Prof. RVRK Prasad (2014,July) “ Pushover Analysis of G+3 Reinforced Concrete Building with soft storey”
5. Aswin Prabhu T (2013) “Seismic evaluation of 4-story reinforced concrete structure by non-linear static pushover analysis”
6. Carlos Augusto Fernandes Bhatt (2007) “Seismic Analysis of Reinforced Concrete Buildings according to Eurocode8 – Linear and Nonlinear Analyses”
7. Code on Seismic evaluation and retrofit of concrete buildings, ATC 40,Vol-1
8. Curt B. Haselton (2006,December) “Assessing seismic collapse safety of modern reinforced concrete moment frame buildings”, Thesis submitted to the University of Stanford for the degree of Doctor of Philosophy in the Faculty of civil and environmental engineering, 2006

9. Eduardo Miranda (1999, April) "Approximate seismic lateral deformation demands in multistory buildings"
10. Joseph M. Bracci, Sashi K. Kunnath and Andrei M. Reinhorn (1997, January), "Seismic performance and retrofit evaluation of reinforced concrete structures"
11. Kenji Okazaki, Krishna S. Pribadi & Dyah Kusumastuti and Taiki Saito (2010), "Comparison of Current Construction Practices of Non-Engineered Buildings in developing Countries"
12. M. K. Rahman, M. Ajmal, M.H. Baluch & Z. Celep (2012) "Non linear Static Pushover Analysis of an Eight Story RC Frame-Shear Wall Building in Saudi Arabia"
13. Mehmed Causevic , Sasa Mitrovic (2010, July) "Comparison between non-linear dynamic and static seismic analysis of structures according to European and US provisions", Paper published in Bull Earthquake Eng journal DOI 10.1007/s10518-010-9199-1.
14. Mehmet Inel, Hayri Baytan Ozmen (March 2006) "Effects of plastic hinge properties in nonlinear analysis of reinforced concrete buildings", Paper published in science direct.
15. N. Lakshmanan, (2006), "Seismic Evaluation and Retrofitting of buildings and structures" published on ISET Journal of Earthquake Technology, Paper No. 469, Vol. 43, No. 1-2, March-June 2006, pp. 31-48.
16. Pre standard and commentary for the seismic rehabilitation of buildings, FEMA 356, November 2000

17. Rahul Rana, Limin Jin and Atila Zekioglu Au (2004, August) "Pushover Analysis of a 19 story concrete shear wall building", Paper published in 13th World Conference on Earthquake Engineering, Vancouver, B.C., Canada
18. Vojko Kilar and Peter Fajfar (1996 September) "Simple Push-over Analysis of Asymmetric Buildings"
19. Wikipedia, the free encyclopedia
20. X.-K. Zou, C.-M. Chan (2005, May) "Optimal seismic performance-based design of reinforced concrete buildings using nonlinear pushover analysis", Engineering Structures